Investigating the Role of CLEC14A and RhoJ in Regulating Endothelial Shear Responses

Jagminder Singh Gill

Word Count 18,234

Submitted May 2023

A thesis submitted to The University of Birmingham for the degree of MSc by Research in Cardiovascular Sciences at The University of Birmingham

UNIVERSITY OF BIRMINGHAM | INSTITUTE OF CARDIOVASCULAR SCIENCES

Abstract

Atherosclerosis is a disease associated with dysregulated hemodynamic shear stress, manifesting in regions of low shear stress and disturbed flow, and contributing to an atheroprone phenotype. CLEC14A, a type I transmembrane glycoprotein, and RhoJ, a small Rho GTPase protein, are both endothelially expressed, involved in angiogenesis and regulated by shear stress. Both may have a role to play in regulating the atheroprotective transcription factor KLF2, which is a master regulator of shear stress responses such as endothelial cell alignment. The aim of this study was to gain insight into the mechanism through which CLEC14A regulates KLF2 expression, focusing on critical regions and interacting partners of CLEC14A. A second aim was to understand the role of RhoJ in regulating shear induced KLF2 expression and shear mediated cell alignment. A third aim was to enhance our understanding of CLEC14A and RhoJ protein biology by analysing bioinformatic transcriptome databases relating to shear stress, atherosclerosis, and endothelial signalling pathway studies. Subjecting HUVECs which were overexpressing CLEC14A to laminar shear stress suppressed the normal upregulation of KLF2 and enhanced MMRN2 expression. These effects were most pronounced with intact CLEC14A. RhoJ expression was negatively regulated by laminar shear stress and siRNA-mediated knockdown of RhoJ revealed no change in KLF2 expression. Key bioinformatic findings included the observation that both proteins could be regulated by EGR1, a transcription factor known to regulate and promote atherosclerosis. CLEC14A was downregulated by the proinflammatory cytokine TNF-α and RhoJ upregulated in a model of ischaemia-reperfusion injury. These studies have given additional insight into the biology of RhoJ and CLEC14A and the bioinformatic database analyses has yielded new avenues for future research.

Acknowledgements

I would like to thank my supervisors Dr Victoria Heath and Dr Peter Hewett for their continued support, guidance, and patience throughout my MSc by Research degree. The skills and qualities I've acquired from being your student has set me up for life and for that I am grateful. To all the staff and students, past and present, at the Institute of Cardiovascular Sciences- thank you for making it such a wonderful experience. It was a pleasure being part of the wonderful team in Professor Roy Bicknell laboratory and I wish you all the very best. Lastly, I would like to thank my mom and my wife for their encouragement and support throughout.

Table of Contents

Abstract ..... ***ii***

Acknowledgements ..... ***iii***

1 Introduction ***2***

1.1 Endothelial Shear Stress Overview **2**

1.2 Endothelial Mechanosensing Mechanism **4**

1.2.1 Overview of Endothelial Glycocalyx 4
1.2.2 Overview of Junctional Mechanosensors 5

1.3 The Role of Mechanosensors in Vascular Health and Atherosclerosis **8**

1.3.1 Endothelial Glycocalyx Mechanotransduction of Atheroprotective Laminar Shear Stress 8
1.3.2 Endothelial Glycocalyx Mechanotransduction of Pro-atherogenic Disturbed Flow 9
1.3.3 Endothelial Junctional Mechanotransduction of Atheroprotective laminar Shear Stress 10
1.3.4 Endothelial Junctional Mechanotransduction of Pro-atherogenic Disturbed Flow 11

1.4 CLEC14A **14**

1.4.1 Overview of CLEC14A 14
1.4.2 CLEC14A Expression and Functions in Endothelial Cells 16
1.4.3 CLEC14A Interacting Molecules 17
1.4.4 CLEC14A and Endothelial Shear Regulation 20
1.4.5 CLEC14A Role in Atherosclerosis 20

1.5 RhoJ GTPase **21**

1.5.1 Overview of RhoJ 21
1.5.2 Endothelial Functions of RhoJ 23

1.6 Hypotheses and Aims **25**

2 Materials and Methods ***28***

Materials ***28***

2.1 Cell Biology **30**

2.1.1 Cells and Media 30
2.1.2 Cell Passaging 31

2.2 Lentiviral Tsransduction of HUVEC **32**

2.2.1 Plasmids 32
2.2.2 PEI Plasmid Transfection 33

2.2.3 HUVEC Transduction 34

2.3 Validation of HUVEC Transduction 36

2.3.1 Flow Cytometry 36
2.3.2 Cell Staining for Flow Cytometry 36

2.4 Preparing Transduced HUVEC for Orbital Shaker 37

2.5 Transfection of HUVEC with siRNA duplexes 37

2.6 Image Analysis 38

2.7 RNA Analysis 38

2.7.1 RNA Isolation and Purification 38
2.7.2 cDNA Synthesis 39
2.7.3 Quantitative Real-Time PCR 39

2.8 Protein Analysis 41

2.8.1 Protein Extraction 41
2.8.2 SDS Polyacrylamide Gel Electrophoresis (SDS-PAGE) 41
2.8.3 Western Blotting 42

2.9 Bioinformatics Methods 43

2.9.1 Database Analysis 43
2.9.2 Data Searches and Data Acquisition 43
2.9.3 Data Unpacking and Annotating 44
2.9.4 Database Selection 45

2.10 Data Analysis 45

3 The Role of CLEC14A and RhoJ in Regulating Endothelial Shear Responses 51

3.1 Introduction 51

3.2 Experimental Results 52

3.2.1 HUVEC Transduction to express GFP and mutant forms of CLEC14A 52
3.2.2 Evaluation of the Overexpression of Wild Type and Mutant Forms of CLEC14A on the Expression of Shear Regulated Genes 59
3.2.2.1 GFP mRNA Expression in Transduced HUVECs 59

3.2.2.2 CXCR4 mRNA Expression in Transduced HUVECs 61

3.2.2.3 KLF2 mRNA Expression in Transduced HUVECs 63

3.2.2.4 MMRN2 mRNA Expression in Transduced HUVECs 64

3.2.3 RhoJ mRNA and Protein Expression During Static and Laminar Shear Stress Conditions 67
3.2.4 *In vitro* RhoJ Regulation of KLF2 Shear Responses in RhoJ SiRNA-treated Cells 69
3.2.5 Image Analysis of RhoJ Knockdown Transfection Cultures to Evaluate Cell Alignment 71

3.3 Discussion 73

3.3.1 Summary 73
3.3.2 Endothelial Shear Reponses of Mutant Forms of CLEC14A 73
3.3.3 RhoJ Shear Stress Responses 76

3.4 Conclusion 77

4 Bioinformatic Analysis of Online Datasets 80

4.1 Introduction 80

4.2 Summary of Bioinformatic Workflow 80

4.3 Bioinformatics results 85

4.3.1 Effect of Shear Stress on CLEC14A and RhoJ Expression 85
4.3.2 Atherosclerosis Related Studies on Clec14a/A and RhoJ Expression 89
4.3.3 CLEC14a and RhoJ Expression Data from Microarray Studies Related to The Effect of Oxidative Stress using the Ischemia and Reperfusion Injury Model in Mice 102
4.3.4 CLEC14a and RhoJ Expression Data from Microarray Studies Related to Proinflammatory Cytokine TNF-α 104
4.3.5 Microarray Studies Related to Endothelial Regulation of CLEC14A and RhoJ 106
4.3.6 CLEC14A and Rhoj Expression Data from Microarray Study Investigating the Molecular Mechanism of Endothelial Barrier Formation 114

4.4 Discussion 116

4.4.1 Summary 116
4.4.2 *In vitro* Regulation of CLEC14A Expression 116
4.4.3 *In vivo* Atherosclerotic Plaque Study Interrogation for CLEC14A Expression 118
4.4.4 *In vitro* Regulation of RhoJ Expression 119
4.4.5 *In vivo* Atherosclerotic Plaque Study Interrogation for RhoJ Expression 120

4.5 Conclusions 121

List of References 123

Appendix 135

List of Abbreviations

AP-1	Activator Protein 1
AHA	American Heart Association
ANOVA	Analysis of Variance
ApoE	Apolipoprotein E
ASK1	Apoptosis signal-regulating kinase 1
BCA Assay	Bicinchoninic Acid Assay
bFGF	Basic Fibroblast Growth Factor
BSA	Bovine Serum Albumin
CD248	Endosialin
CD93	Complement component C1q receptor
Cdc42	Cell Division Cycle 42
cDMEM	Complete Dulbecco's Modified Eagle Medium
CLEC14A	C-type lectin domain family 14 member
CM199	Complete Basal Media
Ct	1 Cycle
CTLD	C-type Lectin Domain
CXCR4	C-X-C Chemokine Receptor Type 4
daRhoJ	Dominant Active Mutant of RhoJ
DMEM	Dulbecco's Modified Eagle's Medium
ECL	Enhanced Chemiluminescent Substrate
ECs	Endothelial Cells
eGCX	Endothelial Glycocalyx
EGF	Epidermal Growth Factor
EGM-2	Endothelial Cell Growth Medium 2
EGR-1	Early Growth Response 1
eNOS	Nitric Oxide synthase
EPCs	Endothelial Progenitor Cells
ERK	Extracellular Signal-regulated Kinase
FACS	Fluorescence Activated Cell Sorting
FBS	Foetal Bovine Serum
FITC	Fluorescein isothiocyanate
G domain	Rho-type GTPase domain
GAG	Glycosaminoglycans
GAP	GTPase-activating-protein
GAPDH	Glyceraldehyde 3-phosphate dehydrogenase
GDP	Guanine Nucleotide Diphosphate
GEFs	Guanine Nucleotide Exchange Factors
GEO	Gene Expression Omnibus
GEOquery	Bioconductor package
GFP	Green Fluorescent Protein
GOI	Gene of Interest
GPL	GEO Platform annotation

GTP	Guanine Nucleotide Triphosphate
GTPase	Guanosine Triphosphatase
HEK298T cells	Human Embryonic Kidney 298T cells
HRP	Horseradish Peroxidase
HSP70-1A	Heat Shock Protein 70-1A
HUVECs	Human Umbilical Vein Endothelial Cells
ICAM-1	Intercellular Adhesion Molecule-1
ICD	Intracellular Domain
JNK	c-Jun N-terminal kinases
KLF2	Krüppel-like factor 2
KLF4	Krüppel-like factor 4
Kda	Kilodalton
KD	Knockdown
MCP-1	Monocyte chemoattractant protein-1
MEK5	Mitogen-activated protein kinase kinase 5
Miro	Mitochondrial Subfamily
MMRN2	Multimerin-2
MT1-MMP	Endothelial Membrane Type-I Matrix Metalloproteinase
NCBI	National Centre for Biotechnology Information
NCD	Negative Control Duplex
NF-κβ	Nuclear Factor-kappa β Signalling
NO	Nitric Oxide
NRF2	Nuclear Factor Erythroid 2-related Factor 2
OS	Orbital Shear
PAK1	p21 protein (Cdc42/Rac)-activated kinase 1
PBS	Phosphate-Buffered Saline
PECAM-1	Platelet Endothelial Cell Adhesion Molecule-1
PEI	Polyethylenimine
PI3K	Phosphoinositide 3-Kinase
PI3K/Akt	Phosphoinositide-3-kinase–protein kinase B/Akt
P-value	probability value
qPCR	Real Time Quantitative PCR
PCR	Polymerase Chain Reaction
RHBDL2	Rhomboid Like 2
Rho	Ras Homology
RhoJ	Ras Homolog Family Member J
RIPA Buffer	Radioimmunoprecipitation Assay Buffer
RISC	RNA-induced silencing complex
RNS	Reactive Nitrogen Species
ROS	Reactive Oxygen Species
SDS-PAGE	Sodium dodecyl-sulphate polyacrylamide gel electrophoresis
SEM	Standard Error of Mean
Sema	Semaphorin
siRNA	Small interfering RNA
SMC	Smooth Muscle Cell

SOFT	Simple Omnibus Format in Text
ST	Static
STAGE	Stockholm Atherosclerosis Gene Expression Study
TBST	Tris-Buffered Saline Tween- 20
THBD	Thrombomodulin
TIE1	Tyrosine Kinase With Immunoglobulin Like And EGF Like Domains 1
TNF-α	Tumour necrosis factor α
T-test	Hypothesis Test Statistic
VCAM-1	Vascular Cellular Adhesion Molecule-1
VE-Cadherin	Vascular Endothelial Cadherin
VEGF	Vascular Endothelial Growth Factor
VEGFR2	Vascular Endothelial Growth Factor Receptor subtype 2
VEGFR3	Vascular Endothelial Growth Factor Receptor subtype 3
vWF	Von Willebrand factor
YAP	Yes-associated protein
wt	Wild type
18S	18S ribosomal RNA

Chapter One

Introduction

1 Introduction

1.1 Endothelial Shear Stress Overview

Haemodynamic shear stress is defined as the intraluminal frictional force of blood flow and is determined by many factors such as velocity, viscosity, and luminal radius (1, 2). It plays a key role in maintaining vascular homeostasis and, when dysregulated, can contribute to the development of vascular diseases such as atherosclerosis (3). The levels and characteristic patterns of arterial shear stress are associated to the location within the arterial tree (4). For example, blood flow within healthy straight luminal arterial vessels is characterised by high pulsatile, uniform laminar shear stress profile (Figure 1.1). These are associated with atheroprotective gene signalling and a healthy vascular phenotype (2). At points of arterial bifurcation and curvatures, like that seen within the carotid sinus, there is a disruption to the preceding uniform laminar flow and the manifestation of disturbed flow, characterised by low velocity shear stress with multidirectional, reverse flow patterns (1, 5) (Figure 1.1). Disturbed flow is associated with atherogenic gene signalling and is one of many factors that contribute to endothelial dysfunction and atherosclerosis (6, 7).

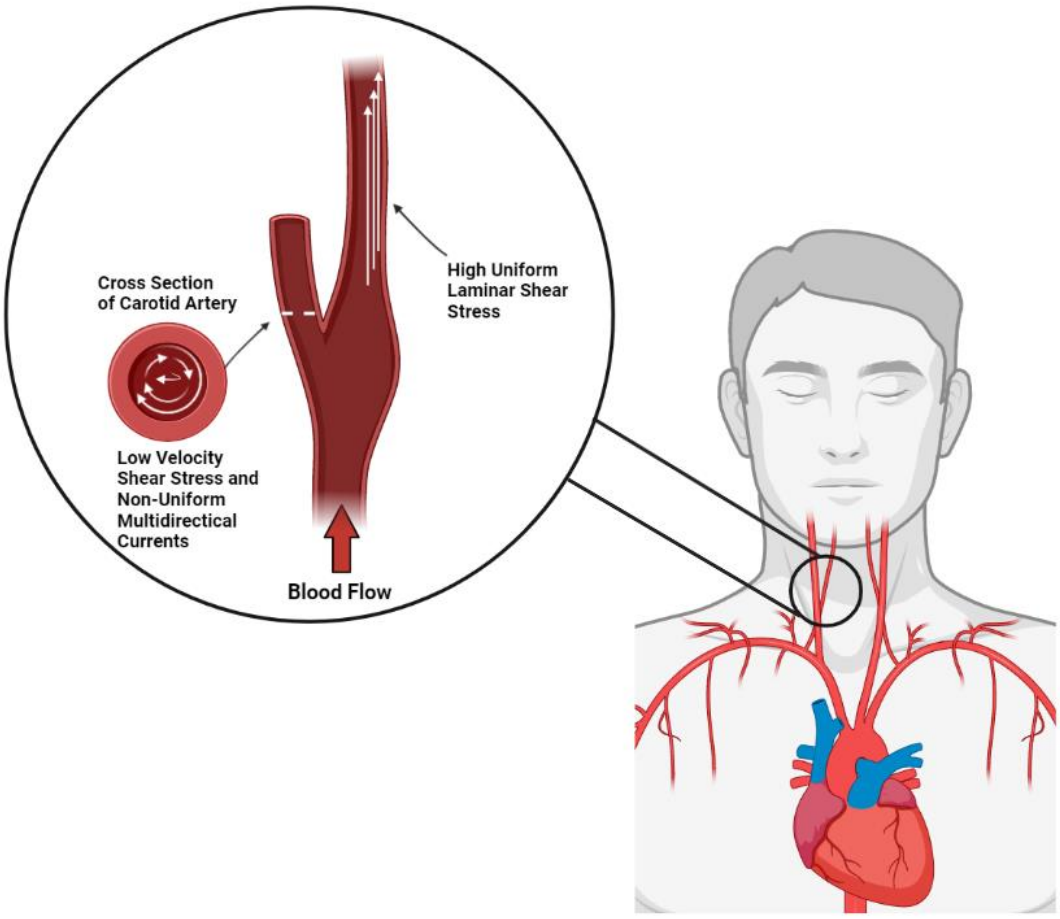

Figure 1.1: Haemodynamics within the human carotid bifurcation. Blood flow within straight arterial vessels is characterised by atheroprotective high laminar, uniform shear stress. Once passing through the carotid artery bifurcations the blood flow is replaced by non-uniform, low velocity shear stress and recirculating flow (disturbed flow) which are associated with the formation of atherosclerotic plaques (4, 7). Figure adapted from Wragg J *et al.*, 2014 (8).

1.2 Endothelial Mechanosensing Mechanism

Cardiovascular blood vessels are lined with Endothelial Cells (EC), which are responsive to haemodynamic shear stress (9, 10). ECs modulate homeostatic and pathological responses by sensing the mechanical shear forces in blood flow through structures known as mechanosensors. These structures transduce external mechanical signals into intracellular biochemical signals via adaptor molecules in a process called mechanotransduction (1, 11). The biochemical signals then pass through the cytoskeleton before being translated into an EC response. The main players involved in EC mechanotransduction are the endothelial Glycocalyx (eGCX) and junctional mechanosensors (Figure 1.2) (2).

1.2.1 Overview of Endothelial Glycocalyx

Coating the luminal surface of ECs, in direct contact with the blood is a complex, thin (~500 nm) gel-like layer of the eGCX, a mechanosensory unit made up of macromolecules such as glycosaminoglycans (GAGs), proteoglycans and glycoproteins (2, 12). The eGCX consists of two distinct layers as depicted and described in Figure 1.2 (12, 13). The eGCX is a dynamic structure and is continuously remodelled in response to environmental changes. The polyanionic constituents in the eGCX structure provide a net negative charge, which interacts with molecules carried by blood flow (12). Proteins in the eGCX structure that interact with GAG side chains are dependent on the microenvironment cation concentration and pH (12). Heparan sulphate, a member of the GAG family of glycosaminoglycans, is the most abundant component in the eGCX structure made up of negatively charged polysaccharide compounds with an amino sugar core (12, 14). Heparan sulphate

proteoglycan has an important role in regenerating the eGCX and acting as a signal transduction molecule in regulating mechanotransduction pathways (15).

The composition and thickness of the eGCX is regulated by the continuous shedding and synthesising of eGCX components, maintaining an intact balance in the healthy vasculature. The shredding of the eGCX is mediated by enzymes such as heparinase, hyaluronidase, and metalloproteases (16). In vascular diseases such as atherosclerosis, the balance shifts as shredding of the eGCX exceeds eGCX biosynthesis (17). As a result, the eGCX becomes thinner, leading to disrupted cell signalling transmission and communication between EC junctions (13). Additionally, this reduces the overall capacity of quencher binding oxygen radicals which are important in preventing oxidative stress and endothelial dysfunction (13, 14). In healthy arterial ECs, the eGCX component balance is intact due to prolonged uniform, laminar shear stress (18). It does this by promoting conformational changes to the eGCX structure which result in a thickened and redistributed eGCX, helping to dampen excessive shear stress before they reach the EC surface and protect the endothelium against turbulent shear stress (19-21).

1.2.2 Overview of Junctional Mechanosensors

Junctional mechanosensors are endothelial-specific complexes located at EC-EC junctions (Figure 1.2). They sense haemodynamic shear stress forces and trigger downstream intracellular signalling pathways that modulate endothelial and vascular homeostasis (1) including flow-dependent vasodilation, physiological vascular remodelling, and pathological remodelling in atherosclerosis (22-24). Junctional mechanosensory complexes are

composed of the proteins Vascular Endothelial (VE)-cadherin, Platelet Endothelial Cell Adhesion Molecule-1 (PECAM-1) and Vascular Endothelial Growth Factor Receptor subtype 2/3 (VEGFR2/VEGFR-3) (Figure 1.2) (1, 25). VEGFR3 has only recently been shown to play a role within this mechanosensory complex working in combination with VEGFR2 (25, 26). It has been proposed that the level of VEGFR3 expression within vessels specifically determines the mechanosensitivity of the junctional mechanosensors by controlling the shear sensing set point (26).

Fluctuations in shear forces at the junctional mechanosensory complex are sensed by PECAM-1 and VE-cadherin which triggers phosphorylation and recruitment of Src family kinases eventually leading to ligand-independent activation of VEGFRs (27, 28). Both VEGFR2 and VEGFR3 are rapidly phosphorylated activating the downstream phosphatidylinositol-3-OH kinase (PI3K) signalling pathway through its binding partner β-catenin (1, 25). β-catenin is also known to be activated by VE-cadherin, linking VE-cadherin to the actin cytoskeleton to facilitate EC-to-EC adhesion and, along with the activation of Rac1, ensuring an intact endothelial protective barrier and function (29, 30).

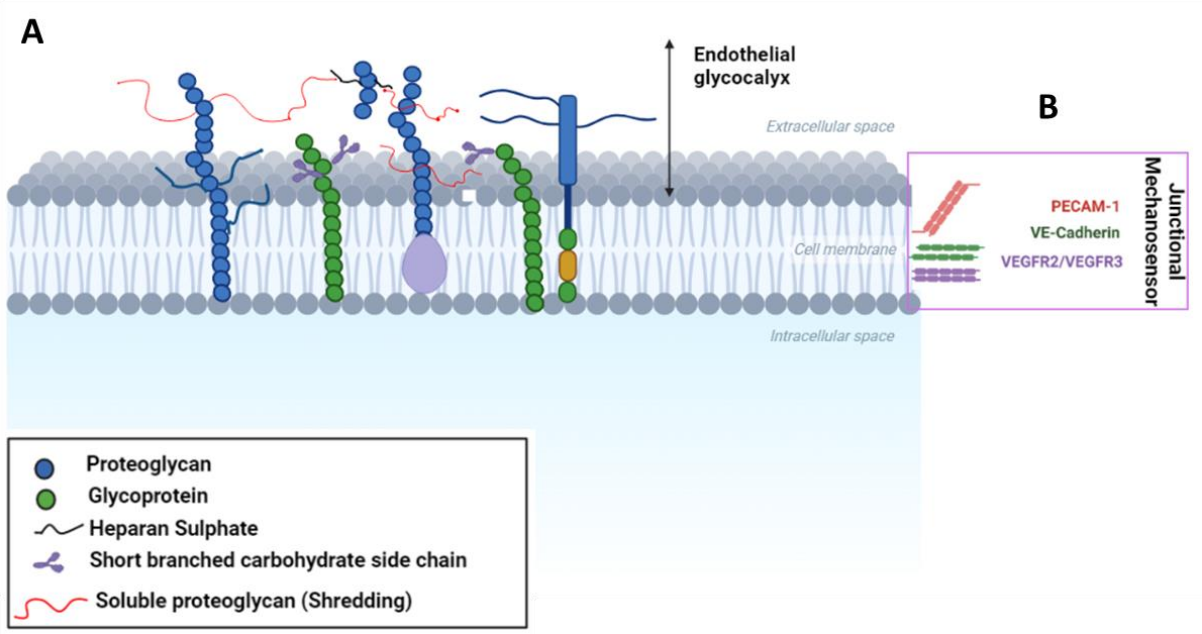

Figure 1.2: The eGCX and junctional mechanosensory complexes function as mechanosensors which transduce external mechanical signals into intracellular biochemical signals. A) The eGCX consists of two layers. The inner layer connects the glycocalyx matrix to the cell membrane and is made up of glycoproteins and proteoglycans. The outer layer consists of soluble molecules that are loosely attached to the inner layer composed of glycolipids and glycoproteins (12, 13). B) Junctional mechanosensors are comprised of a complex between PECAM-1, VE-cadherin and VEGR2/3. The homophilic interactions at the junctions i.e. PECAM-PECAM, VE-Cad-VE-Cad maintains the integrity of endothelial cell junctions and junctional mechanosensory complexes (31, 32). Figure adapted from Naumann D, 2018 (33) and Dorland Y & Huveneers S, 2017 (34) and Reitsma S, 2007 (13).

1.3 The Role of Mechanosensors in Vascular Health and Atherosclerosis

The nature and intensity of shear stress signals determines the mechanosensory signalling pathways activated and the resulting endothelial phenotype (7). For example, low velocity, disturbed flow induces activation of genes that promote an atherogenic gene profile and reduce expression of atheroprotective genes such as Nitric Oxide (NO) and Krüppel-like factor 2 (KLF2). These changes can be reversed by restoring laminar blood flow (6, 35).

1.3.1 Endothelial Glycocalyx Mechanotransduction of Atheroprotective Laminar Shear Stress

An intact eGCX is atheroprotective due to both its structure and its role as a mechanosensor transmitting shear stress signals to activate intracellular pathways (13). This in turn activates the atheroprotective transcription factor KLF2 which maintains endothelial quiescence (36). Hyaluronan, along with heparan sulphate, is a major GAG present in the eGCX whose biosynthesis is regulated by laminar shear stress and KLF2 (18). Under prolonged uniform laminar shear, KLF2 regulated hyaluronan increases the thickening of the eGCX and spatial distribution to the EC-EC junctional regions (37). Another way KLF2 promotes an atheroprotective endothelial barrier is through cytoskeletal-dependent regulation of EC alignment via actin shear fibre assembly and inhibiting atherogenic c-Jun N-terminal Kinase (JNK) signalling (38). The EC barrier protects against vascular permeability to prevent leucocyte infiltration and help ECs withstand higher end shear stress forces (38, 39). In addition, shear induced KLF2 expression promotes the differentiation of Endothelial Progenitor Cells (EPCs) to ECs encouraging endothelium repair, which is important in maintaining EC quiescence (40).

KLF2 achieves an anti-inflammatory phenotype in endothelial cells by inhibiting the pro-inflammatory Nuclear Factor-Kappa β signalling (NF-κβ) pathways and suppressing pro-inflammatory E-selectin expression (41, 42). KLF2 promotes an anti-thrombotic state by binding to the promoter region of the Von Willebrand Factor (vWF) gene to reduce secretion of vWF and inhibiting the coagulation factor plasminogen activator inhibitor-1 and activates thrombomodulin, an anti-coagulant protein (7, 40, 42). PI3K/Akt signalling activates the enzyme Endothelial Nitric Oxide Synthase (eNOS) to increase NO production which as a potent vasodilator promotes vasodilation, inhibits platelet aggregation, and exhibits anti-inflammatory properties (7, 43, 44). KLF2 directly mediates binding to eNOS promoter to increase NO expression (45).

Other atheroprotective roles of KLF2 include protecting against leukocyte recruitment by blocking transcription of leukocyte adhesion molecules such as Vascular Cell Adhesion Molecule-1 (VCAM-1), and Intercellular Adhesion Molecule 1 (ICAM-1) (45). KLF2 expression downregulates the transcription factor AP-1 (Activator Protein 1), which is involved in cell apoptosis, and activates atheroprotective transcription factors such as NRF2 (Nuclear factor erythroid 2-related factor 2) to promote antioxidant gene activation (Figure 1.3) (46). The eGCX sialic acid components are particularly important when it comes to regulating shear induced EC redox signalling (47).

1.3.2 Endothelial Glycocalyx Mechanotransduction of Pro-atherogenic Disturbed Flow

Prolonged low shear, disturbed flow triggers an increase in EC proliferation, Reactive Oxygen Species (ROS), Reactive Nitrogen Species (RNS) and Smooth Muscle Cell (SMC)

proliferation, all important hallmarks in initiating endothelial dysfunction and promoting plaque development (40, 48). It does this by degrading the eGCX resulting in downregulation of heparan sulphate which is required in modulating atheroprotective NO production (39, 49). In addition, disturbed flow induced eGCX mechanotransduction, downregulates atheroprotective KLF2 and NRF2 signalling and activates pro-inflammatory NF-Kβ signalling leading to the expression of inflammatory adhesion molecules such as VCAM-1 promoting monocyte recruitment and the development of atherosclerotic plaques. (2, 16, 47). Disturbed flow also contributes to endothelial dysfunction by modifying eGCX sialic acids resulting in reduced NRF2-mediated antioxidant responses (47).

1.3.3 Endothelial Junctional Mechanotransduction of Atheroprotective laminar Shear Stress

At endothelial junctional mechanosensors, high uniform laminar shear stress leads to the activation of VEGFR2, which in turn triggers the PI3K/Akt pathway (50). The PI3K signalling pathway mediates integrin activation which regulates the actin cytoskeleton and atheroprotective cell alignment to direction of flow. These are essential in reorganising and strengthening the cell-cell junction protecting against inflammation induced vascular permeability (1, 34, 51). PECAM-1 induces ERK activation and downregulates inflammatory transcription factors such as NF-κβ when exposed to a laminar flow environment (7, 52).

Continuous junctional mechanosensor exposure to laminar flow results in the constitutive expression of atheroprotective eNOS (53). Upon remodelling during atherogenesis, NO reverses changes in cell proliferation protecting vessels against pathological changes induced by vascular remodelling (7). Endothelial NO also decreases binding of monocytes

and inflammatory molecules to the endothelium by modulating expression of chemokines and leukocyte adhesion molecules such as MCP-1 (Monocyte Chemoattractant Protein-1), VCAM-1, and ICAM-1 (7). These molecules are known to induce an endothelial inflammatory phenotype in areas of disturbed flow, reinforcing NO role in promoting an atheroprotective phenotype (20). In addition, endothelial NO is involved in redox regulation of shear stress and lower levels of Reactive Oxygen Species (ROS) and Reactive Nitrogen Species (RNS), resulting in an atheroprotective phenotype (Figure 1.3) (54).

VE-cadherin demonstrates an atheroprotective function, as evidenced by its predominant expression in regions of laminar flow compared to its absence in areas of disturbed flow (18). The PI3K signalling pathway, activated by VE-cadherin, mediates integrin activation in response to shear stress. Integrins help maintain the atheroprotective phenotype of endothelial cells by modulating the anti-apoptotic effects observed in uniform laminar shear stress conditions (Figure 1.3) (55, 56). Moreover, ECs lacking VE-cadherin fail to align under laminar flow, while those expressing VE-cadherin do, suggesting that junctional mechanosensors contribute to the activation of atheroprotective genes (3, 24).

1.3.4 Endothelial Junctional Mechanotransduction of Pro-atherogenic Disturbed Flow

Despite promoting atheroprotective gene signalling, the junctional mechanosensory complex has also been implicated in mediating pro-inflammatory NF-Kβ signalling and pathological vascular remodelling in atherogenesis, but this only occurs with acute stimulation (3, 22). Disturbed flow triggers downstream atherogenic events by initiating the activation of the Apoptosis Signal-regulating Kinase 1 (ASK1) pathway, which in turn

influences downstream pathways such as the JNK pathway (Figure 1.3) (48, 54). These result in downstream effects that promote endothelial dysfunction due to inflammatory and oxidative stress responses, ultimately leading to apoptosis and development of atherosclerosis (Figure 1.3) (20).

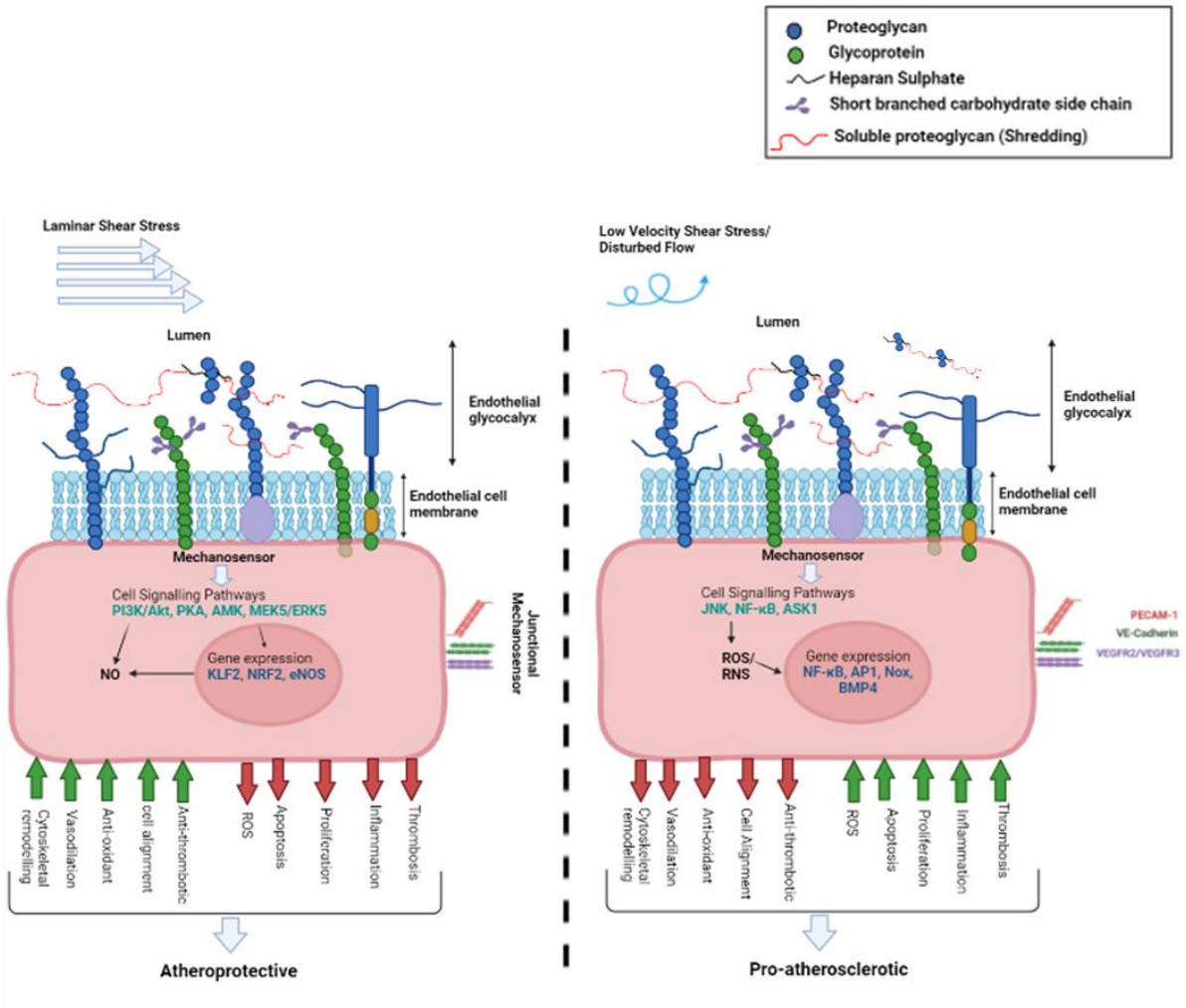

Figure 1.3: Schematic representation of the eGCX and junctional mechanosensory complex as well as the key signalling pathways involved in triggering atheroprone or atheroprotective phenotypes in response to laminar and disturbed flow. The eGCX and junctional mechanosensory signalling pathways, activated upon exposure to laminar shear stress, helps to maintain vascular homeostasis and endothelial function through upregulation of atheroprotective gene expression. Disturbed flow promotes eGCX shredding, and in both mechanosensors, causes downregulation of atheroprotective genes and activation of atherogenic gene signalling pathways leading to inflammation, thrombosis, and oxidative stress, resulting in endothelial dysfunction and atherosclerosis. Figure adapted from Naumann D, 2018 (33), Weinbaum *et al.*, 2007 (12), Reitsma *et al.*, 2007 (13) and Dorland Y & Huveneers S, 2017 (34).

1.4 CLEC14A

1.4.1 Overview of CLEC14A

The C-type lectin domain family 14 member (CLEC14A) is a type I transmembrane endothelial expressed glycoprotein, initially identified via microarray analysis (57-60). CLEC14A localises to vascular endothelial cell junctions, to the leading edge of migrating endothelial cells and to the interface between endothelial cells and pericytes (61). CLEC14A belongs to the C-type lectin domain (CTLD) containing group 14 family, which all are single transmembrane proteins with a conserved CTLD domain but with differing numbers of EGF-like repeats (57, 62). The other members of the CTLD group 14 family of transmembrane proteins are thrombomodulin, endosialin (CD248) and complement component C1q receptor (CD93) (57, 63) (Figure 1.4). The structure of CLEC14A consists of an extracellular portion called the N-terminal CTLD, one sushi domain, one epidermal growth factor (EGF) repeat, a mucin like domain, a transmembrane domain anchored to the cell membrane, and a small intracellular cytoplasmic tail (57, 63, 64). The CTLD domain is comprised of 110-130 amino acid residues and contains a double loop fold held together by two conserved disulphide bonds (65). In addition, CLEC14A exists as a soluble ectodomain as the extracellular domain is cleaved by Rhomboid Like 2 (RHBDL2), an intramembrane serine protease belonging to the RHBDL family (66).

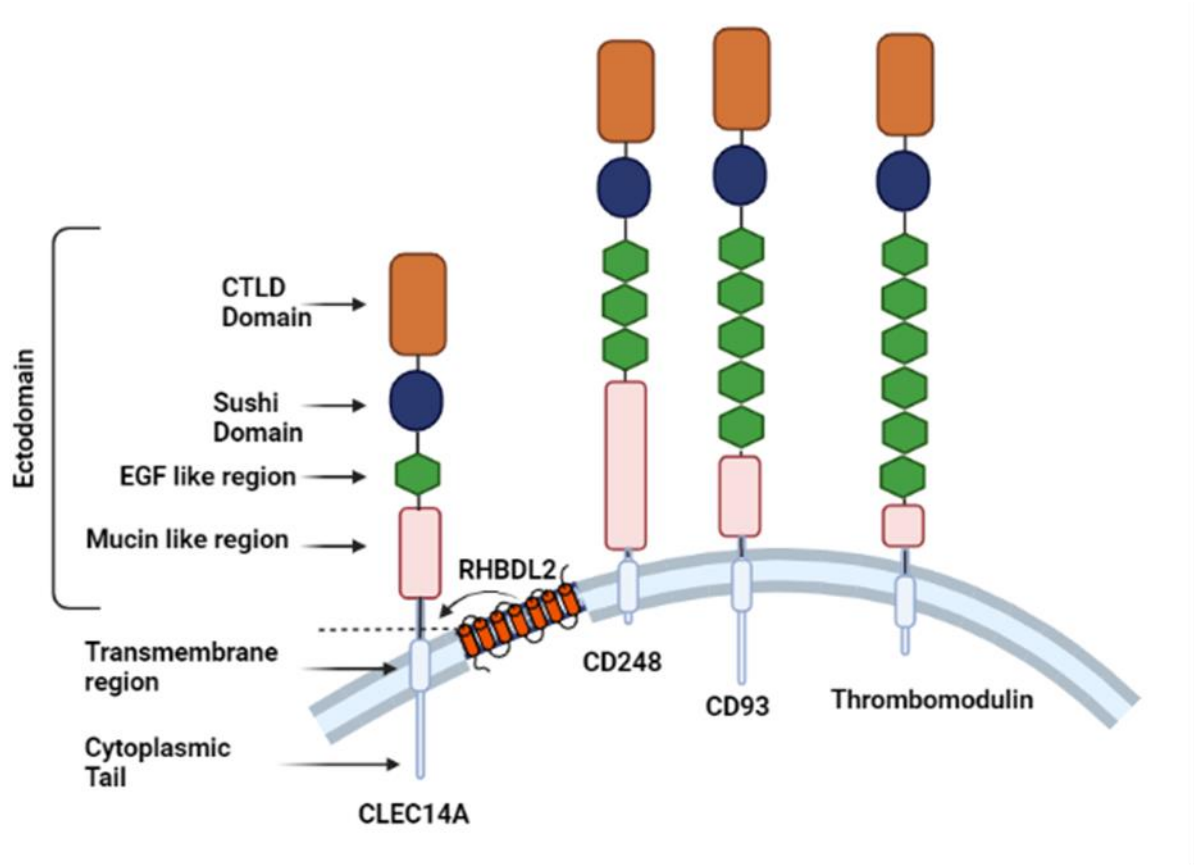

Figure 1.4: The structure of C-type lectin-domain (CTLD) group 14 family members. All the CTLD group 14 family transmembrane proteins share the same CTLD domain within the extracellular matrix denoted in brown, sushi domain in blue and EGF repeat in green. RHBDL2 cleaves CLEC14A along the transmembrane region releasing CLEC14A into the extracellular matrix to interact with ligands. Figure adapted from Khan K *et al.*, 2019 (57).

1.4.2 CLEC14A Expression and Functions in Endothelial Cells

Immunohistochemical staining and immunofluorescence imaging of CLEC14A revealed its expression in the tumour vasculature, but not in healthy vessels, indicating a potential role in tumorigenesis (67, 68). This is supported by the observation that CLEC14A knockout mice showed reduced growth of implanted tumours compared with wild-type mice (69). Moreover, CLEC14A was determined to be one of the signature regulators of tumour angiogenesis from a study looking at approximately 1000 tumour samples (70). This highlights CLEC14A potential as a clinical utility in being a reputable endothelial tumour marker (68) and its potential role in developing novel targeted cancer therapies (67, 69).

CLEC14A is involved in endothelial migration and tube formation. This is exemplified by small inhibitory RNA (siRNA) mediated knockdown of CLEC14A in HUVEC (Human Umbilical Endothelial Cells) resulting in reduced migration in a wound healing assay and impaired sprouting in spheroid assay compared to cells transfected with control siRNA duplex (67). In addition, HUVECs transfected with control siRNA were mixed with HUVEC treated with CLEC14A-specific siRNA, which resulted in less of the latter present at the sprout tips (69). As well as reduced growth of tumours in CLEC14a knockout mice (69), there was also reduced vascularisation of subcutaneously implanted sponges treated basic fibroblast growth factor (bFGF) compared with wild type mice (69).

1.4.3 CLEC14A Interacting Molecules

A number of CLEC14A interacting molecules have been identified including multimerin-2 (MMRN2), heparan sulphate, heat shock protein 70-1A (HSP70-1A) and VEGFR3 (58, 61, 71, 72).

MMRN2 is an endothelial expressed extracellular matrix protein which interacts with the CTLD domain of CLEC14A (69, 73). This matrix protein is also an inhibitor of the pro-angiogenic protein, vascular endothelial growth factor A (VEGF-A) (74). The coiled-coil region of MMRN2 was found to interact with the CLEC14A's CTLD. Replacing residues 97-108 of CLEC14A's CTLD with the analogous region from thrombomodulin (the only member of this family not to bind MMRN2) abrogated the binding to MMRN2. This indicated that MMRN2 interacts with the long-loop region of CLEC14A's CTLD with two cysteine residues within this region being necessary for interaction (61). Inhibiting the CLEC14A-MMRN2 interaction using specific blocking antibodies in HUVECs reduced tube formation and endothelial sprouting in HUVECs *in vitro* (69). I*n vivo,* CLEC14A-MMRN2 blocking antibodies injected into mice with Lewis Lung Carcinoma (LLC) resulted in a reduction in tumour size and weight and reduced vessel density compared to the control group (69). Another CLEC14A binding partner discovered using proteomics and verified by co-precipitation assay is HSP70-1A. Endothelial cell-cell contact, a key event in angiogenesis, was induced by CLEC14A interacting with HSP70-1A in a HUVEC-HUVEC adhesion assay (58). CLEC14A also interacts with the glycosaminoglycan heparan sulphate, which is an important component of eGCX (71). The CLEC14A-heparin binding site domain was mapped; Arginine 161 was

found to be a critical residue with its mutation to alanine significantly reducing its affinity to immobilized heparin in protein assays (71).

VEGFR3 is currently the only binding partner identified to interact with the intracellular domain of CLEC14A (Figure 1.5), though the critical residues within the cytoplasmic tail have not been mapped (57, 72). CLEC14A influences the expression levels and signalling of VEGFR2 and VEGFR3, which are essential for angiogenesis and lymphangiogenesis, respectively (72). Knocking down CLEC14A in ECs increased VEGFR3 signalling and supressed VEGFR2 signalling, with CLEC14A over-expression causing the reverse effect (72). This is of importance because VEGFR2 and VEGRF3 are important components of the junctional mechanosensory complex alongside VE-cadherin and PECAM (1, 25). Immunofluorescence microscopy revealed CLEC14A and VE-cadherin to be colocalised to cell-cell junctions (67).

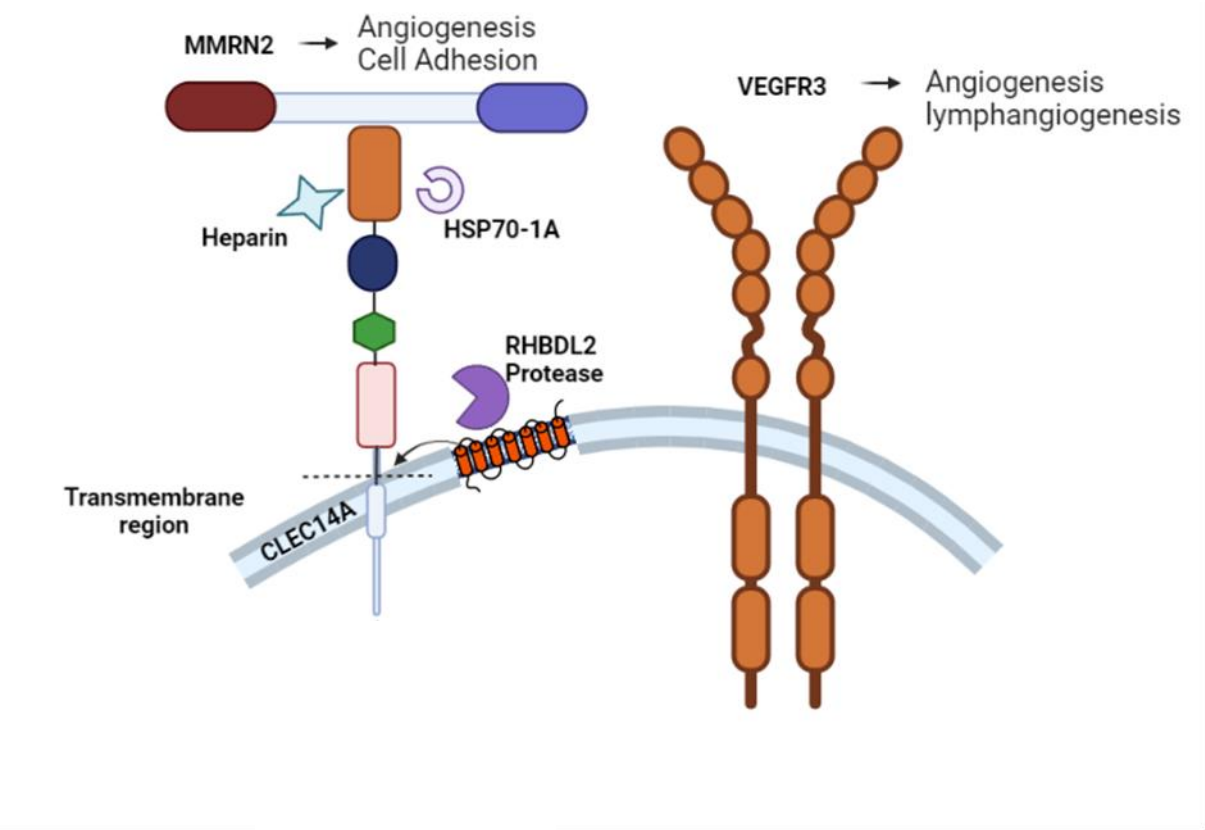

Figure 1.5: Schematic of CLEC14A and its binding partners. The extracellular ligands HSP70-1A and MMR2 interact with CLEC14A CTLD resulting in ERK phosphorylation/activation which promote angiogenesis. Arginine 161 in the CLEC14A CTLD domain is important for CLEC14A-heparin interaction and endothelial tube formation. The rhomboid protease enzyme RHBDL2 can cleave the extracellular domain of CLEC14A to regulate sprouting angiogenesis. The cleaved CLEC14A ectodomain can also bind to adhesion molecules encouraging aggregation. VEGFR3 is important in angiogenesis signalling and is known to interact with CLEC14A. Figure adapted from Kabir K *et al.*, 2019 (57) and Borah S *et al.*, 2019 (63).

1.4.4 CLEC14A and Endothelial Shear Regulation

Gene expression profiles generated from 5600 genes showed that only 379 genes were shear stress regulated in vascular endothelial cells (75). Interrogating SAGE (serial analysis of gene expression) libraries revealed CLEC14A to be one of the few shear-regulated genes involved in multiple cellular functions such as endothelial cell migration, adhesion, and angiogenesis (76, 77). *In vitro*, CLEC14A expression was reduced upon exposure to 2 Pa of shear stress compared with cells cultured under static conditions (67). In addition, CLEC14A shows very similar expression patterns to another endothelial shear regulated gene TIE1 which is a useful validated marker for low shear stress (67, 68). The shear stress regulation of CLEC14A expression may be connected with its interaction with partners such as VEGFR3 present within junctional mechanosensory complexes (25, 72). Alternatively, other ligands such as MMRN2 or heparin present within the extracellular eGCX may be involved in regulating its expression (61, 71). CLEC14A's shear regulation may also explain to some extent the upregulation of CLEC14A seen in vascularised tumours since tumour vessels are highly abnormal and characterised by non-uniform, low shear stress (68).

1.4.5 CLEC14A Role in Atherosclerosis

Increased CLEC14A expression was observed in atherosclerotic plaques. Bioinformatic analyses from the Stockholm Atherosclerosis Gene Expression (STAGE) study, which involved expression profiling of 1,092 individuals from different populations around the world, identified CLEC14A to be raised in atherosclerosis. CLEC14A expression was upregulated with increasing plaque size, being particularly pronounced in stenosed carotid arteries (78). Linkage analyses using the apolipoprotein E (ApoE) mice model of

atherosclerosis on two different mouse strain backgrounds demonstrated a locus containing *Clec14a* which was strongly linked to carotid plaque size (79). Though there is evidence linking CLEC14A to atherosclerotic plaques, nothing is known about its biological function in atherogenesis.

1.5 RhoJ GTPase

1.5.1 Overview of RhoJ

RhoJ is an endothelially expressed Rho GTPase, belonging to the Cdc42 (cell division cycle 42) subfamily of Rho GTPases (80, 81). These proteins function as molecular switches which modulate signal transduction pathways by cycling between active GTP-bound and inactive GDP-bound states (82, 83) (Figure 1.6). Rho GTPases are activated by guanine nucleotide exchange factors (GEFs) which mediate the exchange of GDP for GTP and their inactivation is facilitated by GTPase-activating proteins (GAPs) which promote the intrinsic GTPase activity of Rho proteins (80, 84). In their active GTP-bound state, Rho GTPases regulate cytoskeletal dynamics, cell polarity, cell proliferation, cell migration and apoptosis (82).

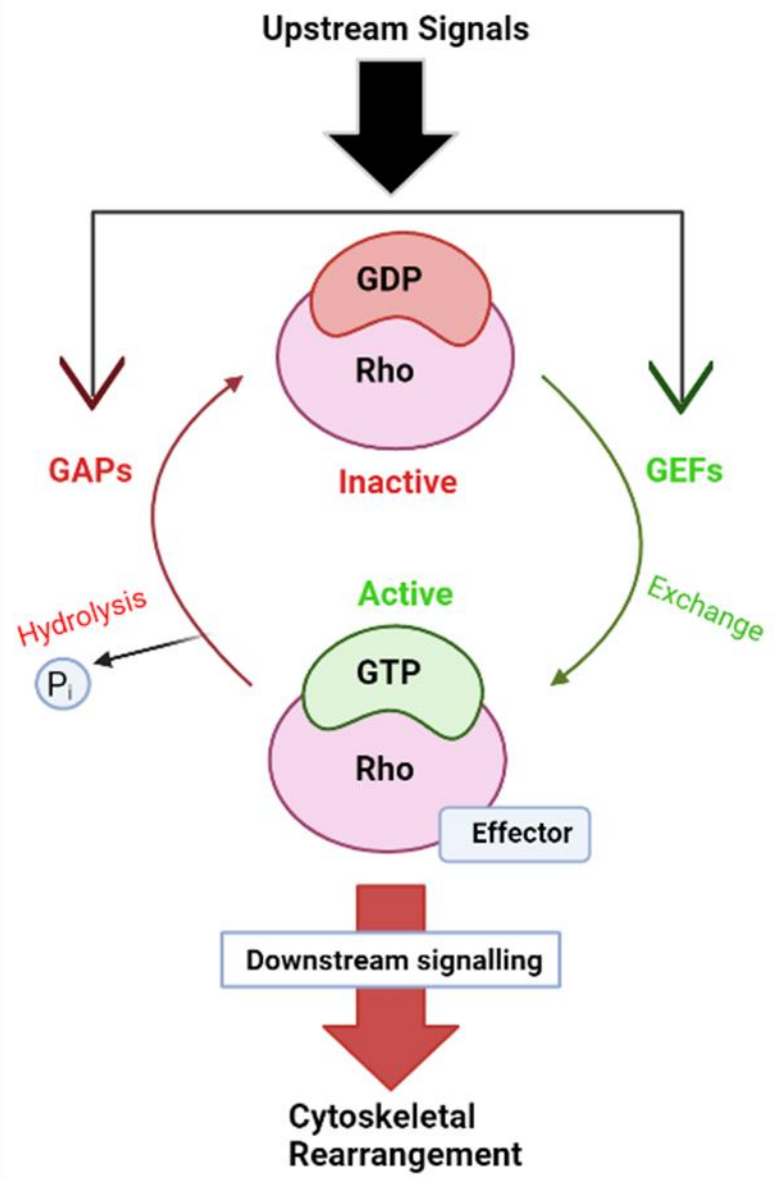

Figure 1.6: Overview of the Rho GTPase cycle and the activation of Rho proteins. GTPase proteins activated by GEFS facilitate the exchange of GDP for GTP. The binding of GTP causes a conformational change in RhoJ which results in activation of downstream effector signalling. Rho GTPases are deactivated by GAPS which promote the intrinsic hydrolysis activity of GTPases. The figure is adapted from Vadodaria K and Jessberger S, 2013, Kwanhyeong K *et al.*, 2019 (85) and Jaffe A and Hall A, 2005 (86).

1.5.2 Endothelial Functions of RhoJ

The endothelial expression of RhoJ has been noted in a number of studies. An early study identified that it was exclusively found in expression libraries from endothelial cells type, but not in those from other cell types (60). Subsequently, it has been localised to both normal and tumour vessels and expression has been noted in the intersegmental vessels in the mouse embryo (87, 88). At the cellular level, its expression is promoted by the transcription factor ERG (89).

A variety of functions of RhoJ in endothelial cells have been elucidated which play a role in angiogenesis and vessel stability. Manipulating the activity of RhoJ *in vitro* impacts tubulogenesis, cell migration and lumen formation, with RhoJ siRNA silencing causing inhibition of these processes (87, 89). *In vivo*, global knockout of RhoJ in mice results in viable organisms, but ectopically implanted tumours grew more slowly and are less vascularised (90). In another study tumour vessels were found to be abnormal – there was reduced vessel integrity, and this was associated with reduced metastasis (91). Transcriptomic studies of multiple tumours identified RhoJ as being part of a core tumour angiogenesis signature, underlining its potential importance in cancer (70). RhoJ knockout also impacted the development of the retinal and cephalic vasculature (92).

A variety of cellular functions of RhoJ have been identified with it having roles in regulating the cytoskeleton, cell polarisation and responses to migratory signals. Knocking down RhoJ expression in HUVECs resulted in increased actomyosin contractility and increased focal adhesion numbers, with expression of an active mutant of RhoJ showing the opposite effect.

The exact mechanism by which this occurs is not known but may be via RhoJ's interaction with the GIT-PIX complex (90), a protein complex known to regulate focal adhesion disassembly (93). RhoJ has also been found to mediate cell trafficking, it co-localised with the actin regulator Formin Like 3 (FMNL3) and facilitated the movement of the glycocalyx glycoprotein podocalyxin to the apical cell membrane. This is a crucial initial step in lumen formation (94). The $\alpha5\beta1$ integrin is another protein whose trafficking is regulated by RhoJ, with RhoJ knockdown associated with increased levels of this integrin at the plasma membrane and enhanced deposition of fibronectin fibrils (95). Interestingly, increased activation of this integrin and ensuing fibronectin fibrillogenesis contributes to the pathology of atherosclerosis (96) and so this may be a way in which RhoJ can impact the pathology of this disease. RhoJ is also involved in regulating responses to migratory signals and is involved in mediating the composition of a receptor complex comprising VEGFR2, Neuropilin1 and PlexinD1. VEGFR2 is the receptor for VEGFA and is an attractive signal while PlexinD1 is the receptor for Semaphorin (Sema) E3 which is a repulsive signal. When VEGFA levels are high, RhoJ promotes association of this complex enabling sustained activation of VEGFR2 signalling and forward migration. By contrast, high levels of Sema E3 cause RhoJ to be released from this complex downregulating VEGF signalling and cell contraction (92, 97). Thus, RhoJ plays multiple roles in regulating the cell biology of endothelial cells and these all contribute to RhoJ's function in promoting vessel stability and angiogenesis.

While there is considerable literature on RhoJ in relation to cancer, little is known about RhoJ's involvement, if any, in atherosclerosis. Its expression is repressed by the constitutive

expression of the shear responsive transcription factor KLF2 (37), suggesting that RhoJ would be at low levels in endothelium experiencing laminar flow. As noted above RhoJ regulates the endothelial cytoskeleton and this has been shown to impact the transmigration of neutrophils, with RhoJ knockdown impeding the motility of transmigrated neutrophils (98). Since leukocyte migration has an important role in the pathogenesis of atherosclerosis (99) it is possible that RhoJ activity may impact this process.

1.6 Hypotheses and Aims

Our laboratory group has shown that the ectopic expression of CLEC14A suppresses EC responses to shear stress by repressing the upregulation of atheroprotective KLF-2 and the downregulation of proinflammatory genes. This suggests a possible role of CLEC14A in the shear sensing mechanism and regulation of shear responsive genes. This has led to the following hypothesis:

CLEC14A plays an important role in mediating endothelial shear stress responses and that the intracellular domain and ligand-binding regions are essential in this process.

The first aim of this thesis is to better understand how CLEC14A regulates endothelial shear responses. This was investigated by using lentiviral transduction to introduce a range of mutant forms of CLEC14A into primary ECs. These were then subjected to laminar shear stress using an orbital shaker system and quantitative PCR was used to assess the level of transcription of shear regulated genes.

Microarray analyses suggest that RhoJ is shear regulated and overexpression of KLF2 represses RhoJ expression (37) suggesting that RhoJ may potentially regulate endothelial shear responses of KLF2 and RhoJ's role in regulating the cytoskeleton may affect shear mediated cell alignment. Thus, the hypothesis investigated in relation to this was:

RhoJ expression is indeed shear regulated and these shear responses are important in regulating KLF2 expression and KLF2-mediated cell alignment.

The second set of aims of this thesis is to confirm shear stress regulation of RhoJ by subjecting ECs to laminar shear stress and measuring RhoJ RNA and protein expression by qPCR and western blotting, respectively. siRNA-mediated knockdown of RhoJ was used to determine if the protein had any impact on shear-mediated expression of KLF2 as determined by qPCR. Finally, the effect of knocking down RhoJ on endothelial alignment under shear stress was investigated using microscopy and image analysis.

The third aim of this thesis was to interrogate bioinformatic databases related to shear stress, atherosclerosis, and endothelial biology for CLEC14A and RhoJ expression to better understand how different stimuli and cellular conditions affect the expression of these genes to determine how their expression may be altered in atherosclerosis.

Chapter Two

Materials and Methods

2 Materials and Methods

Materials

All chemicals used in these studies were purchased from Sigma-Aldrich unless otherwise stated. The composition of buffers used in experiments is stated in Table 2.1. siRNA duplexes are listed in Table 2.2, primary antibodies in Table 2.3, secondary antibodies in Table 2.4 and qPCR primers in Table 2.5.

Table 2.1: Various buffers and solutions used in this project

1× Phosphate-Buffered Saline (PBS)	10 mM Na_2HPO_4, 1.76 mM KH_2PO_4, 2.7 mM KCl, 0.14 M NaCl, pH 7.4
NP40 Lysis Buffer	1% (v/v) NP40, 10 mM Tris pH 7.5, 150 mM NaCl, 1 mM EDTA pH 8, 0.01% (w/v) Sodium Azide, Mammalian protease inhibitor cocktail
2× SDS-PAGE loading sample buffer	100 mM Tris-HCl, pH 6.8, 20% (v/v) Glycerol, 20% (v/v) β-mercaptoethanol, 4% (w/v) SDS, 0.2% (w/v) Bromophenol blue
1 x Stacking gel buffer	125 mM Tris-HCl pH 6.8, 0.1% (w/v) SDS
1 x Resolving gel buffer	375 mM Tris-HCl pH 8.8, 0.1% (w/v) SDS
1× SDS-PAGE running buffer	25 mM Tris, 250 mM Glycine, 0.1% (w/v) SDS, pH 8.3
1× Transfer buffer for western blotting	6 mM Tris-base, 47.6 mM Glycine, 20 % (v/v) Methanol, pH 8.3
Tris-Buffered Saline Tween- 20 (TBST)	20 mM Tris-HCl, pH 7.5, 150 mM NaCl,

	0.1% (v/v) Tween-20
Blocking buffer for Western Blot	5% (w/v) Dried skimmed milk in TBST
FACS buffer	PBS, 0.1% (v/v) NaN_3 1% (w/v) BSA

Table 2.2: Sequence of SiRNA duplex and target region of gene

siRNA duplexes	Sequence	Target region	Source
RhoJ duplex 2	5'-agaaacctctcacttacga-3'	Human RhoJ 455- 474	Eurogentec, UK
Negative Control Duplex	Undisclosed	Non-specific to human gene sequence	Eurogentec, UK

Table 2.3: Primary antibodies used for flow cytometry and western blotting

Antibody	Working Concentration	Application	Supplier
Mouse IgG negative control	0.5 mg/mL	Flow Cytometry	Sigma Aldrich
Purified Mouse Antibody to CLEC14A	0.5 mg/mL	Flow Cytometry	Sigma Aldrich
Rabbit monoclonal anti-human Tubulin	1/1000	Western Blotting	Cell Signalling Technology
Mouse monoclonal anti-human RhoJ	1 µg/mL	Western Blotting	Abcam

Table 2.4: Secondary antibodies used for flow cytometry and western blotting

Antibody	Working Concentration	Application	Supplier
Anti-mouse antibody conjugated to HRP	1:5000	Flow Cytometry	Abcam
Anti-rabbit antibody conjugated to HRP	1:5000	Western Blotting	Cell Signalling Technology
Anti-mouse antibody conjugated to HRP	1:5000	Western Blotting	Abcam

Table 2.5: Primer sequences of various genes quantified through qPCR and annealing temperatures used. *Probes are from the Roche Universal probe library

Gene	Sequence	Annealing Temperature	Probe*	Supplier
β-Actin	5'-TCACCCACACTGTGCCCATCTACGA-3' 5'-CAGCGGAACCGCTCATTGCCAATGG-3'	58°C	N/A	MWG / Eurofins
18S	5'-TAA CGA ACG AGA CTC TGG CAT-3' 5'-CGG ACA TCT AAG GGC ATC ACA G-3'	58°C	N/A	
KLF2	5'-GCAAGACCTACACCAAGAGTTCG-3' 5'-CATGTGCCGTTTCATGTGCAG-3'	59°C	N/A	
MMRN2	5'-AGGCTTCCAGTACTAGCCTCTCT-3' 5'-GGTAGGGGCACCAGTTACG-3'	59°C	N/A	
CXCR4	5'-GCCCTCCTGCTGACTATTCC-3' 5'-GGCAGGATAAGGCCAACCAT-3'	58°C	N/A	
GFP	5'-AAGCTGACCCTGAAGTTCATCTGC-3' 5'-CTTGTAGTTGCCGTCGTCCTTGAA-3'	58°C	N/A	
RhoJ	Fwd:"AAACCCTGCCTCTTACCACA" Rev:"CATCACGGAGATCAATCTGG"	58°C	79	Eurogentec

2.1 Cell Biology

2.1.1 Cells and Media

Pooled human umbilical vein endothelial cells (HUVECs) were purchased from Promocell and were used between passage 2 and 6. These were cultured in complete M199 (cM199) which was made from a mixture of basal media (M199, Sigma), $NaHCO_3$ (2.21 g per 1L of media), 10% (v/v) Foetal Bovine Serum (FBS) (Gibco), 4mM L-glutamine 2.5mL (Sigma) and endothelial growth medium 2 supplement mix (PromoCell). CM199 medium was sterile filtered using 0.22µm pore filter (Corning), aliquoted and stored at 4°C. The immortalised cell line, Human embryonic kidney 298T cells (HEK 298T), were cultured using Dulbecco's Modified Eagle's Medium (DMEM, Sigma) which was supplemented with 10% (v/v) FBS and 4mM L-glutamine as noted above for CM199. EGM-2 (Endothelial Cell Growth Medium 2) was purchased from Promocell and was used to replace cM199 medium in the 6 well plates

prior to orbital shaker use. Culture medium was warmed up to room temperature before use.

2.1.2 Cell Passaging

Cell culture was performed inside a sterile laminar flow hood and cells were incubated at 37°C, 5% (v/v) CO_2 in a humidified incubator (Sanyo). Where necessary, cells were cryopreserved in 90% (v/v) FBS and 10% (v/v) dimethyl sulphoxide (Sigma), and after thawing they were washed with complete media prior to plating. HUVECs were cultured on gelatin-coated plates, prepared by coating sterile 10 cm dishes (Corning) with 0.1% (w/v) porcine gelatin in PBS for at least 20 mins at room temperature. To passage both HEK298T cells and HUVECs, cells were first washed in PBS and then incubated in 0.25% Trypsin/1 mM EDTA (ThermoFisher Scientific) until detachment, at which point the trypsin was neutralised with complete medium and cells were centrifuged at 350 × g for 5 mins and either passaged or used in experiments. Where necessary, cells were counted using a haemocytometer.

Typically, HUVECs were grown to 80-90% confluence and then passaged by diluting 1 in 3 and HEK298T cells were grown to confluence and passaged by diluting 1 in 10. The volumes of medium to resuspend cells were determined by the size of the plates.

Table 2.6: Volumes of 0.1% (w/v) porcine gelatin coating solution in PBS and media required to plate HUVECs and HEK298T cells onto various plate sizes

Plate Size	HUVEC			HEK298T
	Gelatin	cM199 media	EGM-2	cDMEM media
6 Well Plate (per well)	1 ml	2 ml	1.5 ml	NA
6cm Dish	2 ml	3 ml	N/A	3 ml
10cm Dish	4 ml	10 ml	N/A	10 ml

2.2 Lentiviral Transduction of HUVEC

2.2.1 Plasmids

CLEC14A plasmids were constructed by Dr Victoria Heath (unpublished). These and the lentiviral packaging plasmids used in this study are listed in Table 2.7.

Table 2.7: Description of the plasmids as well as the various transfer plasmids used to carry DNA genetic information of the four mutant constructs of CLEC14A to create the four conditions of CLEC14A in HUVECs using lentivirus transduction technology

Plasmid	Description	Source
psPax2	2nd Gen Lentiviral Packaging Plasmid	Addgene
pMD2G	2nd Gen Lentiviral Packaging Plasmid	Addgene
pWPXL- WT CLEC14A-P2A-GFP	CLEC14A over-expression construct	Dr Victoria Heath University of Birmingham (unpublished
pWPXL-CLEC14A THRM B-P2A-GFP	CLEC14A- 97-108 amino acids switched to thrombomodulin (THBD), so CLEC14A binding to MMRN2 ligand is impaired	

pWPXL-CLEC14A R161A-P2A-GFP	Impaired heparin binding CLEC14A construct to prevent heparin ligand binding to CLEC14A by switching Arg161 (R161A) to alanine	
pWPXL-CLEC14A No ICD-P2A-GFP	CLEC14A construct with intracellular domain removed	

The constructs were designed so that CLEC14A has a C-terminal myc tag followed by the sequence encoding the P2A self-cleaving peptide and then GFP (Figure 2.1A). The use of the self-cleaving peptide ensured that GFP and CLEC14A expression were proportionate to each other, allowing detection of successful transduction through florescence microscopy and flow cytometry analysis.

2.2.2 PEI Plasmid Transfection

A day prior to transfection 1×10^6 HEK298T cells were plated on 6 cm plates in 3mL cDMEM for production of lentivirus to infect HUVECs. Cells were transfected with a combination of 1.5 µg transfer plasmid (pWPXL based), 1.1 µg psPAX2, 0.43 µg pMD2G, 300 µL Optimem serum-free medium (Invitrogen, UK) and with 12 µL of 1 mg/mL polyethylenimine (PEI) solution (Sigma-Aldrich). After gently vertexing, the mixture was left for 10 minutes to incubate at room temperature to form DNA/PEI complexes which were then added to the HEK298T cells, gently tilting it to distribute in the plate. The plates were incubated at 37°C, 5% CO_2 for 24 hours in the humidified 37°C incubator (Sanyo) to allow production of

lentivirus. Safety Guidelines for Working with Lentiviruses document produced by the University were adhered to at all times.

2.2.3 HUVEC Transduction

One day before transduction, 4 x 10^5 HUVECs at passage 2 were plated onto 6 cm plates coated with 0.1% (w/v) gelatin in PBS in 3 mL CM199 medium. For each transduction a mix consisting of 400 µL CM199 media, 75 µl Endothelial Growth Medium 2 supplement (Promocell) and 24 µL Polybrene (Sigma) at 8 µg/mL was created. The lentivirus containing-media from the transfected HEK298T plates was passed through a 0.45 µL filter (Corning) and added directly to the supplement/polybrene mix. This was then placed on plated HUVECs, having first removed the HUVEC media in which they were growing. HUVECs were incubated with the lentivirus at 37°C for 24 hours inside a humidified incubator. After 24 hours the lentiviral media was removed, cells were expanded into a 10 cm dish and incubated with CM199, and after a further 3 days levels of transduction were analysed by flow cytometry and these cells were used in experiments. The lentivirus containing media from the HEK298T cells transfected with control pWPI plasmid (GFP) was diluted 1 in 4 with CDMEM prior to use to reduce the titre of lentivirus and give a similar GFP fluorescence seen in other HUVEC samples transduced with CLEC14A containing transfer plasmids. The protocol for lentivirus transduction of HUVECs is shown in Figure 2.1B.

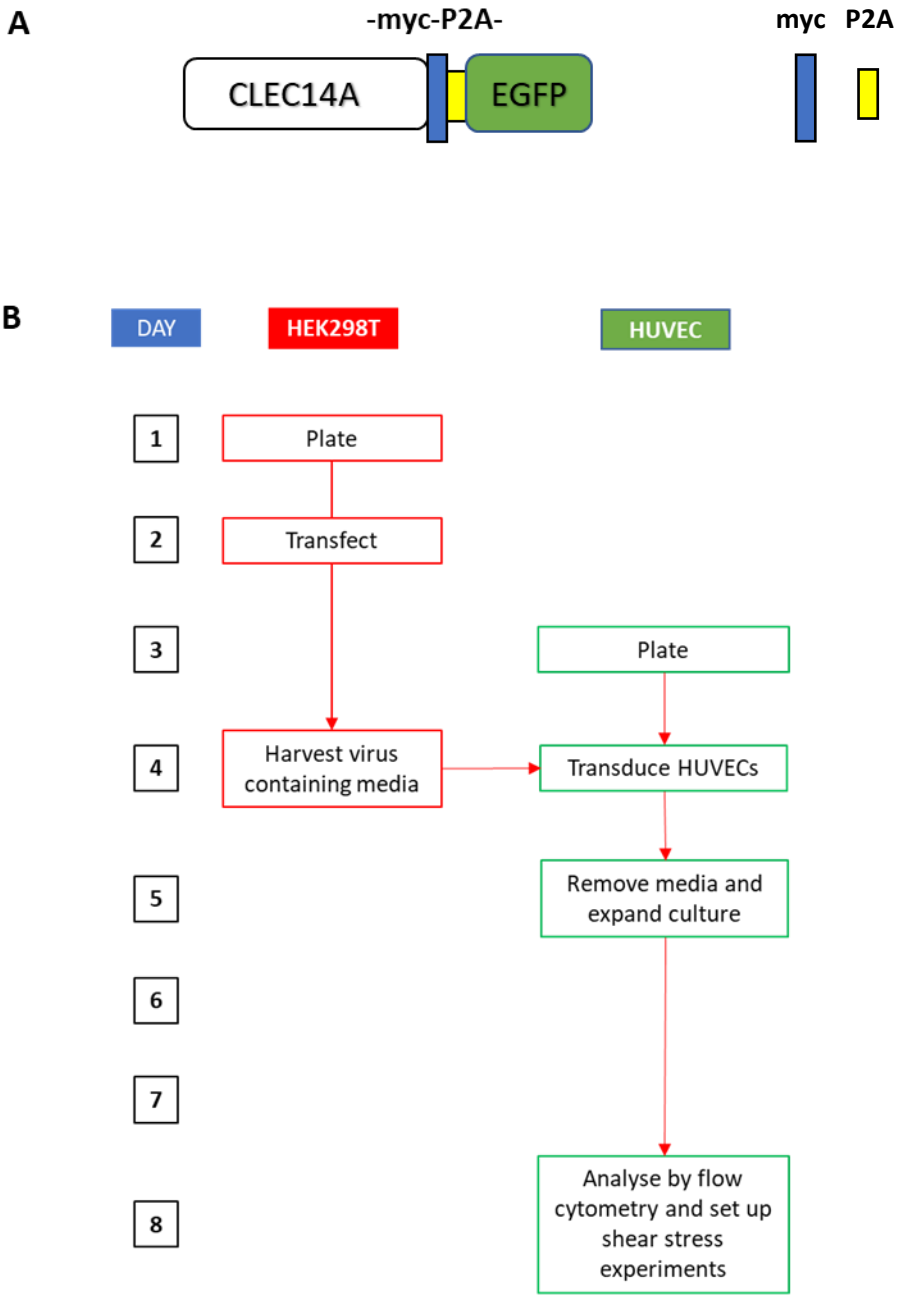

Figure 2.1: Schematic of the mutant CLEC14A transfer plasmid and the HUVEC transduction protocol. A) The transfer plasmids comprised of CLEC14A sequence attached to Myc tag linked to GFP and separated by a self-cleaving peptide sequence. B) Flowchart schematic showing the HUVEC lentiviral transduction protocol.

2.3 Validation of HUVEC Transduction

2.3.1 Flow Cytometry

Quantitative assessment of transduction was done using flow cytometry which enabled the percentage of transduced HUVEC cells emitting GFP fluorescence to be determined, using the untransduced cells to set the gate as a negative control. HUVEC cells were trypsinised and resuspended in cM199 and flow cytometry (CyAn ADP, Beckman Coulter) was performed. The Flowing Software (Turku Bioscience) was used to analyse flow cytometry data.

2.3.2 Cell Staining for Flow Cytometry

HUVEC lysate pellets were trypsinised and first resuspended in 100 µL of Fc block (1:100; Miltenyi Biotech) diluted in FACS buffer to block Fc receptors. Cells were washed once with 1mL FACS buffer and the cell pellets were resuspended in 100 µL of mouse IgG (Sigma-Aldrich) or anti-CLEC14A (CRT2) (61) both diluted in FACS buffer and at a concentration of 10 µg/mL and incubated for 30 minutes on ice. Then cells were washed twice using 1mL of FACs buffer and finally resuspending anti-mouse immunoglobulin conjugated to Alexa647 (1:200; Invitrogen). The cells were incubated for a further 30 minutes on ice before diluting in FACS buffer and analysing by flow cytometry as outlined above. Live cells were gated using forward and side scatter, GFP positive cells were then gated and analysed for fluorescence of the Alexa 647 fluorophore.

2.4 Preparing Transduced HUVEC for Orbital Shaker

The transduced HUVECs were replated onto four 0.1% (w/v) gelatin in PBS coated 6-well plates in duplicate at a cell density of 250,000 HUVECs in 1mL Endothelial Cell Growth Medium 2 (EGM-2) media (Promocell). Two plates were used for static control and kept in 37°C humidified incubator (Sanyo) for 72 hours. The other two plates were transferred to 37°C, 5% CO_2 humified orbital shaker incubators which was set to induce the HUVEC plates to 1.1 Pa of pulsatile laminar shear stress.

2.5 Transfection of HUVEC with siRNA duplexes

To silence RhoJ expression HUVECs were transfected with small interfering RNA (siRNA) duplex (Eurogentec, UK), specifically siRNA D2 was used (87). As a control, a negative control duplex (NCD, Eurogentec, UK) was used. A day before transfection, 300,000 HUVEC cells were plated per well of a gelatin coated 6-well plates (Corning) in cM199 media. The transfection the next day involved initially making up two mixes, the volumes given are for each well transfected and result in a final siRNA concentration of 20nM. The first mix was made up with 0.5µL of siRNA duplex stock solution (20µM) diluted in 169.5µL OptiMEM (Invitrogen, UK) and the second was 3µL of Lipofectamine RNAiMAX (Invitrogen, UK) added to 27µL OptiMEM (Invitrogen). Both mixes were incubated at room temperature for 10 minutes, then they were combined, mixed gently, and incubated for a further 10 minutes at room temperature. Meanwhile the HUVECs to be transfected were washed twice with PBS, before adding 800µL optiMEM media (Invitrogen, UK). After the incubations the transfection mix was added dropwise to the cells and the plates were tilted to distribute the mix evenly. Plates were incubated for 4 hours in humidified incubator at 37°C, 5% CO_2, after

which time the transfection mix was aspirated and replaced with cM199. After 24 hours of transfection CM199 media was replaced with 1.5mL EGM-2 (Promocell) medium per well and plates were placed in 37°C, 5% CO_2 humified orbital shaker incubator or standard incubator (Sanyo). Experimental assays were performed after 24 hours to ensure maximal knockdown efficacy.

2.6 Image Analysis

Incucyte® Live-Cell Analysis System (Sartorius) was used to image cell plates after subjecting RhoJ knockdown and NCD control HUVEC sample plates to static or 24 hours orbital shear. The machine captured 81 image views at a magnification of ×10 in a layout that allowed objective analysis across all plate conditions. For cell alignment analysis the centre top (field 5) and centre bottom (field 77) fields of view were analysed for horizontal alignment using an open-source image processing program called ImageJ (National Institutes of Health). The images were converted to 32 bit and thresholded to give greater contrast of the cell margins. The OrientationJ plugin of ImageJ was used to count the distribution of HUVECs across many degrees of orientation. This provided data that was then analysed and plotted on Microsoft Excel/GraphPad Prism 9.3.1.

2.7 RNA Analysis

2.7.1 RNA Isolation and Purification

RNA was harvested from wells by first adding 175 µL of RL RNA Lysis Buffer (Total RNA plus kit, Norgen Biotek, Canada) per well and pipetting up and down to disrupt the cells. The

wells were set up in duplicate and the lysates from each were combined to give an overall volume of 350 µL, which were stored at -20°C freezer until processing and extraction of total RNA plus kit (Norgen Biotek, Canada). The cell lysates were thawed, mixed, and pulsed down before starting. The first stage involved removal of genomic DNA using DNA removal columns which retained genomic DNA and allowed RNA to flow though into collection tubes after centrifuging lysates at 12,000 × g spin for one minute. The RNA isolation proceeded according to the manufacturer's instructions and finally RNA was eluted in 50 µl of elution solution. The RNA concentration (ng/µL) was measured using a Nanodrop (Thermo-Scientific).

2.7.2 cDNA Synthesis

cDNA was synthesized from 2 µg of total RNA using the High Capacity cDNA Archive kit (Applied Biosystems). The volume of RNA required to give 2 µg was calculated and this was diluted with RNase-free water to make up 10 µL. This was then added to 10 µL of reaction mix made up of 2 µL 10 × RT buffer, 0.8 µL of 25 × dNTP, 2 µL of 10 × random primers, 1 µL of reverse transcriptase and 4.2 µL RNase-free water. After mixing, reactions were placed in a thermal cycler for 10 minutes at 25°C and then for 2 hours at 37°C. cDNA samples were then stored at -20°C until being used for quantitative PCR.

2.7.3 Quantitative Real-Time PCR

Real time quantitative PCR (qPCR) was performed using DNA- binding fluorescent dye SYBR green to quantify gene of interest (GOI) after each cycle on The Applied Biosystems® 7500 Fast Real-Time PCR System machine. A 6.5 µL reaction mix was made per well/reaction,

which consisted of 5.5 µL reaction mix and 1 µL cDNA (diluted 1 in 10 with RNase-free water). The reaction mix/well consisted of 0.048 µL of 50 µM oligo mix (forward and reverse primer – Table 2.5) 3.25 µL Fastgene 2× qPCR universal Mix (Nippon Genetics, Japan), 2.2 µL PCR grade water and 1 µL cDNA per PCR reaction. Primers were designed using Primer-BLAST (100) and the efficiency of primers was analysed by the melting curve produced by the machine. The housekeeping reference genes used were 18S primers (Eurofins Genomics) and β-Actin (MWG/Eurofins). The RhoJ qPCR used a probe-based system, and the reaction mix was adjusted to account for probe using 3.25 µL of 2X Reaction buffer, 0.066 µL of probe, 0.26 µL primers mix (10 µM), 1 µL cDNA and 1.9 H_2O to make up to 6.5 µL. The standard reaction cycle conditions used were as follows: initial denaturation at 95°C for 10 min, followed by 40-45 cycles of 95 °C for 15 seconds, annealing temp (optimised for each primer set – Table 2.5) for 15 seconds and extension at 72°C for 20 seconds. The qPCR reactions were performed in triplicate and replicates within 1 cycle (Ct) were used to calculate the mean, discarding Ct outliers. The Ct values obtained from the machine system were normalised to reference to calculate relative gene expression. The $2^{-\Delta\Delta CT}$ Livak method (101) was then used to calculate fold change for the GOI relative to the static control. Relative expression was calculated using ΔCT values from subtracting each reference control genes mean CT values for each sample from corresponding mean CT values of target GOI. Then ΔΔCT is calculated by subtracting ΔCT of Target Gene by the ΔCT of the Static Control.

2.8 Protein Analysis

2.8.1 Protein Extraction

Cellular lysates were prepared from HUVEC cultures to enable evaluation of protein expression. HUVECs were first washed with PBS and then the cells scraped with the aid of a cell scraper in 1 mL of PBS. The cell pellet was spun down in a micro-centrifuge at 5000 × g for 2 min and then resuspended in ten pellet volumes of NP40 lysis buffer supplemented with protease inhibitor (Sigma). The cells were disrupted both by pipetting and they were then vortexed and incubated on ice for 30 minutes. The cell lysate was centrifuged at 14,000 × g for 10 minutes at 4 °C. The supernatant, which was the cell lysate, was removed. A small volume was reserved for measuring the protein concentration using the bicinchoninic acid assay (BCA assay; Sigma) according to the manufacturer's instructions. To the remainder an equal amount of 2× Sample Buffer was added, and samples were stored at -20°C.

2.8.2 SDS Polyacrylamide Gel Electrophoresis (SDS-PAGE)

Polyacrylamide gels was prepared using the mix described in Table 2.8 using gel cassettes which were used in conjunction with the XCell SureLock™ Mini-Cell electrophoresis tank (Thermofisher). Before loading onto the gel, protein samples in sample-loading buffer were boiled at 95°C for 5 minutes. 10-20 µg of protein exptract was loaded onto the polyacrylamide gel, as was the PageRuler Plus Prestained Protein Ladder (Thermo Scientific) Initially the voltage was set to 100V and was increased to 130 V once the proteins had migrated into the separating gel.

Table 2.8: The volumes of each component used to make up the SDS-Polyacrylamide gel

5% Stacking gel (2 mL volume)	
Solution Component	**Component volume (mL)**
H_20	1.4
30% Acrylamide mix	0.33
1× Stacking gel buffer: 1.0 M Tris (pH 6.8) + 0.1% SDS	0.25
10% Ammonium Persulfate	0.02
TEMED	0.002

12% Resolving gel (10 mL volume)	
Solution Component	**Component volume (mL)**
H_20	3.3
30% Acrylamide mix	4
1× Resolving gel buffer: 1.5 M Tris (pH 8.8) + 0.1% SDS	2.5
10% Ammonium Persulfate	0.1
TEMED	0.004

2.8.3 Western Blotting

Proteins were transferred on to polyvinylidene difluoride membrane using the XCell II™ Blot Module. The membrane was first activated with 100% methanol for 30 seconds and then both it and the gel were soaked in transfer buffer before setting up the transfer. The voltage was set at 30 V and the protein transfer phase was done for 2 hours at 4°C. To assess the protein transfer, the membrane was placed in the Ponceau S stain (Sigma) for 1-2 minutes before destaining in dH_2O. The membrane was then blocked using 5% (w/v) skimmed milk powder in TBST with gentle agitation at room temperature for 1.5 hours. The membrane was then rinsed in TBST and incubated overnight at 4°C in primary antibody diluted in 3 % (w/v) BSA in TBST. The membrane was then washed with TBST for 30 minutes changing the buffer every six minutes before application of secondary antibody diluted in blocking buffer and incubation for two hours at room temperature. Then the membrane was washed again with TBST for five times every six minutes, before developing the membrane with enhanced chemiluminescent substrate (ECL; Geneflow) after leaving for 5

minutes to equilibrate. Within the dark room chemiluminescence was detected after exposure of the membrane with the Hyperfilm-ECL high performance chemiluminescence film (Thermofisher). Films were scanned and densitometry was performed using ImageJ software.

2.9 Bioinformatics Methods

2.9.1 Database Analysis

The Gene Expression Omnibus (GEO) Database is an international public repository that archives raw and processed mRNA expression data generated from various high throughput gene expression studies (102). These studies include the use of technologies such as DNA microarrays, protein arrays, high-throughput nucleic acid sequencing and qPCR which measure the relative or absolute levels of mRNA and genomic DNA (103). This global resource allows researchers to share data as well as replicating the experiments and interpretating the data (102). GEO database is supported by the National Centre for Biotechnology Information (NCBI) and is available for free download through the website http://www.ncbi.nlm.nih.gov/geo/.

2.9.2 Data Searches and Data Acquisition

The pipeline for analysing the gene expression analysis data is depicted in Figure 2.2. While each gene expression database study can be located through its unique accession number ID through the GEO search engine, this study involved identifying studies of interest by inputting key words into the GEO Search engine. For this thesis, databases were located using key words selected based on three over-arching themes: “atherosclerosis”, “shear

stress" and "endothelial biology". From the searches 72 gene expression databases were downloaded. All the data files were compressed into a ZIP folder and downloaded as a Simple Omnibus Format in Text (SOFT) file. A SOFT file is a line-based, plain ASCII text format which allows all the database to be downloaded as a single file (103). The data was downloaded in July/August 2021.

2.9.3 Data Unpacking and Annotating

To process the data, the specialized programming software R (Version 4.0.5) was used to open and convert the SOFT file format to make the data ready for upload and manipulation in Excel and GraphPad Prism (Figure 2.2). Two types of SOFT files were used for bioinformatics analysis: GEO Dataset (GDS) or GEO Series (GSE). Both GDS and G SE SOFT files contained the "VALUE" column for each gene per sample but only GSE SOFT files contained the annotation files that were important in labelling data values to corresponding gene symbols. For GDS files the gene ID identity column was automatically converted to corresponding gene symbol upon downloading further programming packages in R. First the file was converted to an exprSet file using the Bioconductor package (GEOquery). Then the conversion toolset g:Profiler package was downloaded and installed which provided access to many annotation data sources without need to download GEO Platform annotation (GPL) files. The algorithm commands used to install GEOquery on R were found on the following website link https://www.bioconductor.org/packages/release/bioc/html/GEOquery.html, and the g:Profiler package was downloaded from the CRAN repository https://cran.rproject.org/web/packages/gprofiler2/index.html (104).

2.9.4 Database Selection

Databases were interrogated to see if they contained a dataset for CLEC14a/A or RhoJ. 44 databases contained data for CLEC14a/A and RhoJ which were carried forward in the analysis pipeline. Out of these 44 databases for CLEC14a/A, there were two shear stress studies, 12 on atherosclerosis and 30 studies relating to endothelial biology. For RhoJ, there were two shear stress studies, 11 on atherosclerosis and 31 on endothelial biology.

These databases were then filtered on basis of data change or no change using a pre-set criterion. Change was determined to be a relative fold change greater than 1.5 or a statistically significant change as assessed by a paired t-test ($P<0.05$). When accounting for studies that showed change for CLEC14a/A datasets there were two shear stress studies, nine atherosclerosis studies and 16 studies relating to endothelial cell biology (Figure 2.3). RhoJ datasets that showed change were present in two shear stress, seven atherosclerosis and 18 endothelial cell biology studies (Figure 2.4). Although differences were found in multiple databases, only studies that were related to the thesis title were carried forward. These were a subset of databases deemed to be most relevant to shear stress, atherosclerosis, and gene expression regulation.

2.10 Data Analysis

Statistical analysis was performed using GraphPad Prism and results were represented as the Mean±Standard Error of the mean. To calculate statistically significant differences between 3 or more group means a one-way ANOVA was performed and a post-hoc Tukey analysis done to compare individual group means for statistical significance. A paired t-test

was also used to test statistical significance between paired sample measurements. The threshold set for statistical significance was P≤0.05. Statistical significance was denoted as *=P≤0.05, **=P≤0.01 highly significant result and ***=P≤0.001 indicating an extremely statistically significant result.

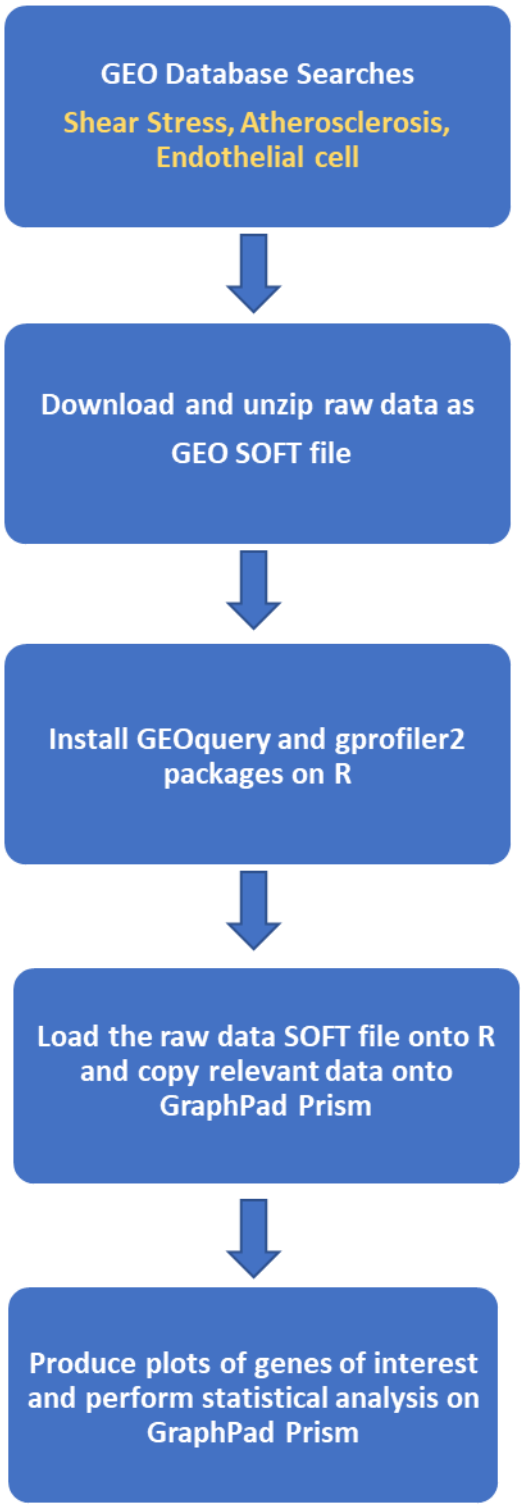

Figure 2.2: Schematic flowchart to summarise the built-in process for bioinformatic data collection, process and analysis of CLEC14A and RhoJ datasets

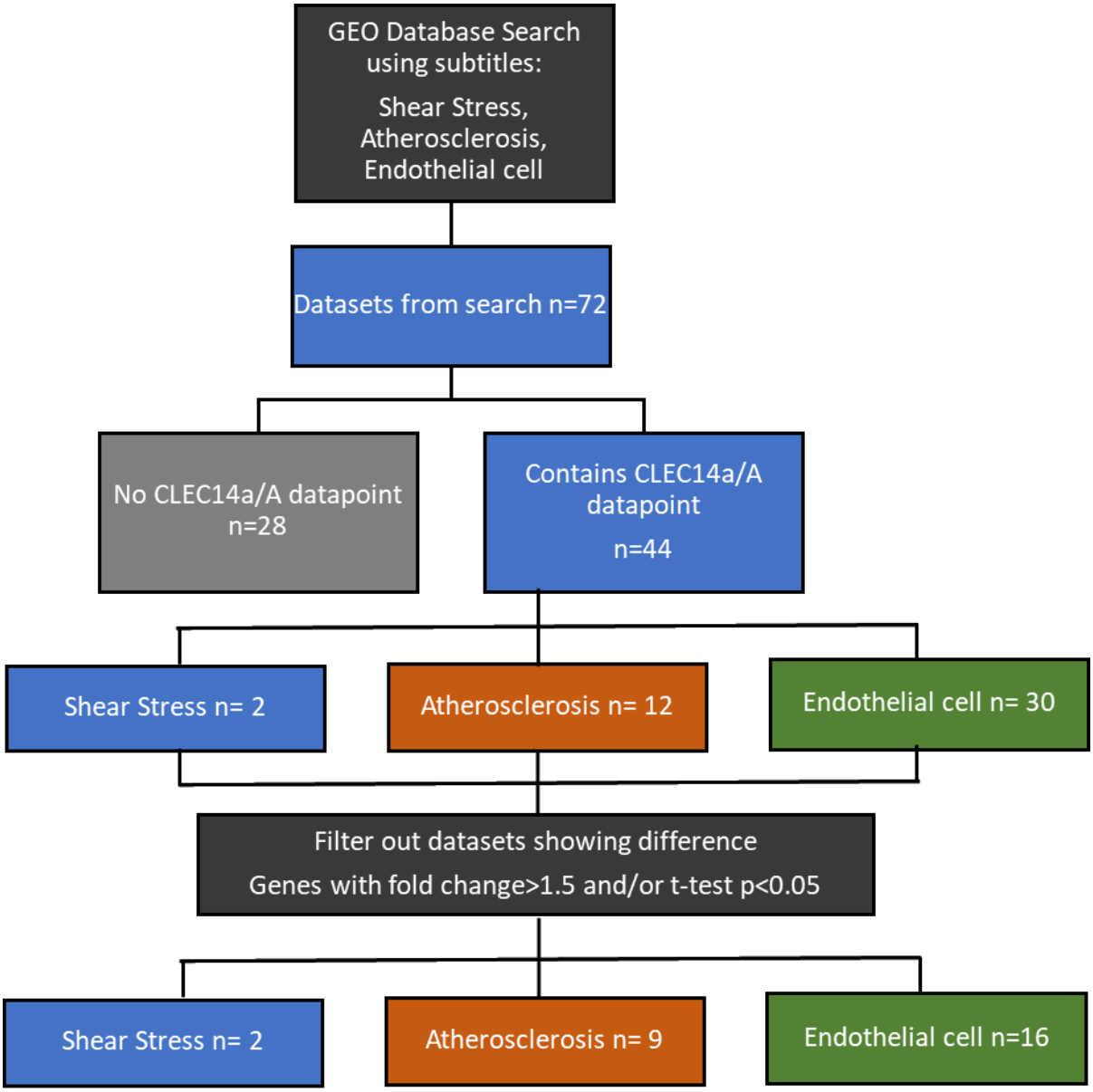

Figure 2.3: Flowchart depicting the workflow process for bioinformatic analysis outlining the search strategy; number of CLEC14a/A database entries and the decision points used to filter out datasets of interest.

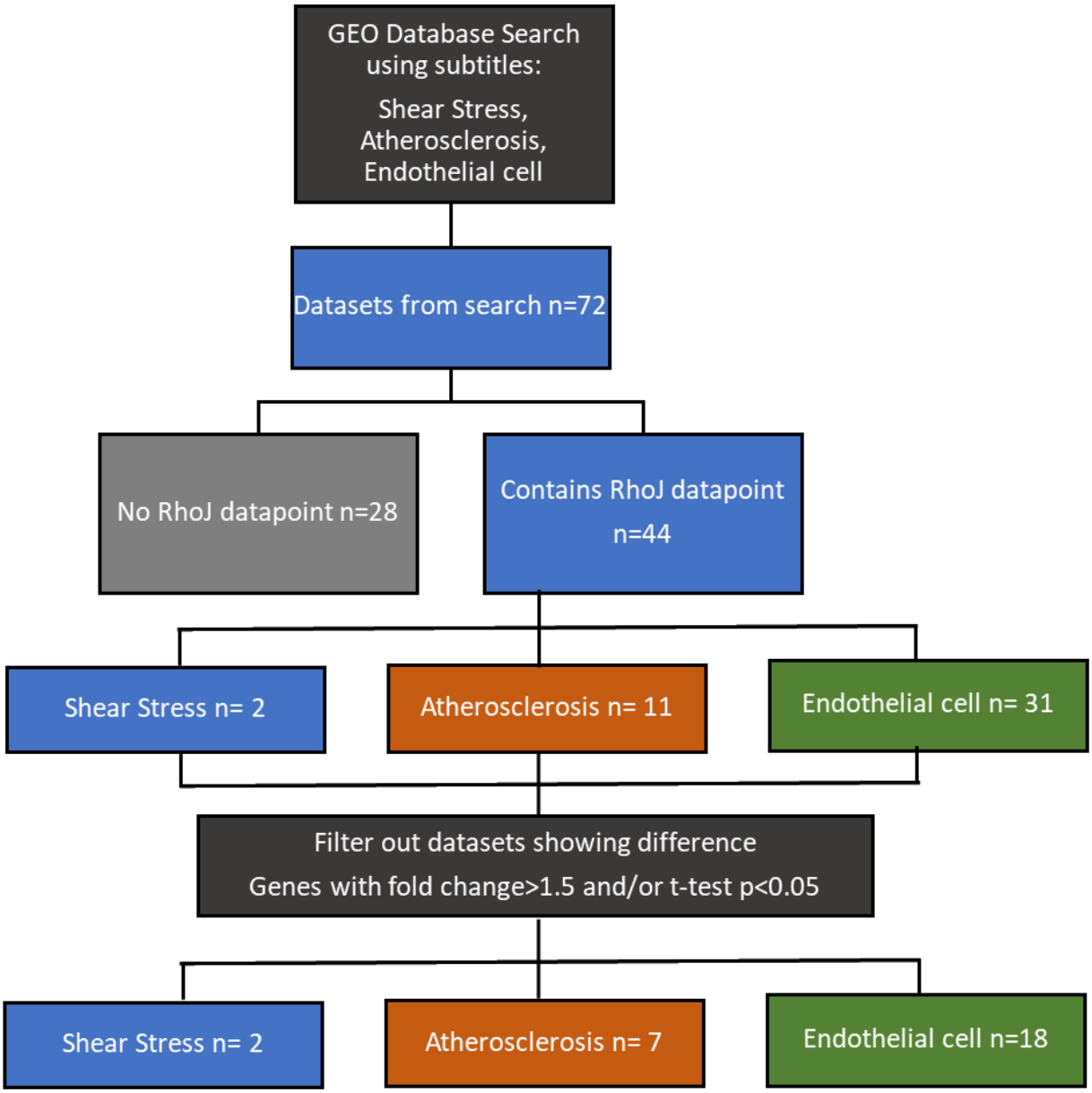

Figure 2.4: Flowchart depicting the workflow process of bioinformatic work outlining the search strategy; number of RhoJ database entries and the decision points used to filter out datasets of interest.

Chapter Three

The Role of CLEC14A and RhoJ in Regulating Endothelial Shear Responses

3 The Role of CLEC14A and RhoJ in Regulating Endothelial Shear Responses

3.1 Introduction

CLEC14A is an endothelial, transmembrane protein that belonging to CTLD containing group 14 family members, which is regulated by haemodynamic shear stress (67). CLEC14A is involved in regulating pathological angiogenesis and is associated with tumour growth and atherosclerosis, diseases characterised by neovascularisation and disturbed flow (67, 69). CLEC14A expression is suppressed by laminar flow inside and its expression has been associated with atherosclerotic plaques (67, 78). Previously unpublished data in our laboratory had demonstrated that constitutive expression of CLEC14A in HUVECs reduced the shear stress-mediated induction of the transcription factor KLF2, a master regulator of shear stress responses (37). The aim of experiments described in this chapter is to further explore this finding and evaluate the effect of a number of mutant forms of CLEC14A in this assay. This would establish which regions of CLEC14A are critical, and by extension which of CLEC14A's interacting partners might be involved in mediating this effect.

RhoJ protein is a small Rho GTPase which like CLEC14A is expressed in endothelial cells (60). It has a number of diverse functions in modulating signal transduction pathways of angiogenesis, cytoskeletal dynamics and endothelial cell migration (105). In a second set of experiments described in this chapter we explored how expression of RhoJ was affected by laminar shear stress and determined whether it played any role in regulating KLF2 expression. RhoJ levels were reduced by using siRNA-mediated knockdown and the effects on KLF2 expression and cell alignment were evaluated.

3.2 Experimental Results

3.2.1 HUVEC Transduction to express GFP and mutant forms of CLEC14A

To investigate the role of CLEC14A in regulating endothelial shear stress responses, HUVECs were manipulated to express wild type and various mutant forms of CLEC14A using lentivirus transduction technology. The process involved transfecting HEK298T cells with three plasmids, a transfer plasmid (coding for the different forms of CLEC14A), an envelope vector and a packaging vector, to generate lentivirus particles. Within a day, the HEK298T cells started producing lentiviral particles which were later used to transduce the HUVEC cultures (Figure 3.1A). Upon infection with these replication deficient virus particles, wildtype, or various mutant forms of CLEC14A were stably integrated into the HUVEC genome (Table 3.1). Transfer plasmids were generated by Dr Victoria Heath (University of Birmingham, UK) and were designed such that the CLEC14A sequence was joined to the GFP sequence, separated by a P2A self-cleaving peptide sequence. Thus, when CLEC14A was expressed, an equal amount of GFP was also released resulting in the levels of CLEC14A and GFP being proportionate to one another (Figure 3.2). This allowed detection and quantification HUVEC transduction to determine whether it was successful. As well as the various CLEC14A transfer plasmids, a transfer plasmid expressing GFP alone (pWPXL) was used as a control to evaluate the effect of lentiviral transduction and subsequent ectopic gene expression on HUVEC responses in the various assays undertaken. Untransduced HUVECs were also included in all assays, such that comparison to the GFP control with the parental cells would allow evaluation the effects of lentiviral transduction on cells.

Table 3.1 Summary of the various mutant forms of CLEC14A transduced in HUVECs. This table describes the different forms of CLEC14A used, the changes in the amino acid sequence and consequence for CLEC14A function.

CLEC14A mutant	Transfer Plasmid	Details of what each mutant form of CLEC14A does
CLEC14A WT	pWPXL-CLEC14A-P2A-GFP	Wild-type CLEC14A
CLEC14A THBD 98-107	pWPXL-CLEC14A THBD 97-108-P2A-GFP	The amino acids 97-108 are replaced with the analogous region from thrombomodulin. This mutant does not bind to the ligand MMRN2 (61)
CLEC14A R161A	pWPXL-CLEC14A R161A-P2A-GFP	This R161A point mutant impairs CLEC14A's interaction with heparan sulphate (71)
CLEC14A- ICD	pWPXL-CLEC14A No ICD-P2A-GFP	This is a truncated form of CLEC14A which lacks an intracellular domain

Transduced HUVECs were subjected to flow cytometry to determine levels of HUVEC transduction. Live cells were gated based on forward and side scatter, and untransduced HUVECs were used as a negative control and to set the gate for determining the percentage of transduced cells. Three transduction experiments were performed in total. In the case of the GFP control sample, the first experiment was performed differently to the subsequent two experiments in that the there was no dilution of the lentivirus containing media produced by the HEK298T cells before it was added to the HUVEC. This resulted in extremely high levels of GFP expression and poor proliferation of the HUVECs compared with the CLEC14A transduced cells and untransduced cells. These HUVEC samples were subjected to only 48 hours of orbital shear stress due to evidence of cell senescence through light microscopy, a likely consequence of GFP toxicity. To address this problem, in experiments 2 and 3 HUVECs were transduced with control GFP lentivirus containing media

diluted 1 in 4. This reduced the virus titre and subsequent expression levels of GFP by the transduced HUVECs. A representative example of HUVEC transduction for experiment 2 is shown in Figure 3.1B. The flow cytometry plots indicate that the majority of HUVECs were transduced, and levels of fluorescence were similar in each sample suggesting that similar levels of GFP were expressed in all samples (Figure 3.1B). Table 3.2 shows the percentage of cells transduced for each of the three experiments from the flow cytometry data.

It was also important to evaluate levels of CLEC14A expression resulting from the transduction in comparison to endogenous levels of CLEC14A expression and this was assessed by both western blot and flow cytometry, with the latter enabling assessment of levels of CLEC14A at the cell surface (Figure 3.3). Western blotting for CLEC14A in transduced samples (Figure 3.3A) showed that CLEC14A levels were considerably greater than endogenous levels of this protein in all HUVEC transduced with CLEC14A constructs whether they be the wild type or mutant forms. Western blotting for tubulin served as a loading control, indicating that similar levels of cell extract were loaded in each lane. CLEC14A is a highly glycosylated protein, and this results in multiple bands representing the different glycosylated forms. There is variation in banding patterns between the wild type and mutant forms suggesting that the mutations introduced have impacted on glycosylation of CLEC14A. The different banding patterns are not evident in the untransduced and GFP-transduced HUVEC and this is due to the large differences in protein levels and the short exposure time required to capture the signal from the CLEC14A-transduced cells.

To determine levels of CLEC14A at the cell surface, flow cytometry was performed staining cells with a monoclonal antibody specific for CLEC14A and an Alexa-647 fluorophore conjugated secondary antibody, live cells were gated via forward and side scatter and histograms for fluorescence in the APC channel displayed (Figure 3.3B). For all samples a negative control staining using a mouse immunoglobulin was performed. There is an evident increased shift in fluorescence for cells expressing wild type CLEC14A, CLEC14A R161A and CLEC14A-ICD, compared with the untransduced and GFP-transduced samples which express only endogenous CLEC14A. The CLEC14A THBD97-108 showed a less marked shift in fluorescence suggesting that this mutant may not be so well expressed at the cell surface. Overall, these data indicate that the transduction of HUVEC with the various CLEC14A constructs leads to high levels of expression of CLEC14A and for most mutants this is accompanied by increased levels of CLEC14A at the cell surface.

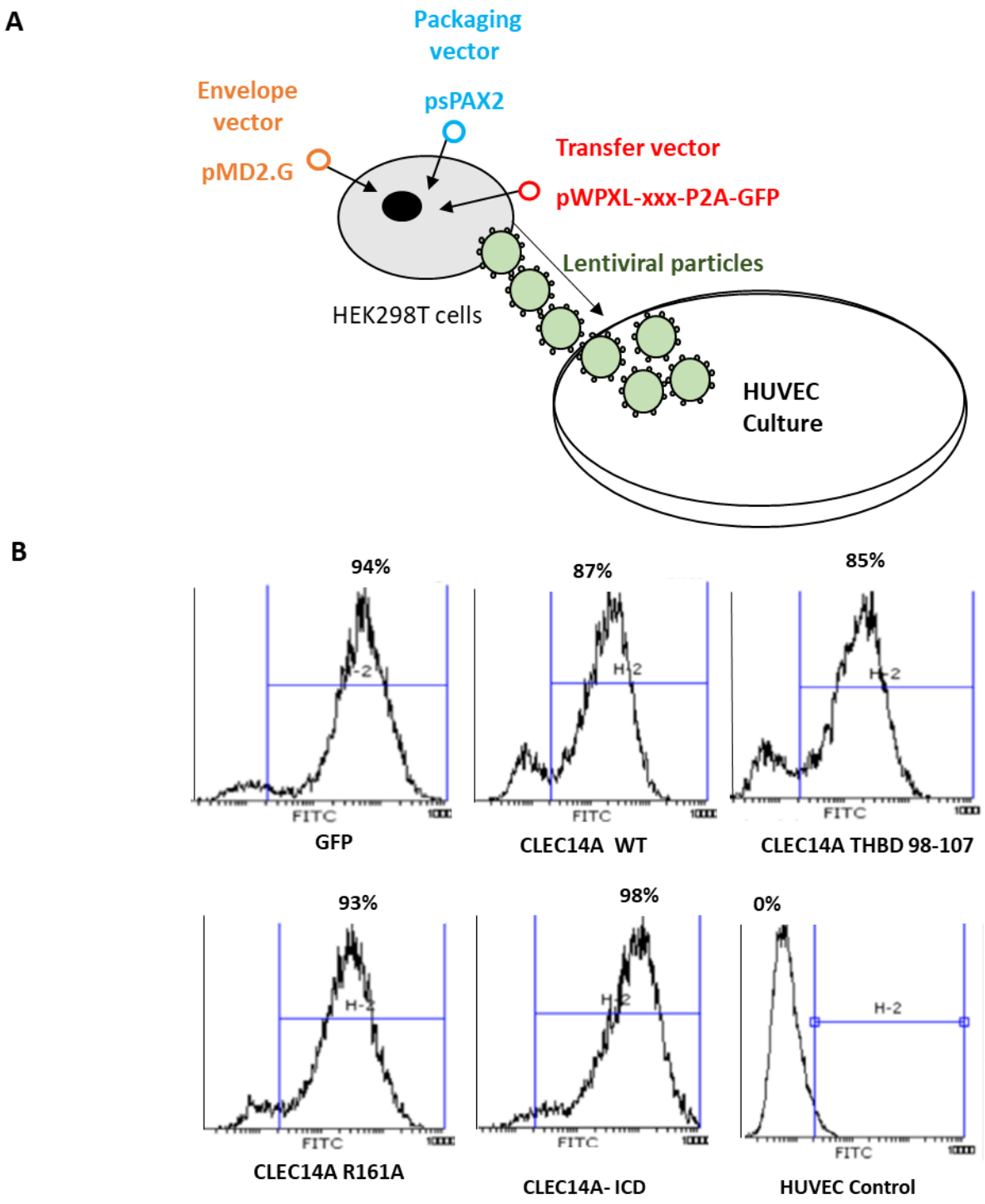

Figure 3.1: Transduction of HUVEC cells with mutant forms of CLEC14A. A) HEK298T cells were transfected with plasmids to generate lentivirus to transduce HUVEC with different mutant forms of CLEC14A. Four days after transduction, cultured HUVECs were subjected to flow cytometry to determine levels of transduction. B) Using the histogram for untransduced control cells, a gate was set on forward and side scatter and the percentage of GFP positive cells was determined (labelled on the histograms).

Table 3.2 Summary of GFP positive cell percentages from three replicate experiments. This table describes the percentages from the flow cytometry for each sample from the three experiments.

Transduced CLEC14A conditions	Transduction Efficacy %			
	EXPT 1	EXPT 2	EXPT 3	Mean
CLEC14A WT	99%	83%	94%	92%
CLEC14A THBD 98-107	97%	79%	87%	88%
CLEC14A R161A	98%	84%	85%	89%
CLEC14A- ICD	98%	75%	93%	89%
CLEC14A WT	99%	98%	98%	98%
HUVEC Control	0%	0%	0%	0%

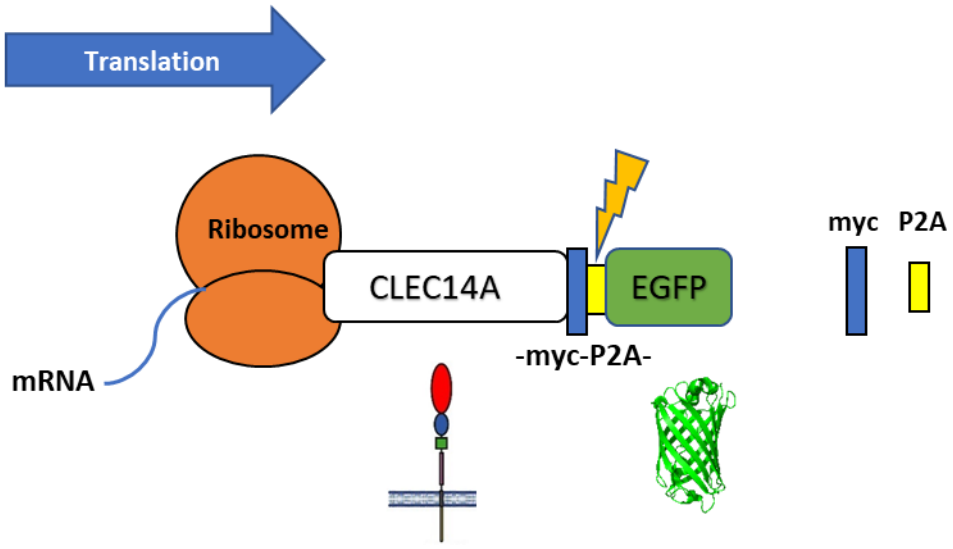

Figure 3.2: Translation of mutant CLEC14A transfer plasmid. The transfer plasmids comprised of CLEC14A sequence attached to Myc tag linked to GFP and separated by a self-cleaving peptide sequence. GFP expression reports transduction and expression of the CLEC14A constructs.

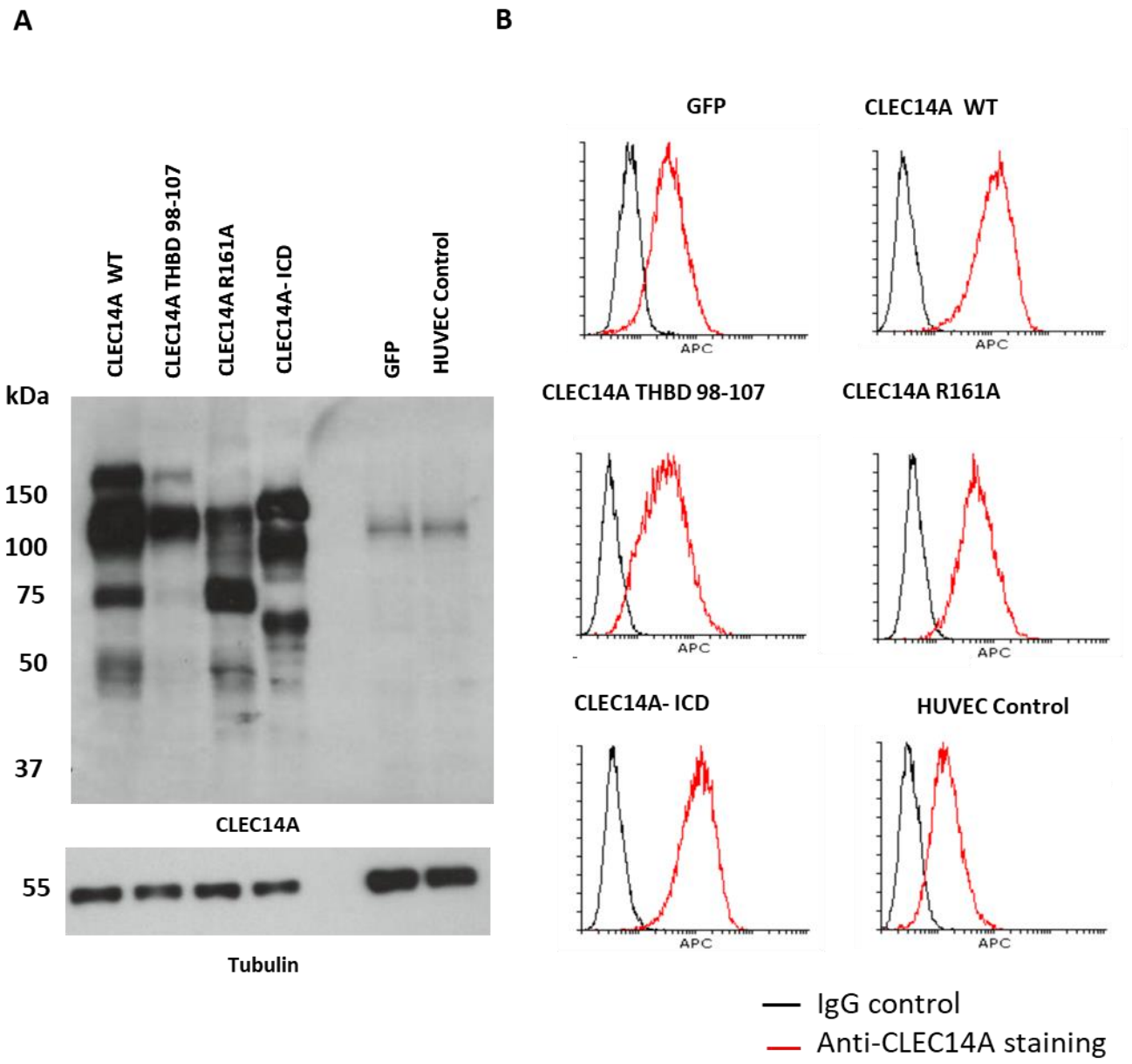

Figure 3.3: Wild type CLEC14A and mutant forms of CLEC14A constructs were at the cell surfaces. Both transduced and control HUVEC were analysed both western blotting and flow cytometry to determine expression levels of CLEC14A. A. Protein lysates were subjected to SDS-PAGE and western blotted for CLEC14A and tubulin as a loading control. B. Transduced and control HUVEC were harvested and incubated with either CLEC14A primary antibody or negative control mouse IgG, followed with secondary antibody conjugated with APC. Live cells were gated based on forward and side scatter. Histograms of APC fluorescence were depicted as the IgG control (black) or anti-CLEC14A staining (red) for each of the different transduction samples and untransduced control.

3.2.2 Evaluation of the Overexpression of Wild Type and Mutant Forms of CLEC14A on the Expression of Shear Regulated Genes

CLEC14A is regulated by shear stress with laminar shear stress decreasing its expression (67). In addition, our laboratory has generated some evidence that CLEC14A expression may influence the expression of other shear-stress regulated genes such as KLF2. To better understand how CLEC14A might be doing this, mutant forms of CLEC14A affecting it ability to interact with various ligands or intracellular signalling proteins were used in a series of shear stress experiments. HUVECs were transduced with these various mutant forms (as described above) were cultured and subjected to 1.1 pa laminar shear stress using an orbital shaker system or incubated in static conditions for 48 hours for experiment 1 or 72 hours for experiment 2 and 3. The cells were collected, and RNA was extracted and purified and converted to cDNA which was then used to probe for the expression of a number of different genes. Initially the expression of GFP and CXCR4 was interrogated.

3.2.2.1 GFP mRNA Expression in Transduced HUVECs

GFP is encoded by the lentiviral transfer plasmid either as part of the CLEC14A expression cassette or on its own in the control pWPXL plasmid. Expression levels of GFP relative to β-actin from each of the three biological replicates is shown in Figure 3.4, and clearly shows expression in all transduced samples but none in any of the untransduced HUVEC control. There is some variation between the different experimental replicates and groups within the replicates, but overall, there is no discernible pattern. There is no consistent effect of the orbital shear stress on the different samples suggesting that shear stress was not affecting expression of the transduced genes.

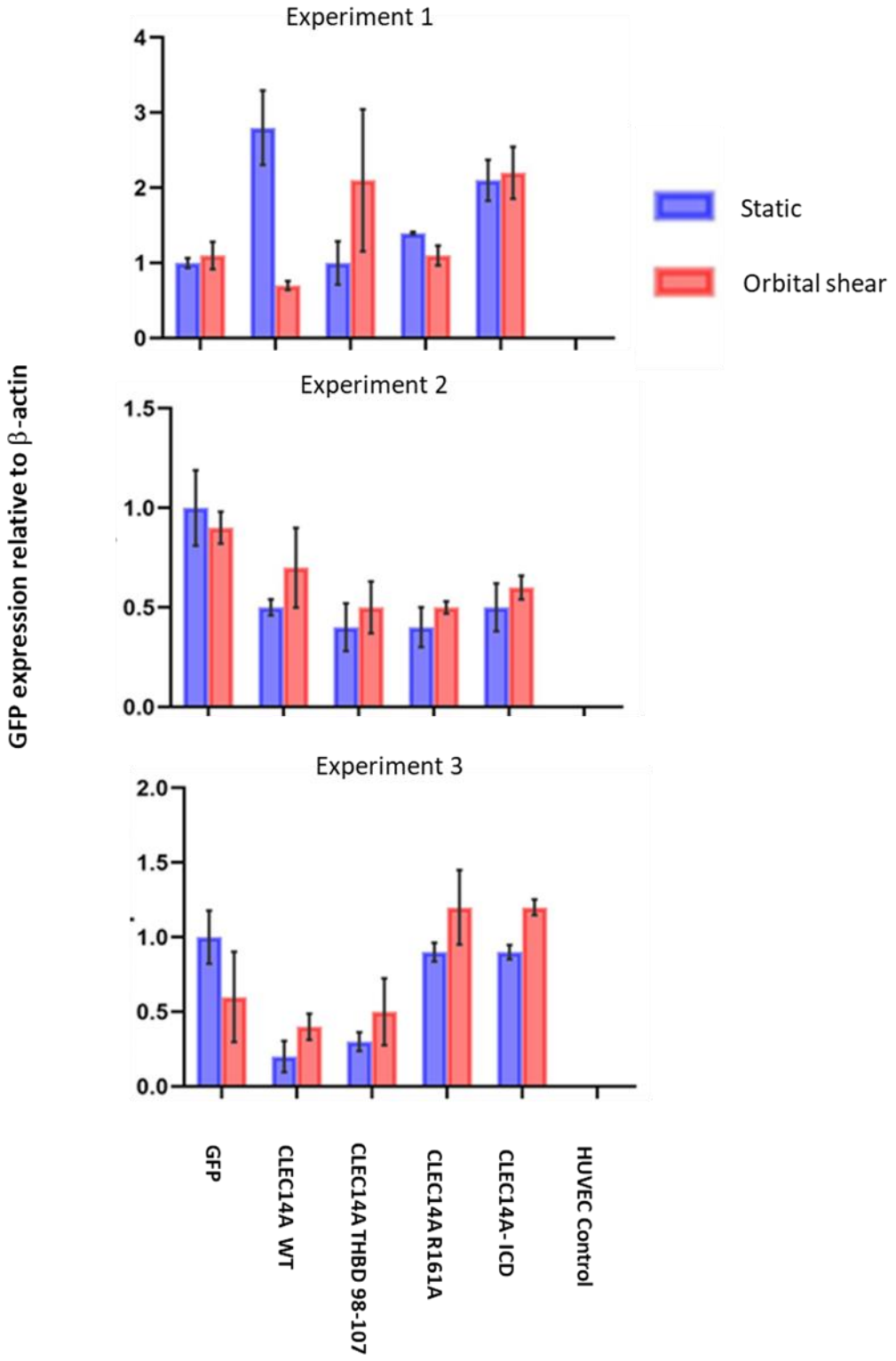

Figure 3.4: GFP is expressed in all transduced cells and its expression is unaffected by the shear stress. HUVECs were transduced with various mutant forms of CLEC14A as indicated in the graphs and subjected to either static culture or 1.1 Pa laminar shear stress for 72 hours. RNA was extracted from cell lysates, converted to cDNA and subjected to qPCR using primers specific for GFP and β-Actin. The blue and red bar depict expression of GFP relative to the β-Actin housekeeping genes in cells subjected to static (ST) and laminar orbital shear (OS) culture conditions, respectively. The error bars present the Mean ±SD from three technical replicates.

3.2.2.2 CXCR4 mRNA Expression in Transduced HUVECs

CXCR4 expression was also investigated because this gene is a known marker of disturbed flow showing reduced expression under laminar flow conditions (106). Before proceeding onto probing other genes of interest, it was important to validate the setting used on the orbital shaker that introduced pulsatile laminar flow to the HUVEC culture plates. For all three experiments, the data showed that the relative expression of CXCR4 to the housekeeping gene β-Actin decreased under laminar shear stress in relation to static conditions across all transduced HUVEC conditions (Figure 3.5). This indicates that the orbital shaker system was introducing laminar flow as programmed and gave confidence to proceed to quantifying other genes of interest.

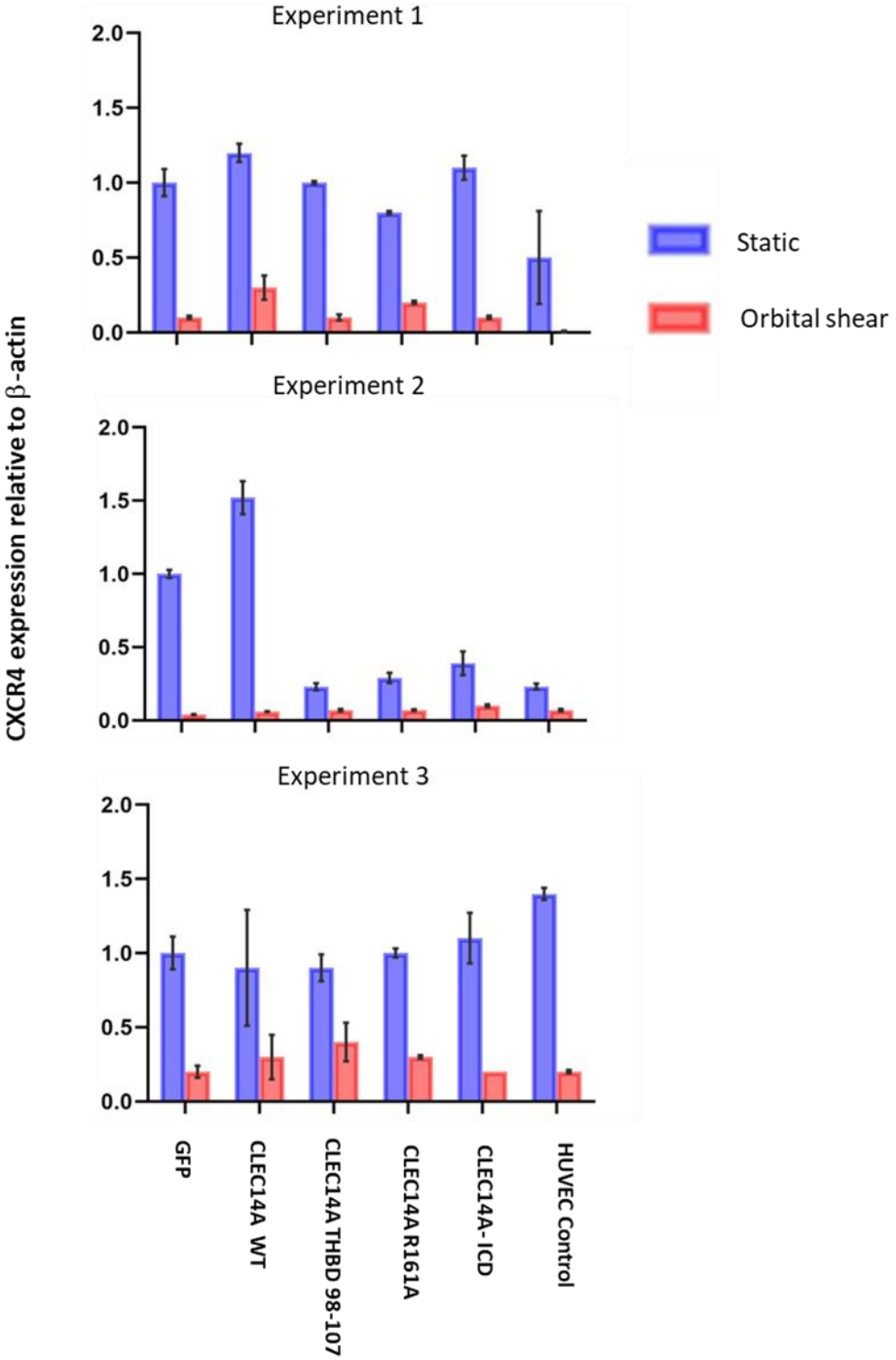

Figure 3.5: CXCR4 is downregulated by laminar flow in all transduced HUVEC. HUVECs were transduced with various mutant forms of CLEC14A as indicated and subjected to either static culture or 1.1 Pa laminar shear stress for 72 hours. RNA was extracted from cell lysates, converted to cDNA and subjected to qPCR using primers specific for CXCR4 and β-Actin. The blue and red bar depict expression of CXCR4 relative to the β-Actin housekeeping genes in cells subjected to ST and OS culture conditions, respectively. The error bars present the Mean ±SD from three technical replicates.

3.2.2.3 KLF2 mRNA Expression in Transduced HUVECs

Having established that the orbital shear system was functioning to regulate CXCR4, the expression of KLF2 was examined. This gene is known to be regulated by laminar shear stress with laminar flow upregulating KLF2 expression (107). Preliminary data from our laboratory indicated that forced expression of CLEC14A down-regulates shear stress induced expression of KLF2 but the mechanism by which this occurs is unknown. To investigate which region of CLEC14A is involved in regulating KLF2 shear stress response, mutant forms of CLEC14A were transduced in HUVECs cultures and subjected to laminar shear stress for 72 hours before harvesting the cell lysates to quantify KLF2 through qPCR. In experiment 1, very high expression of GFP in the GFP control sample compromised the cell viability of this experimental group. Despite there being the expected decrease in the expression of CXCR4 as a consequence of shear stress, a concomitant increase in KLF2 expression was not observed (Figure 3.6). It is therefore difficult to interpret the data from this experimental replicate.

Reduced titres of lentivirus used for the GFP control samples in experiments 2 and 3 resulted in better cell viability and control GFP transduced and untransduced samples show the expected induction of KLF2 upon application of shear stress (Figure 3.6). In experimental replicates 2 and 3, expression of transduced wild type CLEC14A modestly abrogated the induction of KLF2 expression, as we had previously observed. Since all the samples showed an increase in KLF2 mRNA levels relative to β-Actin under laminar flow, the ratio of OS/ST was calculated to enable a better comparison of KLF2 induction between experimental groups. The reduced OS/ST ratio in HUVEC transduced with WT CLEC14A was largely due to the slightly elevated levels of KLF2 expression in the HUVEC cultured under static conditions. The various mutant forms of CLEC14A had minimal effects in altering induction of KLF2

expression which was comparable with control samples. Though the data is variable, and the effects observed small, these data suggest that functional intact extracellular and intracellular domains are necessary for CLEC14A to regulate KLF2 expression.

3.2.2.4 MMRN2 mRNA Expression in Transduced HUVECs

Data from Bicknell laboratory suggests that MMRN2, a ligand for CLEC14A (61), is another shear regulated gene (*unpublished*). Like KLF2, it is thought to be regulated by CLEC14A since previous yet unpublished work from our laboratory suggested knocking down CLEC14A expression in HUVECs resulted in downregulated MMRN2 expression under static conditions. It was thus interesting to investigate how overexpression of CLEC14A affected MMRN2 expression. In experiment 2 and 3, shear stress did increase expression of MMRN2 in control groups and there was an increase in MMRN2 levels relative to the housekeeping gene β-Actin suggesting MMRN2 is positively regulated by shear stress (Figure 3.7). With the over-expression of CLEC14A there was a significantly enhanced shear enhanced upregulation of MMRN2, although the degree of enhancement varied in the three experimental replicates. The levels of shear stress induced upregulation of MMRN2 in HUVECs expressing the various mutant forms of CLEC14A varied across the experiments. In experiment 2 there was reduced induction of MMRN2 for all mutant forms of CLEC14A, whereas in experiment 3 expression of the CLEC14A mutant lacking the intracellular domain had the most impact. Across all three experiments it was the CLEC14A R161A mutant with reduced binding to heparan sulphates that consistently reduced levels of MMRN2 induction. The variability in data make interpretation difficult and the complex nature of this multi-step experiment are likely to result in variations in conditions between experimental replicates that are difficult to determine.

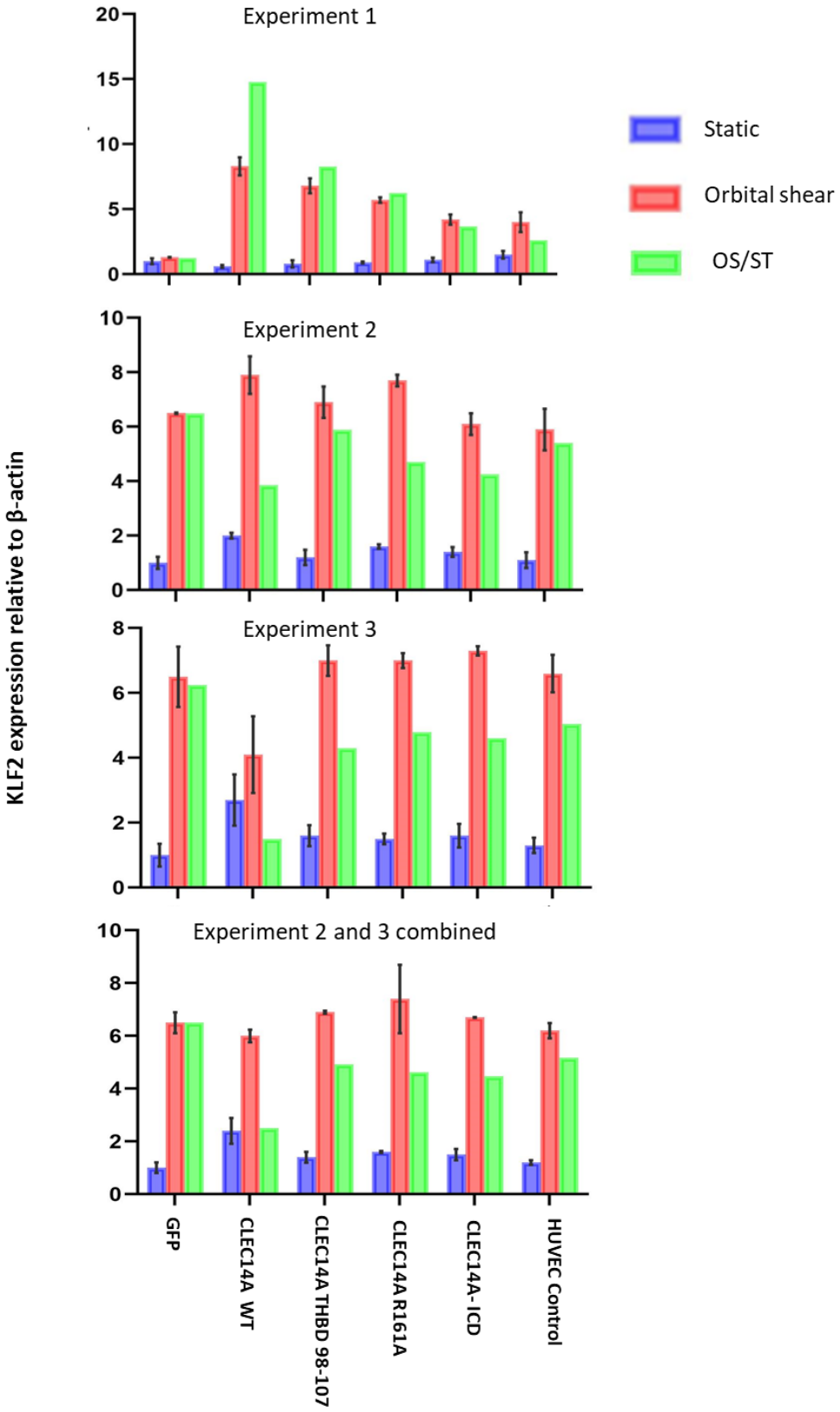

Figure 3.6: CLEC14A over-expression is affecting the normal KLF2 shear response. HUVECs were transduced with various mutant forms of CLEC14A and subjected to either static culture or 1.1 Pa laminar shear stress for 72 hours. RNA was extracted from cell lysates, converted to cDNA and subjected to qPCR using primers specific for KLF2 and β-Actin. The blue and red bar depict expression of KLF2 relative to the β-Actin housekeeping genes in cells subjected to ST and OS culture conditions, respectively. The error bars present the Mean ±SD from three technical replicates.

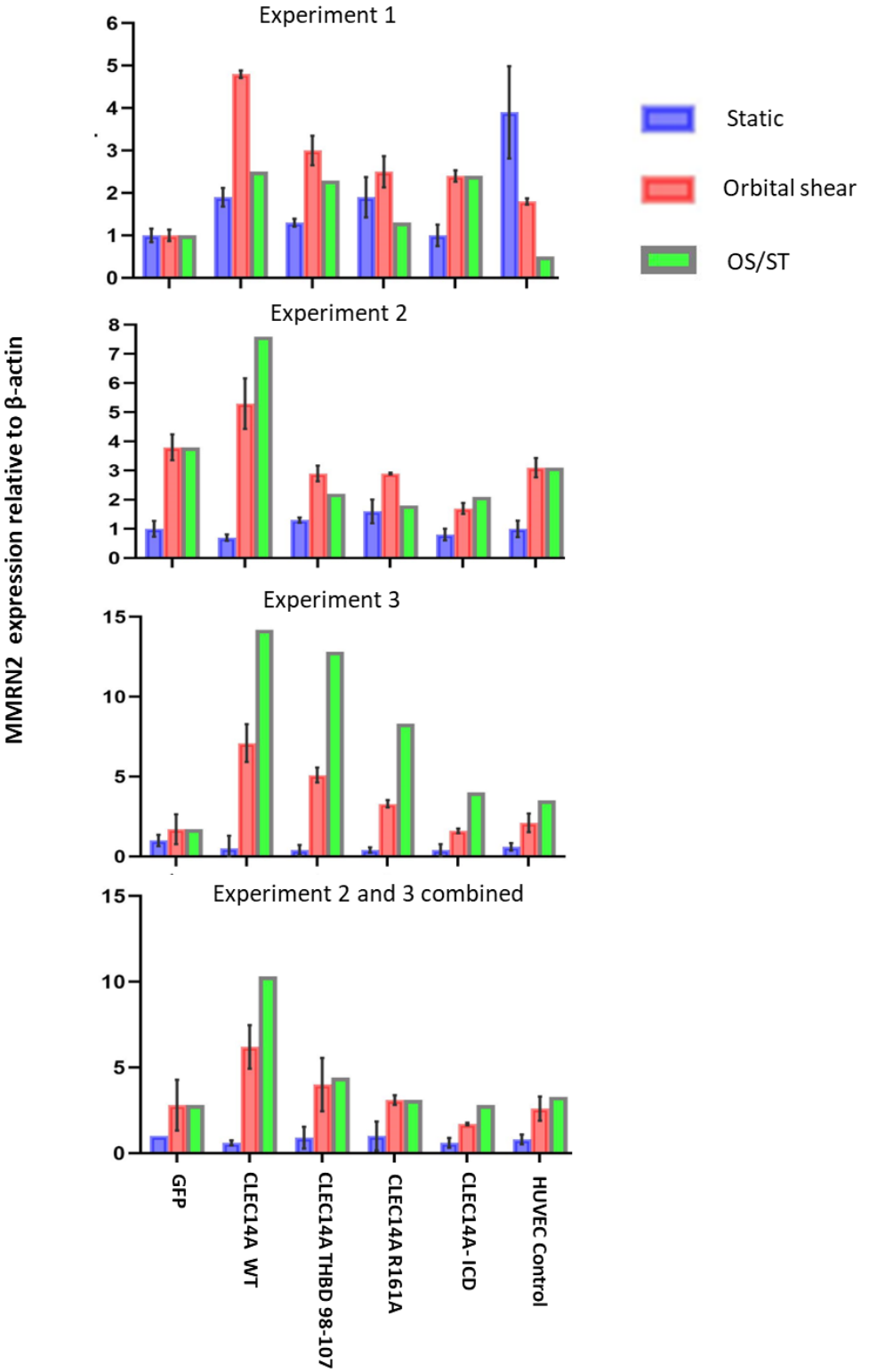

Figure 3.7: MMRN2 expression increases with CLEC14A over-expression and this is reduced with the mutant forms of CLEC14A. HUVECs were transduced with various mutant forms of CLEC14A and subjected to either static culture or 1.1 Pa laminar shear stress for 72 hours. RNA was extracted from cell lysates, converted to cDNA and subjected to qPCR using primers specific for MMRN2 and β-Actin. The blue and red bar depict expression of MMRN2 relative to the β-Actin housekeeping genes in cells subjected to ST and OS culture conditions, respectively. The green bar represents the relative fold change calculated using OS/ST ratio. The error bars present the Mean ±SD from three technical replicates.

3.2.3 RhoJ mRNA and Protein Expression During Static and Laminar Shear Stress Conditions

RhoJ is an endothelial expressed Rho GTPase involved in regulating cell migration and tube formation (105). Both our laboratory and published microarray data indicated that laminar shear stress downregulated RhoJ expression (108). The experiments in the second part of the chapter aimed to confirm this and investigate a potential role for RhoJ in regulating shear stress responses. HUVEC cultures were subjected to 72 hours of laminar flow, RNA and protein lysates were isolated and analysed for RhoJ RNA and protein expression using qPCR and western blot quantification assays, respectively. This experiment was performed three times and qPCR data showed that RhoJ expression relative to β-Actin was significantly downregulated upon application of shear stress compared to static conditions ($P<0.01$; Student t-test) (Figure 3.8A). This was also reflected in the Western blot which showed clear downregulation of RhoJ protein (Figure 3.8B); tubulin was used as a loading control and densitometry quantification was performed using ImageJ software, this showed that levels of RhoJ relative to tubulin were significantly reduced in HUVEC subjected to shear stress ($P<0.05$; Student t-test) (Figure 3.8C).

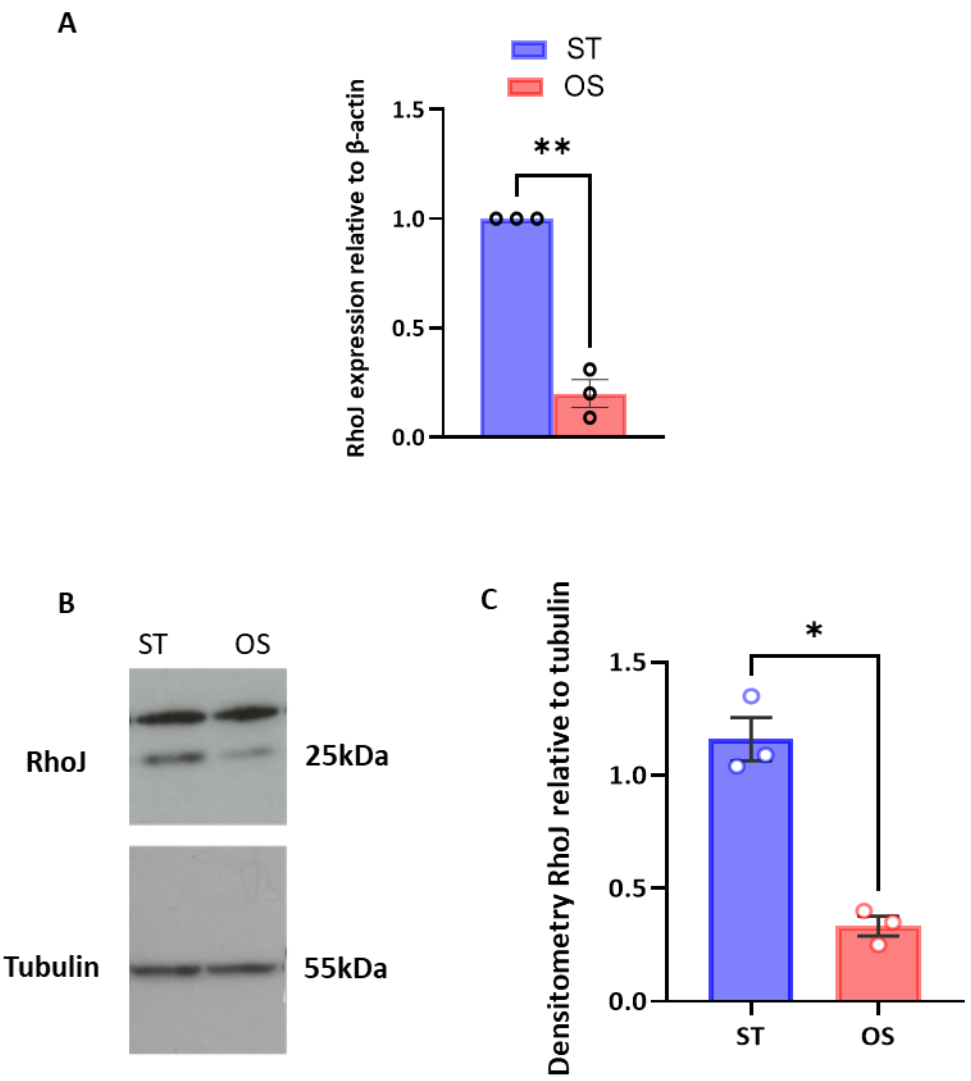

Figure 3.8: RhoJ mRNA and protein is downregulated by laminar shear stress at the protein and mRNA level. A) HUVECs were subjected to either static culture or 1.1 Pa laminar shear stress for 72 hours. RNA was extracted from cell lysates, converted to cDNA and subjected to qPCR using primers and probes specific for RhoJ and β-Actin. The blue and red bar depict expression of RhoJ relative to the β-Actin housekeeping genes in cells subjected to ST and OS culture conditions, respectively. The error bars present the mean±SEM from three independent experiments. Statistical analyses were performed using a paired t-test indicating a statistically significant difference (**=P<0.01). B) Protein lysates were extracted, subjected to SDS-PAGE and western blotted for RhoJ and tubulin, with tubulin acting as a loading control; one representative example of three independent experiments is shown. C) Densiometry of the RhoJ and tubulin bands was performed for all three replicate experiments using the ImageJ software and statistical analyses were performed with a paired t-test showing statistically significant differences between RhoJ 72hr Static and 72hr OS samples (*= P<0.05).

3.2.4 *In vitro* RhoJ Regulation of KLF2 Shear Responses in RhoJ SiRNA-treated Cells

Since RhoJ is regulated by shear stress, the next step was to investigate whether RhoJ played any role in regulating the responses of genes known to be regulated by shear stress. The transcription factor KLF2 is a key regulator of shear stress responses with knockdown studies showing that of all the genes that are shear stress regulated, approximately 15% of them are KLF2-dependent (107). Microarray studies have demonstrated that overexpression KLF2 in HUVECs under flow suppressed expression of RhoJ (37) suggesting that KLF2 is involved in regulating expression of RhoJ. It is not known if the converse is true. HUVECs were treated with either RhoJ specific siRNA duplexes or negative control duplex and after 48 hours cells were subjected to 24 hours of either static or laminar flow conditions inside an orbital shaker for another 24 hours of incubation. In two of the replicate experiments cells were then imaged using the phase contrast microscopy to determine the cellular alignment prior to the extraction of RNA and proteins from the cultures to determine expression of KLF2 and successful knockdown of RhoJ. Western blotting confirmed reductions in RhoJ protein levels relative to the loading control Tubulin, a representative blot is shown Figure 3.9A showing a reduction in the lower RhoJ-specific band. As expected, KLF2 expression levels were increased upon the application of shear stress in both control siRNA and RhoJ-siRNA transfected cells (Figure 3.9B). Knockdown of RhoJ did not have a significant impact on KLF2 upregulation when combining data from three independent replicate experiments.

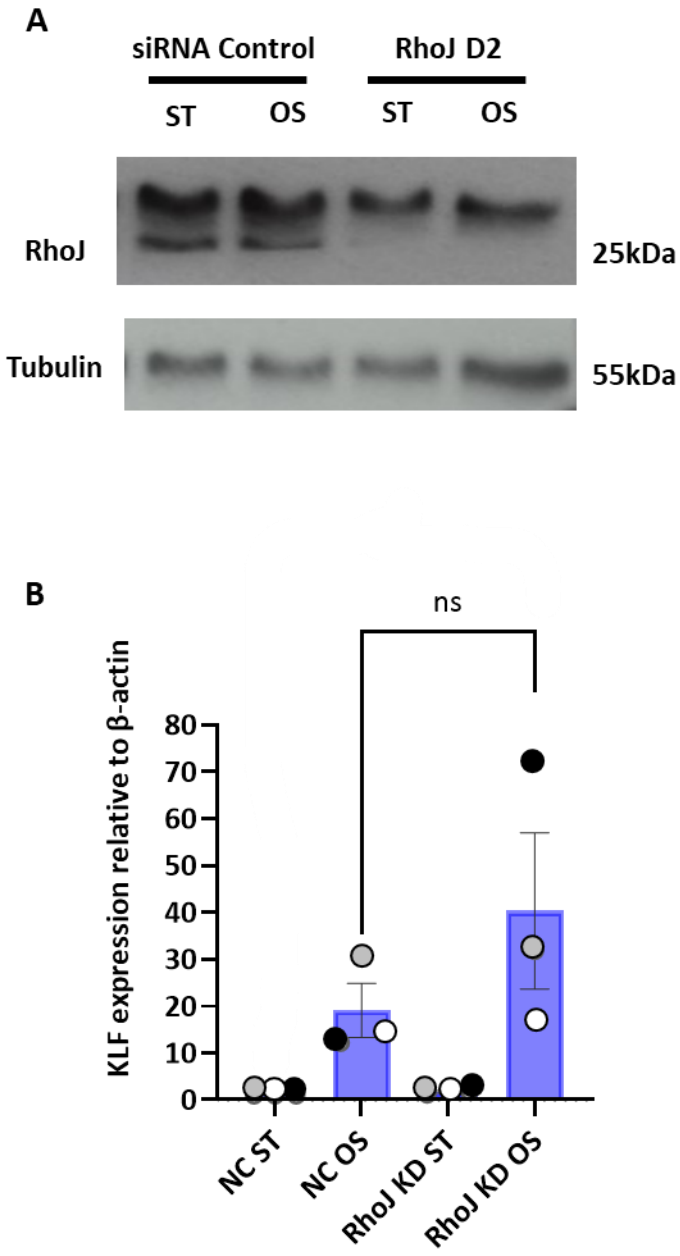

Figure 3.9: Knocking-down RhoJ in HUVECS upregulated KLF2 expression at the mRNA level. SiRNA gene silencing technology was utilised to knockdown RhoJ protein in HUVEC cultures which were then subjected to either 1.1 Pa of laminar shear stress or static culture for 24 hours. A) To confirm RhoJ knockdown, cells were lysed and protein extracts subjected to SDS-PAGE and western blotted for RhoJ and tubulin as a loading control. B) RNA was isolated, purified, converted to cDNA, and qPCR was then used to quantify KLF2 gene expression. Each bar in the KLF2 qPCR run indicates the mean of three independent experiments with each dot representing a single datapoint, and error bars representing the SEM. Kruskal-Wallis test was used to test for statistical analysis ($P<0.05$) and Dunn's multiple comparison test was used to compare negative duplex control ST and RhoJ KD OS conditions (ns=$P>0.05$).

3.2.5 Image Analysis of RhoJ Knockdown Transfection Cultures to Evaluate Cell Alignment

In the orbital shear stress model, cells around the periphery of the plate are subjected to the greatest levels of shear stress and demonstrate cell alignment with the direction of the flow conditions (107). Visual examination of the HUVEC with reduced RhoJ levels suggested that these cells were more elongated and showed a more marked alignment. To investigate this further fields of view at the periphery of the wells captured by the Incucyte (field 5 and 77; Figure 3.10A & B) where alignment was most prevalent were analysed using the OrientationJ Plugin programme in the ImageJ software to investigate cell alignment. The images were imported into ImageJ, converted to 32-bit and then underwent thresholding to give greater contrast to the cell margins to enable the OrientationJ programme to pick out the events for counting. The measurements are presented in histograms which enumerate the number of cells aligned at each degree of orientation (ranging from -180^{o} to +180 ^{o}). The one marked peak in histograms for the cells under laminar flow conditions indicate cell alignment and these contrast with the relatively flat peaks seen in the static conditions. Differences between the histograms for the RhoJ-siRNA treated and negative control siRNA-treated cultured under shear are not markedly different (Figure 3.10C). The slightly narrower and higher peak seen in field 5 of the RhoJ-siRNA treated samples may be indicative of greater alignment in this field, but a similar pattern is not observed in field 77.

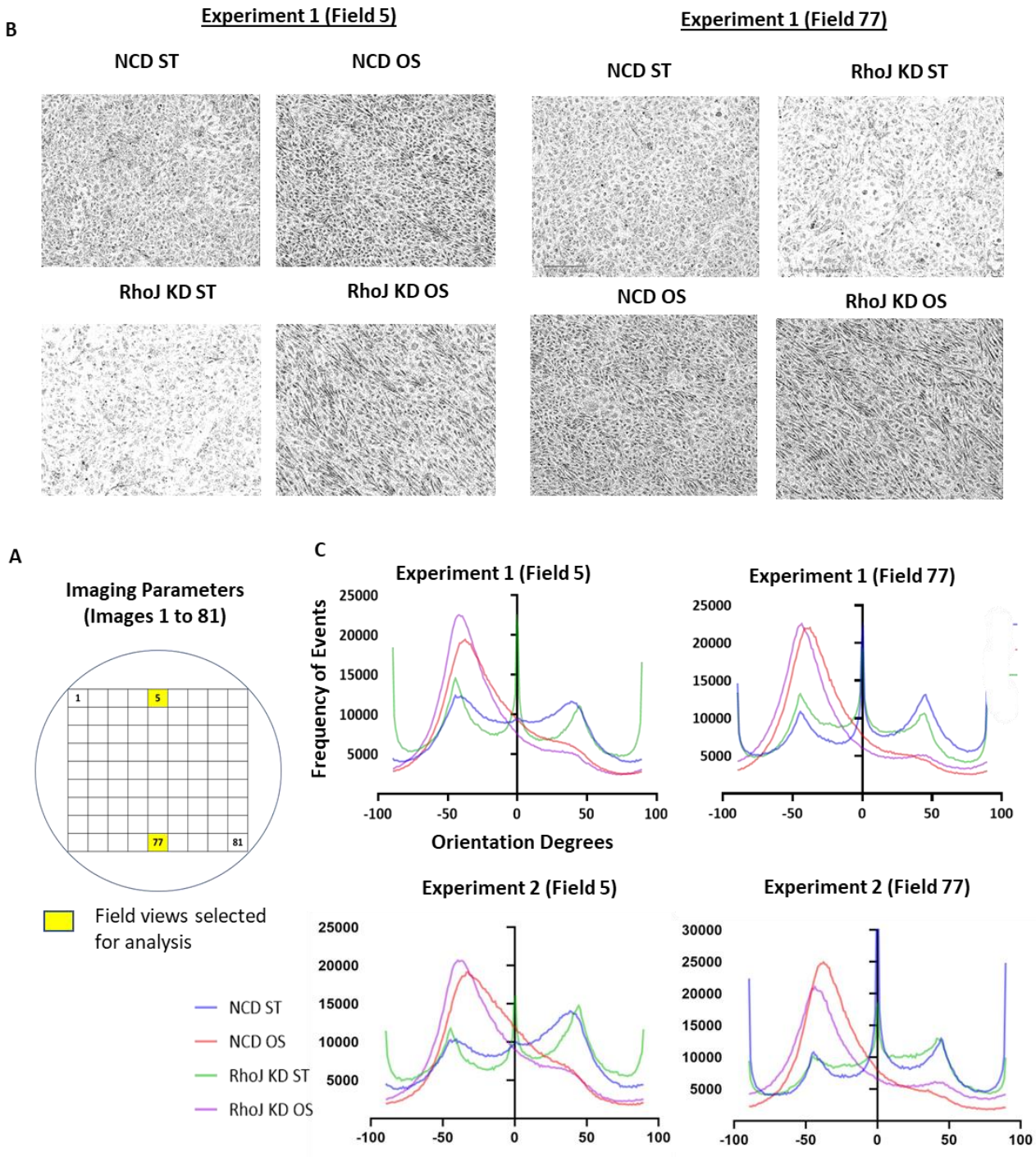

Figure 3.10: Endothelial cells aligned more in response to laminar flow in RhoJ knockdown HUVEC cultures. HUVECs were transfected with control and RhoJ siRNA D2, two days cells were subjected to 1.1 Pa of laminar shear stress or static culture for 24 hours. On completion, 81 high resolution images of each culture well were obtained using the Incucyte® imaging system. From these imaging sets, only two field views were selected to evaluate cell horizontal alignment using the OrientationJ package within ImageJ as depicted in A). B) Representative images of field 5 and 77 from two experiments after 24 hours of exposure to either static or oscillatory shear stress. C) Images were analysed by ImageJ and graphs prepared depicting the average number of events across the -90° to 90° degree orientation spectrum from field 5 and 77.

3.3 Discussion

3.3.1 Summary

CLEC14A is a shear regulated gene with its expression being downregulated by laminar shear stress, however its role in regulating responses to shear stress is not known. Consistent with unpublished data previously generated by the laboratory, these data showed that overexpression of CLEC14A reduced the upregulation of expression of the shear responsive transcription factor KLF2 upon application of pulsatile laminar shear stress in HUVECs. We further sought to determine which regions of CLEC14A were critical in mediating this blunted expression of KLF2. Though technical difficulties and experimental variability hampered these studies, they suggested that intact extracellular and intracellular domains of CLEC14A were required. These data also show that MMRN2 expression is upregulated by shear stress, and in contrast to KLF2 this upregulation was enhanced by the increased expression of intact CLEC14A, with all mutant forms of CLEC14A showing diminished upregulation. RhoJ expression was also shown to be down-regulated by shear stress, however its knockdown did not impact shear-induced KLF2 expression. Finally, there was some evidence that siRNA-mediated knockdown of RhoJ resulted in altered alignment of endothelial cells with the direction of flow.

3.3.2 Endothelial Shear Reponses of Mutant Forms of CLEC14A

KLF2 is a key transcription factor induced by atheroprotective laminar flow and is involved in regulating the expression of almost half of the flow responsive genes. It plays a critical role in inducing the expression of genes involved in regulating vascular tone, thrombosis, endothelial permeability and metabolism and it functions to promote endothelial

quiescence (109). CLEC14A expression is downregulated by shear stress, and it would be informative to determine if KLF2 were involved in repressing its expression as this is currently unknown. The experiments performed in this study show that forced expression of CLEC14A reduced the flow-mediated upregulation of KLF2 (Figure 3.6), suggesting that its presence may influence the signalling pathways that mediate KLF2 upregulation. It may affect the mechanosensory complexes such as the channel PIEZO or the PECAM1/VE Cadherin/VEGR2 complex (1, 110). Indeed, CLEC14A has been shown to interact with VEGFR3, influencing VEGFR2 signalling (72) and this may be a mechanism by which CLEC14A could affect mechanosensing, and in turn KLF2 expression. The interaction between CLEC14A and VEGF3 depended on CLEC14A's cytosolic domain. A range of mutant forms of CLEC14A were tested in these experiments including a truncated form of CLEC14A which lacked a cytoplasmic domain. The data obtained suggested that all the mutant forms of CLEC14A tested were not as active as the wild type CLEC14A indicating that both intracellular and extracellular domains, and presumably interactions with both intracellular and extracellular binding partners were required for CLEC14A to be able to maximally affect KLF2 expression.

Of interest was our observation that shear stress upregulated MMRN2 expression, something not previously reported in the literature. In contrast to KLF2, overexpression of CLEC14A enhanced its expression, and this was less marked with the overexpression of the various mutant forms of CLEC14A (Figure 3.7). Thus, wildtype CLEC14A can positively regulate the expression of MMRN2 under conditions of shear stress. The concomitant upregulation of MMRN2 and downregulation of CLEC14A expression under conditions of

shear stress is surprising given that MMRN2 is a ligand of CLEC14A. However, MMRN2 has alternative ligands – it can bind both CD93 and CD248 expressed on endothelial cells and pericytes, respectively (61, 111) – and MMRN2 is also able to bind and sequester growth factors such as VEGF (74). Under conditions of laminar shear stress MMRN2 is likely to have CLEC14A independent roles.

There were a number of technical difficulties associated with these experiments which resulted in considerable variation in the data. There was some variation in the viral titres with the control GFP virus being produced at higher titres than the virus containing the CLEC14A constructs, in the first experiment the very high levels of GFP expression resulted in significant toxicity of this control group, something that has been previously reported with high levels of GFP expression (112). There were also some differences observed between the GFP control transduced HUVECs and untransduced HUVECs, suggesting that lentiviral infection is likely to have impact the behaviour and phenotype of the endothelial cells. Overall, a key problem was the reproducibility of the data and had time permitted these experiments would have be carried out more times to give more definitive data.

Different CLEC14A mutants were used to determine which regions of CLEC14A may be critical in mediating this altered expression of KLF2 and MMRN2. The R161A point mutation reduces binding to heparan sulphate (71) and our laboratory had demonstrated that this mutant form of CLEC14A does bind MMRN2. The CLEC14A THBD97-108 mutant form of CLEC14A does not bind MMRN2 (61), however it is of concern that its cell surface expression was reduced compared with wild type CLEC14A and this may be indicative of trafficking or

folding problems with this mutant form of CLEC14A. Subsequent to these experiments, a point mutant of CLEC14A has been identified which specifically prevents MMRN2 binding while expressing at the cell surface in a comparable way to wild type CLEC14 (A. Baber, unpublished) and this would be a better tool with which to determine the impact of MMRN2 binding. It should also be noted that the lentiviral transduction of CLEC14A resulted in considerably higher levels of expression seen with endogenous CLEC14A expressed under static conditions. The use of an inducible lentiviral transduction system (113) would enable the level of CLEC14 protein to be better regulated and would allow the effect of CLEC14A expression levels on shear stress-induced KLF2 expression to be evaluated, it would also reduce difficulties associated with toxicity.

3.3.3 RhoJ Shear Stress Responses

Our data showed that RhoJ expression was significantly downregulated by 1.1Pa of laminar shear stress (Figure 3.8). These findings are consistent with the expression analyses performed by Dekker et al. (37) who demonstrated that constitutive expression of KLF2 in endothelial cells cultured under static conditions reduced RhoJ expression. Thus, collectively these studies indicate that KLF2 downregulates expression of RhoJ.

We also demonstrated that knocking down RhoJ did not significantly impact shear induced KLF2 expression (Figure 3.9). We investigated the impact of knocking down RhoJ on alignment of HUVECs subjected to shear stress in the orbital shaker model. Visual inspection of the HUVEC suggested that HUVECs better aligned to flow in these cultures, but this was not clearly reflected in the analysis of alignment using ImageJ (Figure 3.10). That

RhoJ knockdown should affect alignment is not surprising, since our laboratory has previously demonstrated that RhoJ regulates actomyosin contractility and focal adhesion dynamics (87, 90). Knockdown of RhoJ increases actomyosin contractility and this may enhance alignment in the direction of flow. RhoJ belongs to the primary tumour angiogenesis gene signature (70) and it is expression is likely to be associated with endothelial activation, and so its shear-stress induced down-regulation may be important for promoting endothelial quiescence. It would be interesting to determine whether expression of an active mutant of RhoJ had any impact on endothelial shear stress responses.

For both studies, laminar shear stress was applied using an orbital shaker. However, while the majority of the well experiences laminar flow, the flow patterns in the centre of the plate are characterised by low velocity, multidirectional and eddying currents mimicking disturbed flow (114). Because cells were harvested from the entire well, altered gene expression in these central cells may affect the data generated. In future experiments either removing cells from this region prior to harvesting or not plating cells in the centre of the well could avoid this confounding factor.

3.4 Conclusion

In conclusion, these data show that RhoJ expression is decreased and MMRN2 expression is upregulated by shear stress. They also demonstrate that high expression of CLEC14A blunts the shear-mediated upregulation of KLF2 expression and enhances the flow-induced upregulation of MMRN2 expression. These effects of CLEC14A are most pronounced with

intact CLEC14A and are thus likely to require both its intracellular and extracellular domains. Though further work is required to more definitely demonstrate these findings, they do give additional insight into the relationship between shear stress responses and our proteins of interest, CLEC14A, MMRN2 and RhoJ.

Chapter Four

Interrogation of CLEC14A and RhoJ Bioinformatic Datasets

4 Bioinformatic Analysis of Online Datasets

4.1 Introduction

CLEC14A and RhoJ are two endothelial expressed genes are both involved in the regulation of angiogenesis (69, 105). CLEC14A expression is known to be regulated by shear stress (67), while RhoJ is regulated by the transcription factor ERG (89). The aim of the analyses described in this chapter was to further our understanding of the biology of these two proteins by investigating their expression *in vitro* and *in vivo* through the use of publicly available data microarray datasets. In particular their expression in response to different endothelial shear stress patterns, in atherosclerosis and in response to a number of cellular signalling pathways was interrogated.

4.2 Summary of Bioinformatic Workflow

To understand more about how CLEC14a/A and RhoJ gene expression is regulated, bioinformatic studies were analysed from the Gene Expression Omnibus (GEO) Database. The online search engine available was used to identify GEO Databases of interest using the workflow process described in Figure 2.2 in the methods chapter. The searches made using GEO were based on three over-arching themes: shear stress, atherosclerosis, and endothelial biology, and imputing these key words generated 72 databases of interest. Databases were scrutinised to determine if there was data for either CLEC14a/A or RhoJ, and from these 44 contained data for both genes. Out of these 44 databases for CLEC14a/A there were two shear stress studies, 12 on atherosclerosis and 30 studies relating to endothelial biology. For RhoJ, there were two shear stress studies, 11 on atherosclerosis and 31 on endothelial biology (details of all studies are found in Appendix 1). These were then

filtered on basis of change or no change using a set criterion that determined change to be a relative fold change greater than 1.5 or a statistically significant change as assessed by a paired t-test ($P<0.05$). As a result, for CLEC14a/A there were two shear stress studies, nine atherosclerosis studies and 16 studies relating to endothelial cell biology studies that showed change (Figure 2.3). On the other hand, for RhoJ two shear stress, seven atherosclerosis and 18 Endothelial cell biology studies showed change (Figure 2.4). Although differences were found in multiple databases, data from only a subset of databases most relevant to shear stress, atherosclerosis and gene expression regulation were pursued for further analysis. Tables 4.1, 4.2 and 4.3 summarise the findings for CLEC14A/Clec14a and RhoJ with respect to shear stress, atherosclerosis, and endothelial biology, respectively. These tables indicate the titles of each of the studies, whether changes were seen in CLEC14A/Clec14a and RhoJ levels and whether the study is explored further in this Chapter.

Table 4.1: Table highlighting CLEC14a/A and RhoJ changes in databases relating to endothelial shear stress. Change is highlighted in green and the studies pursued for further analysis are in grey.

DataSet	Shear Stress Dataset Study Name	CLEC14a/A	RhoJ
GDS4525	Aortic endothelial cell a response to very high wall shear stress	Change	Change
GDS3868	Elevated laminar shear stress effect on umbilical endothelial cells	Change	Change

Table 4.2: Table highlighting CLEC14a/A and RhoJ changes in databases relating to atherosclerosis. Change is highlighted in green, with no change coloured light orange and the studies pursued for further analysis are in grey.

DataSet	Atherosclerosis DataSet Study Name	CLEC14A	RhoJ
GSE120521	RNA-seq of stable and unstable section of human atherosclerotic plaques	Change	No Change
GDS3698	Differential gene expression in atherosclerotic coronary artery presenting at least 75% stenosis with calcified plaques.	Change	No Data
GDS5083	Comparing gene expression between intact arterial tissue and carotid plaque	Change	Change
GDS1597	Human coronary artery study	Change	Change
GSE163614	Gene expression profile in cerebral ischemia-reperfusion injury of rat model	Change	Change
GDS2773	Endothelial cell response to acute vs chronic activation by tumour necrosis factor	Change	Change
GDS4262	Oxidized low-density lipoprotein effect on LOX-1 overexpressing aortic endothelial cell line HAECT: time course	Change	Change
GSE166162	Expression data from the cortex after middle cerebral artery occlusion (MCAO) between young and aged rats	Change	No Change
GDS1300	Hyperlipidemic model of adaptive immunity in aorta during atherogenesis	Change	No Change
GSE162072	Transcriptome profiling following focal ischemic stroke in female rats	No Change	No Change
GDS4527	Atherosclerosis susceptibility model: macrophages	No Change	No Change
GDS3818	Atherosclerotic lesion regression: aorta	No Change	No Data

Table 4.3: Table highlighting CLEC14a/A and RhoJ changes in databases relating to Endothelial Biology. Change is highlighted in green, with no change coloured light orange and the studies pursued for further analysis are in grey.

DataSet	Endothelial Biology Study Name	CLEC14a/A	RhoJ
GDS2009	Sustained EGR1 expression in endothelial cells: time course	Change	Change
GDS2040	Endothelial cell morphogenesis	Change	Change
GDS2322	Vascular endothelial cell differentiation in vitro	Change	Change
GDS1701	Endothelial progenitor cells in fetal liver	Change	Change
GDS5651	DNA methyltransferase inhibitor 5-Aza-2'deoxycytidine effect on partially-ligated left carotid artery	Change	Change
GDS3060	Endometriosis: endometrial endothelial cells	Change	Change
GDS2902	Hypoxia and lymphathic endothelial cells	Change	Change
GDS3177	Confluent and sub-confluent umbilical vein endothelial cell cultures	Change	No Change
GDS3848	HMEC-1 endothelial cell line response to infection by Rickettsia prowazekii	Change	Change
GDS4777	Freshly-isolated and cultured arterial and venous endothelial cells	Change	Change
GDS5432	Age effect on corneal endothelium	Change	Change
GDS3790	Erk5 activation effect on endothelial cells	No Change	Change
GDS3557	ERG transcription factor depletion effect on endothelial cell	No Change	Change
GDS1354	Cirrhosis and liver endothelial cells	No Data	Change
GDS3310	Human herpesvirus-8 infection of primary pulmonary microvascular cells	Change	No Change
GDS3600	Endothelial cell response to estradiol in vitro	Change	No Change
GDS4463	Endothelial cells from P8 neonatal retina	No Data	Change
GDS5417	Embryonic lung and brain cortex- endothelial cells	Change	No Change
GDS5914	YAP transcriptional regulator depletion effect on endothelial cells	No Change	Change
GDS1968	Endothelial cell response to hypoxia and subsequent reoxygenation	No Change	No Data
GDS1553	Fullerene effect on vascular endothelial cells	No Change	No Change

GDS2484	Dermal lymphatic endothelial cell response to tumor necrosis factor alpha	No Change	No Change
GDS2571	Bone morphogenic protein 6 effect on an endothelial cell line: time course	No Change	No Change
GDS5083	Carotid artery atheroma	Change	No Change
GDS5007	Fetal and neonatal ductus arteriosus and aorta: endothelial cells	No Change	Change
GDS3683	ACE inhibitor captopril effect on atherosclerosis model: aorta	No Change	Change
GDS3355	Angiopoietin-1 stimulation of vascular endothelial cells	No Change	No Change
GDS3440	Aortic endothelial cell response to dominant negative PPAR gamma expression in vitro	No Change	No Change
GDS3810	TNF receptor and lymphotoxin beta -receptor activation effect on aortic endothelial cells in vitro	No Change	No Change
GDS4773	Peripheral venous congestion model: endothelial cells	No Change	No Change
GDS4778	Freshly-isolated umbilical cord arterial and venous endothelial cells	No Change	No Change
GDS5633	Peroxisome proliferator-activated receptor β,δ agonist and hypoxia effects on umbilical vein endothelial cells	No Change	No Change

4.3 Bioinformatics results

4.3.1 Effect of Shear Stress on CLEC14A and RhoJ Expression

CLEC14A expression is negatively regulated by shear stress, with in vitro studies showing that exposure of HUVECs to 2 Pa of laminar shear stress reduced CLEC14A mRNA levels compared to static conditions (67). However, the effect of higher arterial shear on CLEC14A, like the blood flow through regions of stenosed arteries, remains unknown. From the GEO Database searches, two *in vitro* microarray studies were used to compare the effect of normal and elevated shear stress generated using a parallel plate flow apparatus on endothelial cell expression. In the first study, different batches of pooled (passage 2-4) HUVEC were cultured for 48-72 hours, and flow was introduced at 1.5 Pa shear stress and high 7.5 Pa shear stress independently for 24hr (Figure 4.1). A known shear regulated gene KLF2 was interrogated to determine the validity of the data and indeed there was significant upregulation of this gene when shear was raised from 1.5 Pa vs 7.5 Pa. Data from four biological repeats showed that CLEC14A expression under higher 7.5 Pa shear stress was significantly decreased when compared to 1.5 Pa shear stress, and results showed that CLEC14A was one of the 50 most downregulated genes in the whole database through Gene Set Enrichment Analysis (GSEA) (115).

A second similar study was examined which used bovine aortic endothelial cells and subjected them to static conditions, normal arterial laminar flow at 2 Pa and very high at 10 Pa each for 24 hours, with three experimental repeats (Figure 4.2). As expected, CLEC14a expression showed a statistically significant decrease when comparing static conditions with 2 Pa laminar shear stress. However, at 10 Pa, there was a statistically significant elevation in

CLEC14a expression to a level like that seen in endothelial cells exposed to static levels. KLF2 expression showed a statistically significant stepwise increase between each of the three levels of shear stress, with the highest expression at 10 Pa. These two studies are consistent with a bimodal expression of CLEC14A/a with high expression levels in static conditions and very high shear stress, and lowest levels seen at intermediate arterial levels of shear stress.

RhoJ was another gene probed to determine its expression profile when subjected to various levels of shear stress. In the first study, where expression was measured at 1.5 Pa to 7.5 Pa, RhoJ expression showed a slight but not statistically significant increase at the higher level (Figure 4.1). However, with the second study, in which expression was measured at 0, 2 and 10 Pa, there was a statistically significant reduction in RhoJ expression from endothelial cells exposed to 0 Pa and 10 Pa and between 2 Pa and 10 Pa (Figure 4.2). This suggests that RhoJ expression is downregulated in response to very high shear stress levels of 10 Pa.

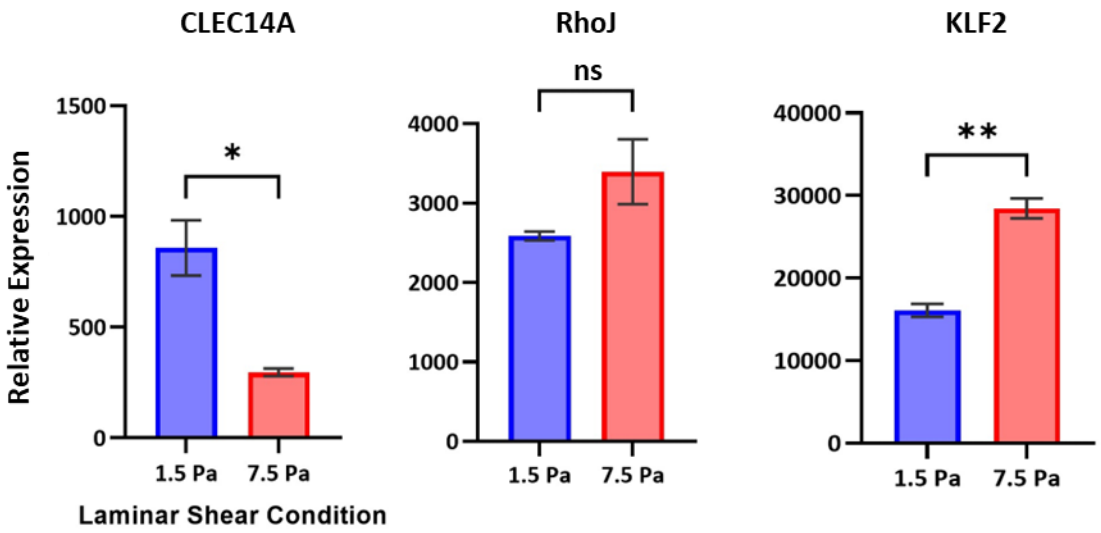

Figure 4.1 Higher laminar shear levels influences CLEC14A expression, and RhoJ expression shows small increase with higher laminar shear (GEO DataSet ID GDS3868). HUVECs were cultured and subjected to normal arterial laminar shear stress at 1.5 Pa for 24 hours and compared to cultured HUVECs exposed to 5 times more shear stress at 7.5 Pa for 24 hours. The mean was calculated using 4 independent biological replicates with each bar representing log2-transformed gene expression normalised using inter-array quantile normalisation. Error bars present the standard error of the mean (SEM). Statistical analyses were performed using paired t-tests (*=P<0.05).

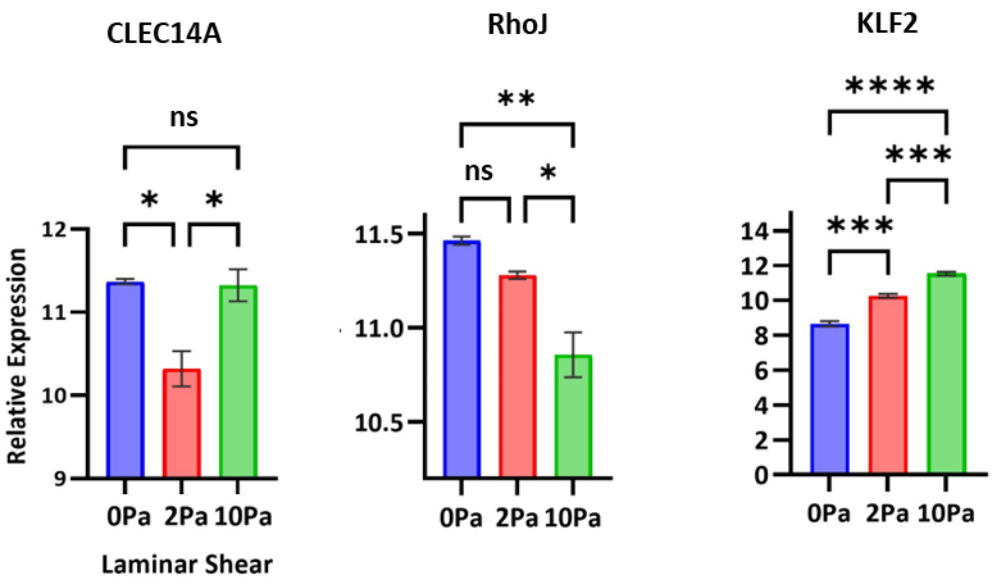

Figure 4.2 Very high shear stress levels at 10 Pa, similar to those found around early plaque formation, reverse shear dependent downregulation of CLEC14a. On the other hand, RhoJ shows a shear stress dependent decrease in expression (GEO DataSet ID GDS4525). Bovine Aortic Endothelial Cells were subjected to 3 different shear stress profiles for 24 hrs in an in-flow chamber using flow loop system inducing: very high wall shear stress (10 Pa), normal wall shear stress (2 Pa) and no flow (0 Pa) static controls to see molecular mechanism involved in adaptive remodelling at higher shear. KLF2 confirms that the shear stress apparatus worked since KLF2 is positively upregulated by higher laminar shear. The gene expression was normalised to 18srRNA. The mean was calculated using 3 biological replicates and error bars represent the SEM. Statistical analyses were performed using one-way ANOVA which showed that CLEC14A was significantly reduced $P<0.01$. Tukey's multiple comparison test was used to compare 0 Pa vs 2 Pa (*=$P<0.05$) and 2 Pa vs 10 Pa (*=$P<0.05$).

4.3.2 Atherosclerosis Related Studies on Clec14a/A and RhoJ Expression

Since atherosclerosis is a disease of shear stress dysregulation (116), bioinformatic microarray studies relating to plaque formation were analysed. CLEC14A expression, unlike RhoJ, is known to be directly linked to atherosclerosis, with a stenosis dependent increase in human atherosclerotic vessels (78), but the cause is yet to be determined. One of the areas of interest was to gain insight into whether CLEC14a/A or RhoJ expression is different because of the altered flow conditions associated with the plaque formation or whether there may be other factors associated with atherosclerosis affecting its expression. For example, it could be the disturbed flow induced by the plaque that is upregulating CLEC14a/A or there could be something inherent in the plaque that is upregulating CLEC14a/A irrespective of flow. It may be that plaque condition, presence of pro-inflammatory cytokines such as TNF-α and/or oxidative stress also modulate the expression of CLEC14a/A. Microarrays related to these areas were explored to answer this question.

The first plaque bioinformatic study looked at CLEC14A expression relative to the expression of the ubiquitin C housekeeping gene from the RNA-sequencing of four patients, comparing stable sections of human atherosclerotic plaques with unstable plaques. The samples were harvested during carotid endarterectomy surgery and were categorised using the American Heart Association (AHA) classification into stable (type I-II, III, VII, VII) or unstable/ruptured plaques (type IV-V, VI) based on their histological characteristics (117). CLEC14A expression between the two plaque types revealed higher CLEC14A expression in unstable plaques opposed to stable plaques across all the four patients (Figure 4.3). The expression of two other genes were also interrogated in these samples. vWF expression was used to

determine the endothelial cell content per sample, as this gene is expressed exclusively by endothelial cells and the plaque samples consist of a mixture of cell types. The expression of CLEC14A is also restricted to endothelial cells (67), and a high CLEC14A expression could simply reflect a high plaque endothelial content. In patient 1-3 but not patient 4, CLEC14A mirrors vWF expression data suggesting this may be the case. However, when plotting the CLEC14A:vWF ratio, the trend seen between stable vs unstable plaque shows that even when accounting for endothelial content, the expression of CLEC14A is slightly higher in the unstable plaques, however this is not statistically significant when combining the data from each of the patients. A third gene investigated was TIE2, this was of interest because like CLEC14A, its expression is both endothelial and it is regulated by shear stress with its expression down regulated in areas of high laminar shear stress (118). If CLEC14A expression followed the expression of TIE2, it would suggest that flow is a major determinant in regulating CLEC14A expression, and if it did not then it might suggest other factors, such as those mentioned above, may have a more major influence on plaque expression of CLEC14A. Data from all patients show that Tie 1 and CLEC14A expression mirror each other closely, with the exception of patient 1, the CLEC14A:TIE2 ratio shows no difference between stable and unstable plaques, suggesting that in these samples flow is the major determinant in regulating CLEC14A expression. CLEC14A expression in the unstable plaque from patient 1 was particularly high and its expression was elevated relative to TIE2 expression, so it is possible that in the plaque different factors may have influenced CLEC14A expression, but it is not possible to draw conclusions from this single data point.

Next RhoJ gene was interrogated which revealed that RhoJ expression was unchanged in stable and unstable plaques. The vWF expression data did not match the RhoJ expression for the exception of patient 3 (Figure 4.3). TIE1 expression also did not mirror RhoJ expression data as was the case for RhoJ:vWF and RhoJ:TIE1 ratios suggesting that both endothelial cell content and flow were not major determinants in regulating RhoJ expression although more datapoints are needed to be conclusive. The RhoJ:vWF and RhoJ:TIE1 ratio for patient 1 is markedly higher in the stable plaque than the unstable plaque compared to the other 3 patients. This is reflected in the large error bars in the mean plot for RhoJ:vWF ratio which resulted in an overall insignificant difference between the 2 plaque conditions (Figure 4.3).

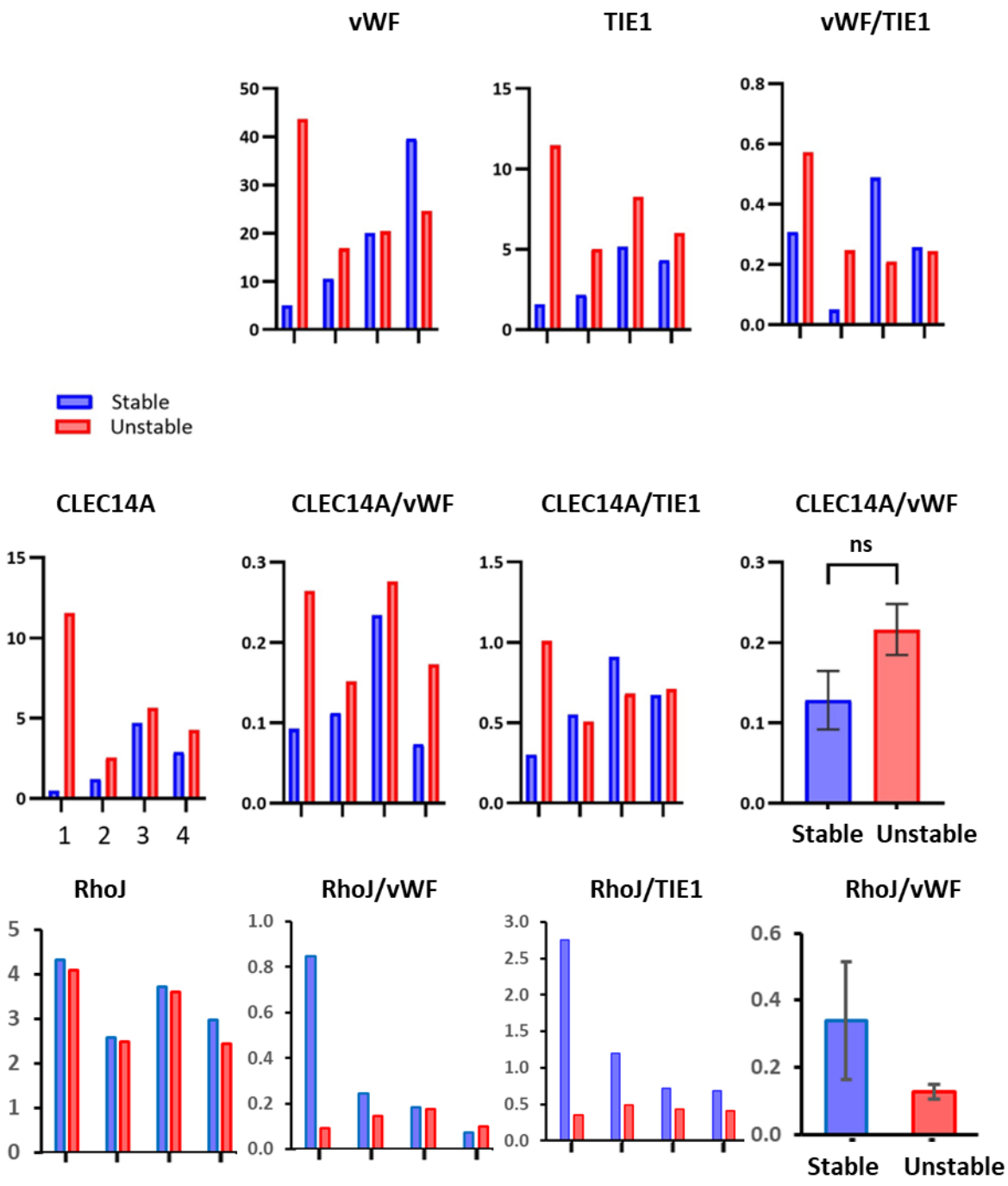

Figure 4.3 CLEC14A expression is elevated in unstable vs stable plaques and RhoJ expression was reduced (GEO DataSet GSE120521). RNA was extracted from 4 unstable (ruptured) sections of human atherosclerotic plaque and 4 from stable regions obtained during carotid endarterectomy operation, and the gene expression relative to ubiquitin C housekeeping gene of each condition were compared. Each bar represents the mean and the expression fold value was calculated as log 2 base. Data of CLEC14A/vWF and RhoJ/vWF ratio is presented as SEM. Statistical analyses were performed using a paired t-test to compare stable plaque with unstable plaque (ns=P>0.05).

Other atherosclerosis microarray studies were looked at to better understand the molecular processes of involved in atherosclerosis. Firstly, the expression data of CLEC14A was analysed from a database study containing 32 individual samples of atheroma plaques and healthy adjacent carotid arterial tissue from patients undergoing endarterectomy surgery. As both diseased and healthy control samples were from same patient a comparison within patients could be made without issues surrounding control tissue collection (119). Each sample pair was numbered by a pathologist and blindly examined for histology using the AHA type I and II criteria to categorise intact control tissues, and AHA stage IV or over for diseased samples which contained both core and shoulder of the plaque (119). CLEC14A expression inside the plaque tissues was significantly greater than the adjacent healthy tissue (Figure 4.4). vWF expression was also examined as a marker of endothelial cells, and like CLEC14A there was a significant increase in vWF expression in the plaque tissue compared with the normal arterial tissue, indicating a significantly greater endothelial content in the plaque tissue. However, the ratio of CLEC14A:vWF expression was found to be significantly lower in plaque tissue compared with the normal arterial tissue indicating that CLEC14A was not specifically upregulated in endothelial cells from the plaque tissue. This suggests that regulation of plaque expression of CLEC14A expression is complex.

RhoJ expression profile was interrogated to understand its role in atherosclerosis pathology. The data revealed RhoJ expression was slightly downregulated in the plaque tissues compared to adjacent healthy control tissue, but this difference was not statistically significant (Figure 4.5). However, given the statistically significant increase in vWF expression in the plaque tissue, normalisation of RhoJ expression to vWF expression

indicated a significant decrease in the RhoJ:vWF ratio, suggesting that endothelial expression of RhoJ was lower in atherosclerotic plaques.

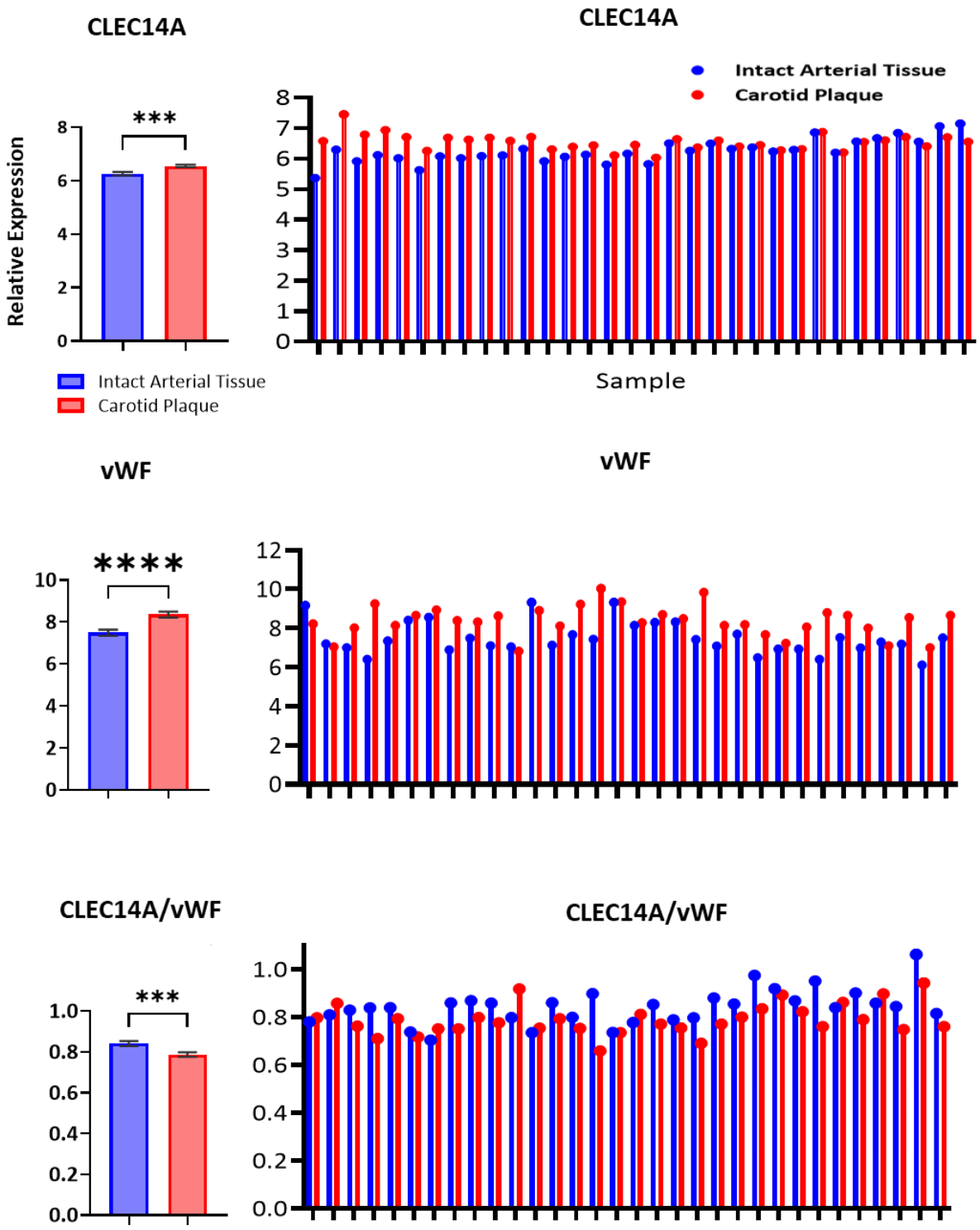

Figure 4.4 When corrected for changes in flow and endothelial content, human carotid plaques caused a downregulation in CLEC14A and RhoJ expression compared to intact arterial tissue (Dataset ID GDS5083). A microarray was done to analyse mRNA gene expression from 32 pieces of carotid atherosclerotic plaque samples containing core and shoulders of the plaque (stary classification stage IV and over). These were taken from hypertensive patients during endarterectomy surgery and paired with a corresponding intact tissue sample (stage I and II). Each bar represents the mean of 32 biological replicates; error bars present the SEM and relative plots are from ratios of individual datapoints. Statistical analyses were performed using a paired t-test to compare the means of intact tissue data with plaque tissue data (ns=P>0.05, *=P<0.05, ****=P<0.0001).

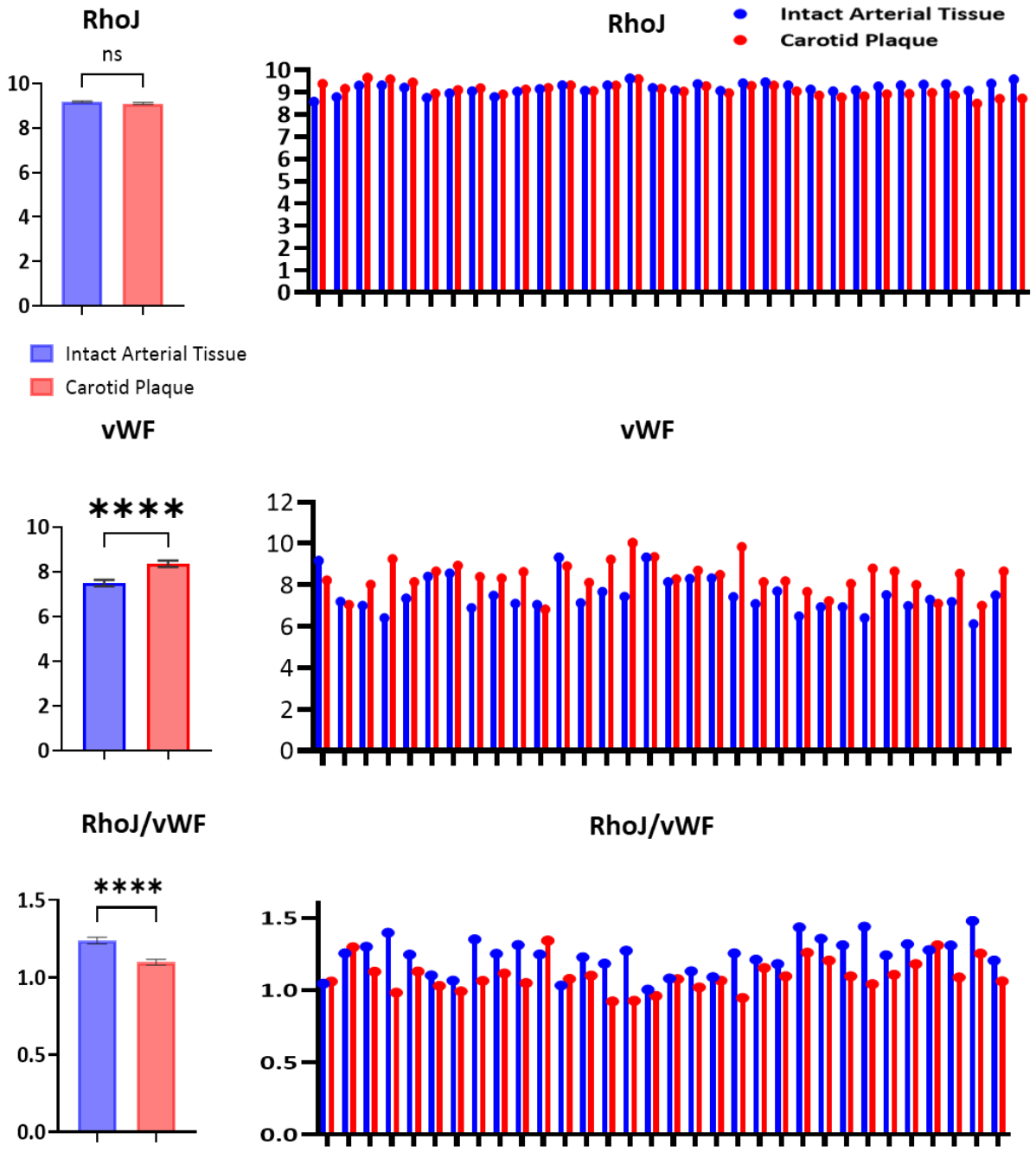

Figure 4.5 When corrected for changes in flow and endothelial content, human carotid plaques caused a downregulation in CLEC14A and RhoJ expression compared to intact arterial tissue (Dataset ID GDS5083). A microarray was done to analyse mRNA gene expression from 32 pieces of carotid atherosclerotic plaque samples containing core and shoulders of the plaque (stary classification stage IV and over). These were taken from hypertensive patients during endarterectomy surgery and paired with a corresponding intact tissue sample (stage I and II). Each bar represents the mean of 32 biological replicates; error bars present the SEM and relative plots are from ratios of individual datapoints. Statistical analyses were performed using a paired t-test to compare the means of intact tissue data with plaque tissue data (ns=P>0.05, *=P<0.05, ****=P<0.0001).

The third atherosclerosis microarray analysis looked at how calcified plaques effect human coronary gene expression, and CLEC14A expression relative to control GAPDH (Glyceraldehyde 3-phosphate dehydrogenase) gene was interrogated in this dataset. Different sections of calcified plaques (AHA type VI or VII) from coronary arteries with at least 75% stenosis were harvested from eight symptomatic patients and compared with a pool sample of 10 healthy control coronary arteries (120). Of the eight patients only 6 had datapoints for CLEC14A. Not only were there differences in CLEC14A expression between all the patients but also in the individual samples themselves highlighting extensive variation in individual patients (Figure 4.6). Patient 1, 5 and 6 showed an upregulation of CLEC14A whereas patients 2, 3 and 4 showed a downregulation suggesting each patient plaque sample was behaving differently. Patients 3 and 6 had upregulated vWF expression with patient 1,2,4 and 5 showing a downregulation in expression of this gene. Patients 1, 4, 5 and 6 showed an upregulation of TIE1 expression whereas the converse observed in patient 2. Highlighting the variability in the data further was complete inconsistency in the CLEC14A:vWF and CLEC14A:TIE1 ratios between patients. These data are difficult to interpret but indicate that there are likely to be significant differences in the composition of the plaque samples and possibly how these samples are treated post-mortem, so it is difficult to infer information about CLEC14A expression from these studies. There was no data for RhoJ in this study.

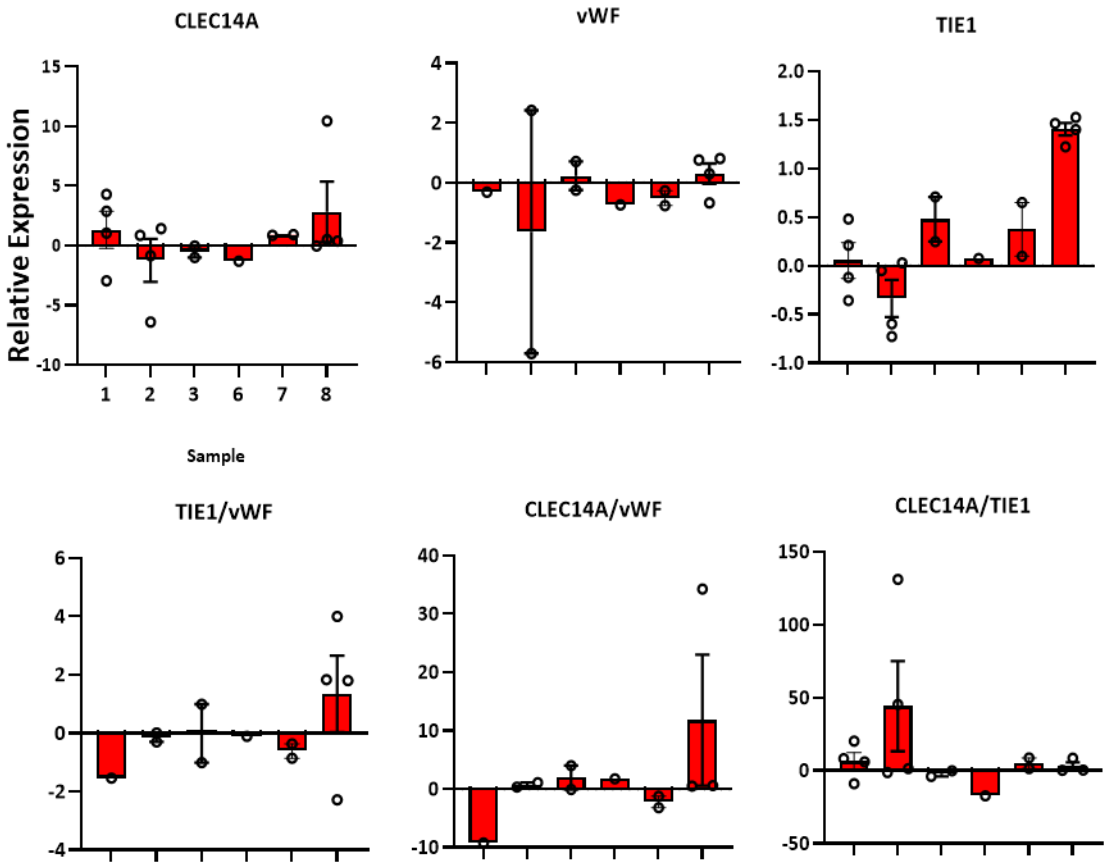

Figure 4.6 CLEC14A plaque expression is variable (GEO DataSet GDS3698). A DNA microarray study was done using type VI or VII atherosclerotic calcified plaques (stenosis ≥ 75%) harvested from coronary arteries from 8 patients, using 10 pooled samples without plaque as the control. The relative fold change was represented as log2 of fold change relative to GAPDH gene. The individual datapoints are represented by the small circles, and the bar represents the mean, and the error bars represent the SEM.

In another similar microarray analysis, RNA was extracted from 51 segments of coronary arterial plaques from 22 patients and expression was quantified relative to a pooled control of healthy RNA samples to produce a gene profile from each segment. The database was mined for CLEC14A and RhoJ expression data and analysed. CLEC14A expression between the plaque samples was highly variable both between samples from the same patient and between patients (Figure 4.7) and did not follow the expression of vWF and TIE1 suggesting that factors other than endothelial cell content and shear stress are responsible for the differences.

RhoJ expression revealed a downregulation across all samples suggesting that RhoJ expression is lower in plaque tissue relative to pooled controls (Figure 4.8). To some extent this does mirror the expression of vWF, but again high variation between samples make evaluation of this difficult.

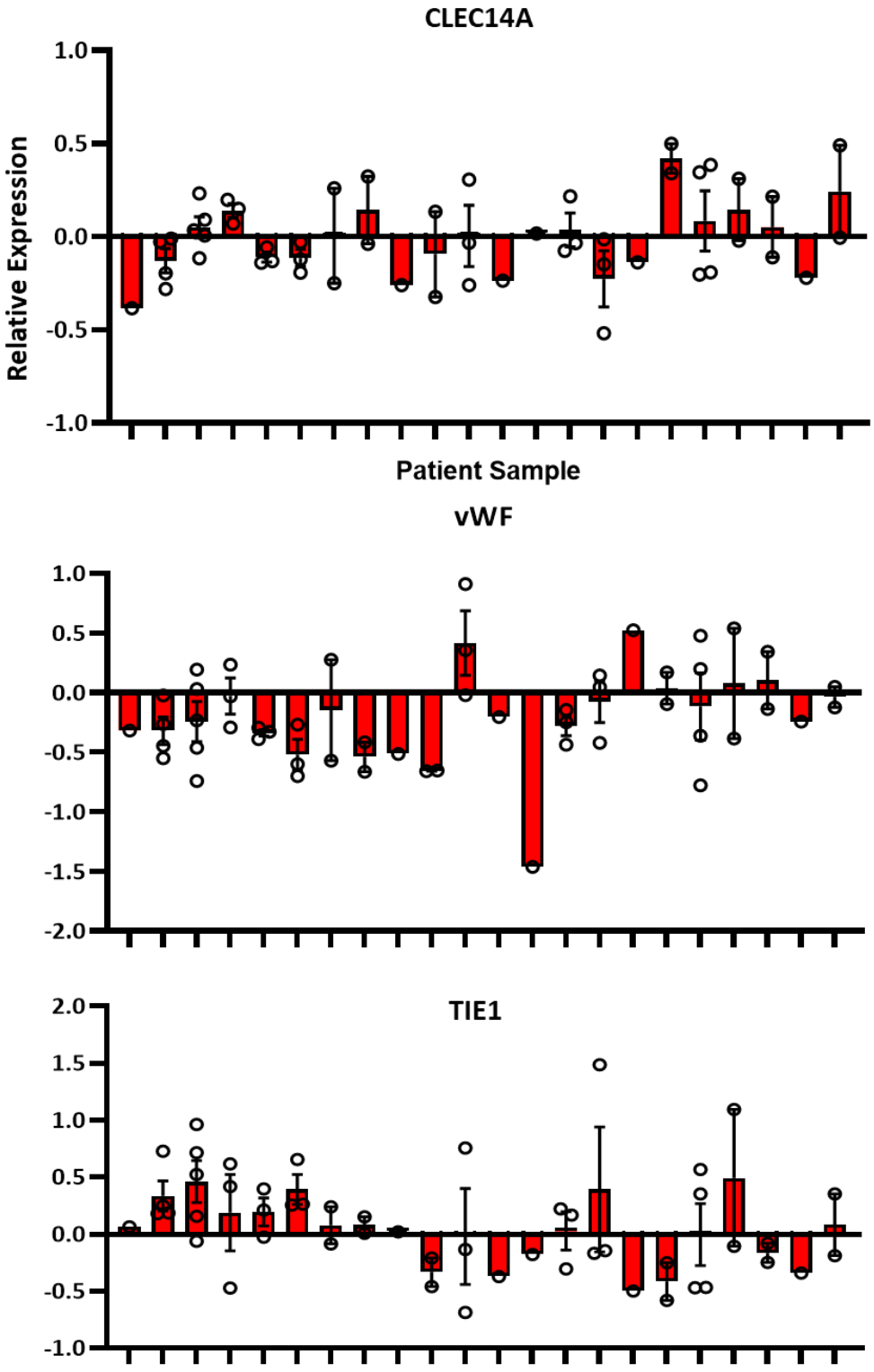

Figure 4.7 CLEC14A and RhoJ expression fluctuates vastly between human atherosclerotic plaques (Dataset ID GDS1597). 51 segments of coronary arterial plaques were obtained after heart transplantation surgery from 22 patients, and total RNA retrieved used for analysis was compared to a pooled disease-free sample group. RNA was quantified using a Microarray Scanner System to measure the fluorescence given off from the biomolecules conjugated to fluorescent dye within each sample RNA. Data was presented as a relative fold change [log2(FC)]; each individual bar represents mean calculated using 5 biological replicates and error bars were presented as SEM of each patient sample. The small circles represent individual datapoints.

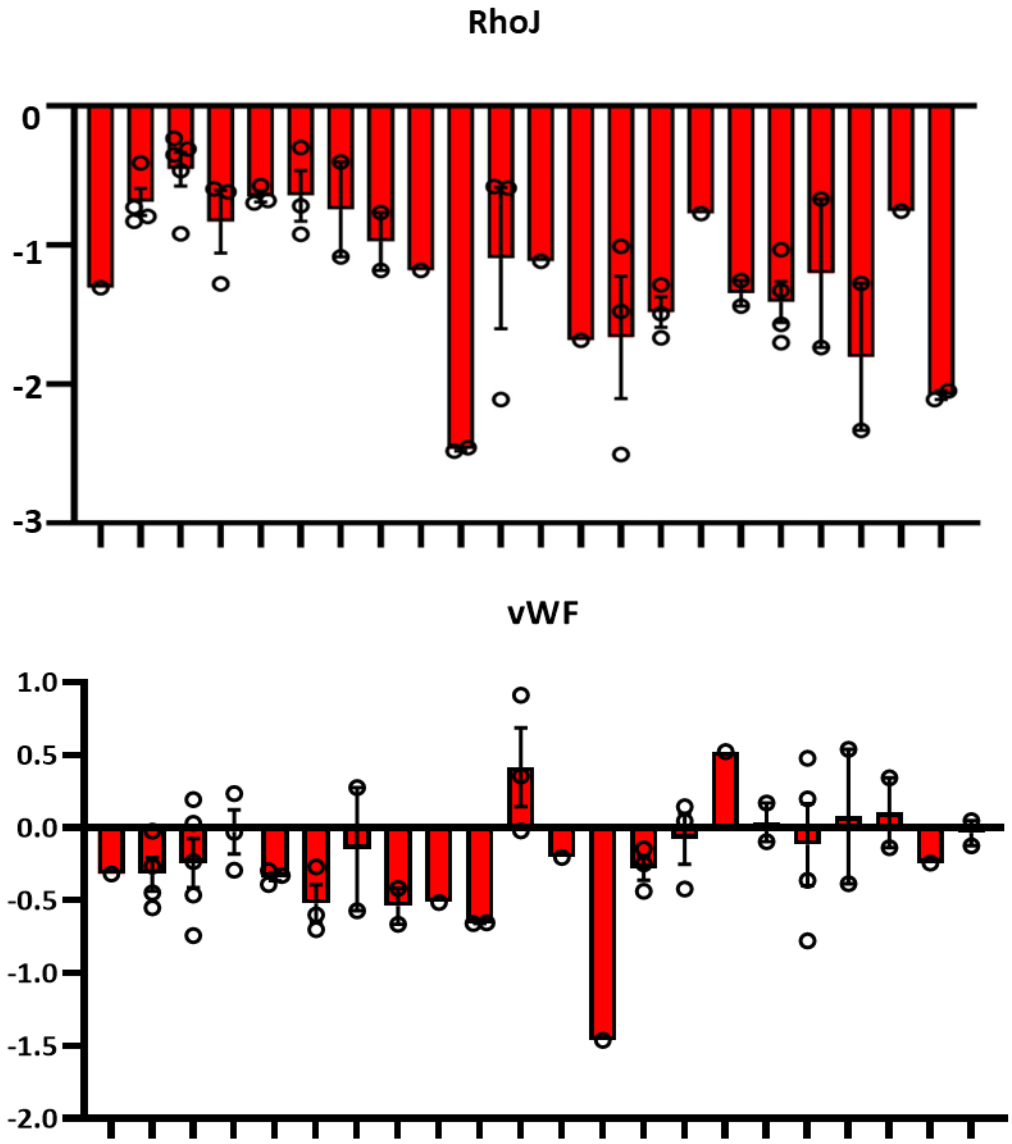

Figure 4.8 CLEC14A and RhoJ expression fluctuates vastly between human atherosclerotic plaques (Dataset ID GDS1597). 51 segments of coronary arterial plaques were obtained after heart transplantation surgery from 22 patients, and total RNA retrieved used for analysis was compared to a pooled disease-free sample group. RNA was quantified using a Microarray Scanner System to measure the fluorescence given off from the biomolecules conjugated to fluorescent dye within each sample RNA. Data was presented as a relative fold change (log2(FC)); each individual bar represents mean calculated using 5 biological replicates and error bars were presented as SEM of each patient sample. The small circles represent individual datapoints.

4.3.3 CLEC14a and RhoJ Expression Data from Microarray Studies Related to The Effect of Oxidative Stress using the Ischemia and Reperfusion Injury Model in Mice

Oxidative stress is one of the key components in the pathophysiology of vascular disease such as atherosclerosis (121). To explore this further, data from high throughput RNA transcriptome sequencing database was used to study how oxidative stress modifies gene expression in cerebral ischemia-reperfusion injury in rats. To induce cerebral ischemia-reperfusion injury a suture was applied to occlude the middle cerebral artery in three rats for 90-minutes to induce ischaemia. After 90 minutes the suture was removed to cause reperfusion for 24 hours (MCAO/R) before the rat was sacrificed and brain cortex RNA was extracted, purified and sequenced for transcriptome analysis (122). CLEC14a expression showed no significant difference between MCAO/R samples compared to control sham brain samples, and overall, its expression was low compared with vWF and TIE1. vWF expression was interrogated because of the difficulty in standardising sample collection and this was significantly higher in MCAO/R samples. Changes in CLEC14a expression were mirrored by the changes in vWF, and the CLEC14a:vWF ratio showed was very similar between MCAO/R and Sham control samples. These data suggest CLEC14a is not modulated by oxidative stress (Figure 4.9).

RhoJ expression showed a significant upregulation in MCAO/R sample compared to the sham control, and this upregulation was higher than that observed for wWF expression. This resulted in an increased RhoJ:vWF ratio in samples that had experienced ischaemia-reperfusion. This suggests RhoJ expression is affected by oxidative stress and may have a role in endothelial cell responses to this stress (Figure 4.9).

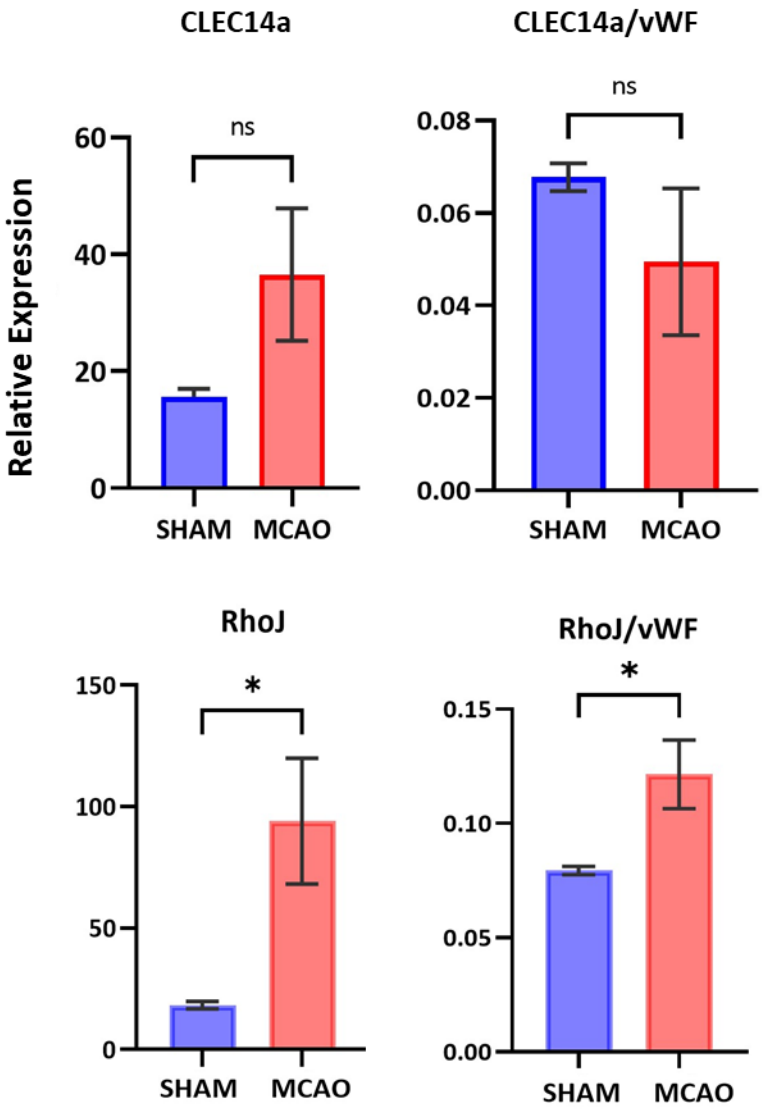

Figure 4.9 Reperfusion injury does not consistently effect CLEC14a expression but it has a significant effect on RhoJ expression (GEO DataSet GSE163614). In this RNA transcriptome sequencing study, a suture was applied to occlude rat middle cerebral artery (MCAO) to cause a 90-min ischemic period and released to restore blood flow and induce oxidative stress. Samples were harvested from sham rat models (control) and cerebral ischemia-reperfusion injury (oxidative stress) rat models. The mean was calculated using 3 independent experiments and is presented as bar in the plot. The error bars are presented as SEM of each condition. Statistical analyses were performed using an unpaired t-test to compare the Sham control sample with MCAO/R model samples (ns=P>0.05, *=P<0.05)

4.3.4 CLEC14a and RhoJ Expression Data from Microarray Studies Related to Proinflammatory Cytokine TNF-α

Inflammation is a key driver of atherogenesis and the inflammatory cytokine TNF-α is involved in endothelial activation and leukocyte recruitment (123). To understand its role in regulating the expression of CLEC14a and RhoJ, microarray data was interrogated to look at the response of vascular endothelial cells undergoing either an acute TNF-α challenge or continuous challenge induced by the transfection of a plasmid encoding non-cleavable TNF-α. Endothelial cells over-expressing non-cleavable transmembrane mutant form of murine TNF (tmTNF) were cultured, along with TNF-α treated control endothelial cells and non-treated mock transfected control cells (124). RNA was extracted and subjected to microarray analyses. CLEC14a expression was significantly downregulated in both acute and chronic TNF-α activation conditions relative to untreated control suggesting CLEC14a expression is regulated by TNF-α (Figure 4.10). RhoJ expression profile showed no significant difference in response to acute or chronic TNF- α exposure.

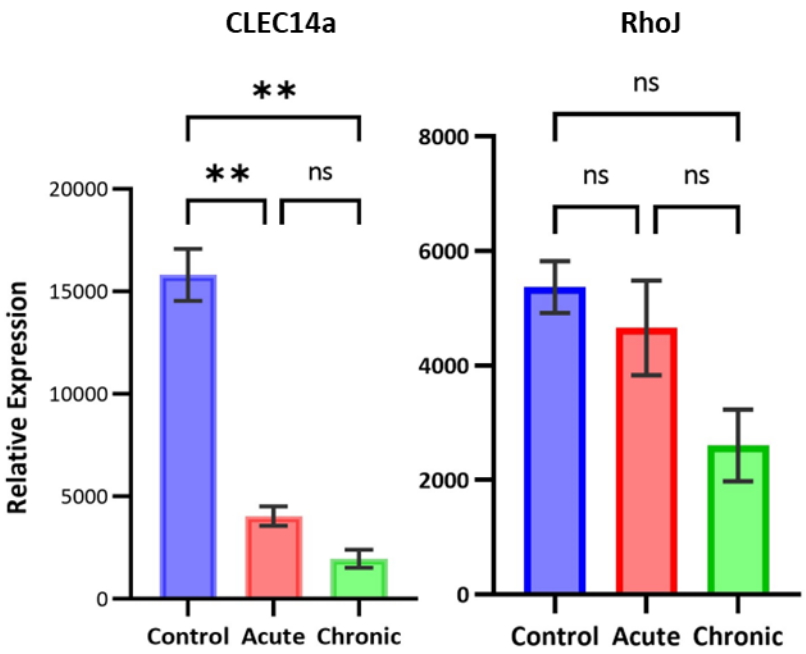

Figure 4.10 CLEC14a expression is regulated by TNF-α inflammatory cytokines and RhoJ expression shows an insignificant reduction under chronic inflammation (GEO DataSet GDS2773). This experiment compared the response of vascular endothelial cells from newborn mice that were either treated with soluble TNF-α (20ng/ml) for 4 hours to induce acute inflammation or stably transfected with a non-cleavable transmembrane mutant form of mice TNF-α (over-expression) to induce chronic inflammation. The mean is depicted in the bars from 2 independent experiments using 3 independent clones of each cell type and error bar presents the SEM of each condition. Statistical analyses were performed using one-way ANOVA which showed a significant difference in CLEC14a expression between control, acute and chronic inflammation (*=P<0.01). Tukey's multiple comparison test was used to compare control and acute condition (**=P<0.01) and control vs chronic (**=P<0.01).

4.3.5 Microarray Studies Related to Endothelial Regulation of CLEC14A and RhoJ

Transcription factors play an important role in regulating normal vascular and pathologic endothelial biology (125, 126). CLEC14A and RhoJ genes were interrogated in three bioinformatic microarray studies to understand how CLEC14A and RhoJ gene activity is being regulated and further our knowledge of the molecular pathways involved. Firstly, data from a study looking into the possible targets of the transcription factor Early Growth Response 1 (EGR-1) were analysed. EGR-1 has a role in regulating and promoting atherosclerosis and is known to be activated by various stimuli such as inflammatory cytokines and shear stress (127). In this study, HUVECs were transduced with either control adenovirus or adenovirus encoding EGR-1 and the effect of over-expression of EGR-1 was assessed over a 48-hour period. Successful EGR-1 adenovirus transduction was confirmed by measuring EGR-1 mRNA and protein levels though qPCR and western blot. The RNA was extracted after 16, 24 and 48 hours for each sample type and a microarray was performed. In response to EGR-1 overexpression CLEC14A showed a time-dependent decrease from 16 hours to 48 hours compared to the no vector control and empty vector control suggesting EGR-1 has a role in regulating CLEC14A gene activity (Figure 4.11). RhoJ followed the same trend showing greater reduction at 48 hours of sustained EGR1 expression suggesting it is an EGR-1 target gene. However, any conclusions drawn are limited by the one data point.

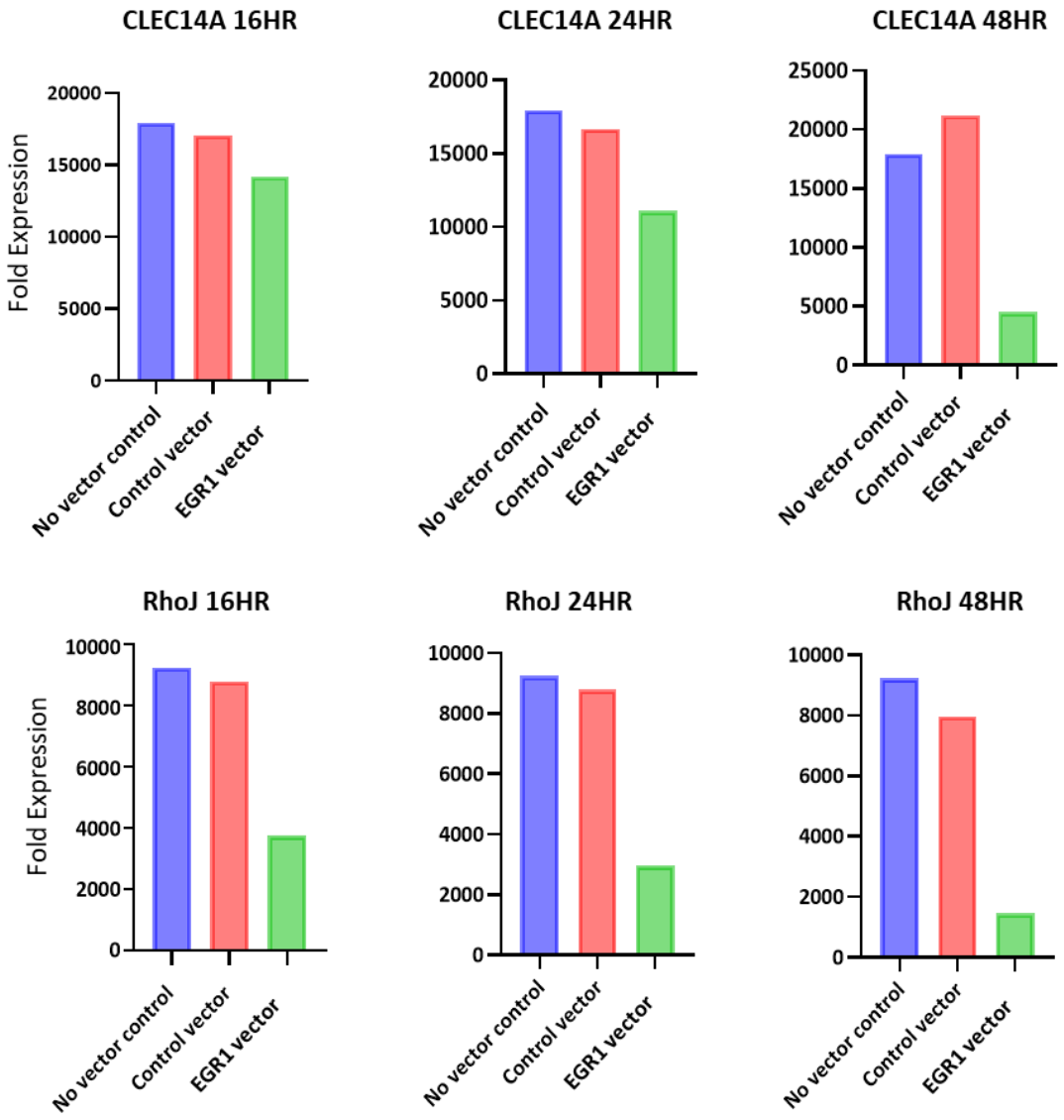

Figure 4.11 EGR1 regulates CLEC14A and RhoJ expression in a time-dependent manner (GEO DataSet GDS2009). Densely cultured HUVEC were infected with recombinant adenoviruses expressing EGR-1 or empty control and RNA was extracted at 16, 24 and 48 hours of infection, and analysed using Affymetrix U133 GeneChip-set to identify EGR-1 target genes. Transient induction of EGR1 decreased CLEC14A and RhoJ expression in relation to both controls with 48hr induction producing the largest reduction. Gene expression changes for EGR1 expressing adenoviruses were calculated relative to non-infected control cells.

Another transcription factor investigated was ETS (erythroblast transformation-specific) related gene (ERG). This transcription factor is specific to endothelial cells and is a known regulator of RhoJ (89) and can act as transcriptional activators, repressors or both (128). A microarray study utilising siRNA gene silencing was analysed to determine ERG's involvement in the regulation of RhoJ expression in endothelial cells (89). HUVECs were cultured and treated with either ERG-specific siRNA or a non-specific siRNA or an empty control vector. RNA was extracted at 48 hours and knockdown was confirmed using qPCR relative to GAPDH. A microarray was performed using two controls as references, the control vector without any and a negative control siRNA. The data showed a statistically significant reduction in RhoJ mRNA levels in the ERG knockdown samples compared to the controls confirming that RhoJ is regulated by ERG (Figure 4.12). There was no CLEC14A expression dataset from this microarray expression database.

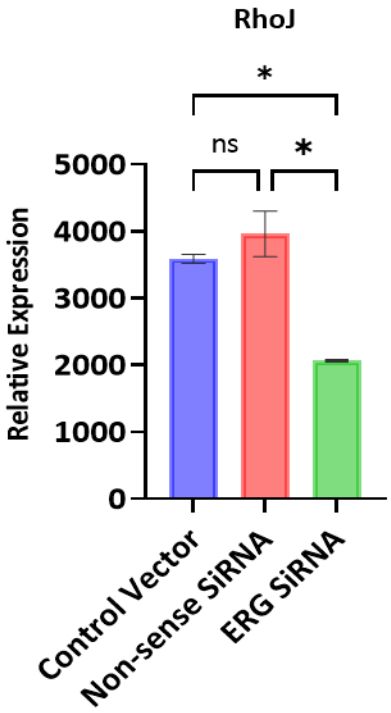

Figure 4.12 ERG siRNA treatment reduces RhoJ expression (GEO Dataset GDS3557). Cultured HUVECs were treated with either ERG SiRNA control vector (no SiRNA) or non-sense SiRNA and microarray analysis was done to help identify targets of ERG and to better understand regulation of normal endothelial cell function. The mean was calculated by 2 biological replicates for each condition and error bars depict SEM. Data was presented as fold changes relative to control SiRNA treated cells. Statistical analyses were performed using one way ANOVA which showed significant decrease between groups (*=P<0.05). Tukey's multiple comparison test was used to compare control convector vs ERG SiRNA and non-sense SiRNA vs ERG SiRNA (*= P<0.05).

Another microarray bioinformatic study was analysed to determine whether RhoJ gene expression is modulated by the MEK5/Erk5 signalling pathway mediated endothelial cell responses to laminar shear. The MEK5/Erk5 pathway belongs to a family of MAPK protein kinases which are activated by laminar shear and are important in modulating angiogenesis as well as atheroprotective responses such as regulating flow induced anti-inflammatory KLF2 and KLF4 gene expression (129, 130). In this microarray study, HUVECs underwent transduction with either control virus or virus to induce expression of a constitutively active form of MEK5, an upstream kinase of ERK5 activation. After 40 hours, RNA was extracted for microarray analysis. The transduced sample data expression was normalised relative to GAPDH housekeeping gene and this was then used to calculate fold change by comparing data from the experimental samples with empty vector control expression data. RhoJ expression was significantly increased in the MEK5D-infected HUVECs samples compared to the empty vector control indicating that activating the MEK5/ERK5 signalling pathway promotes RhoJ expression (Figure 4.13).

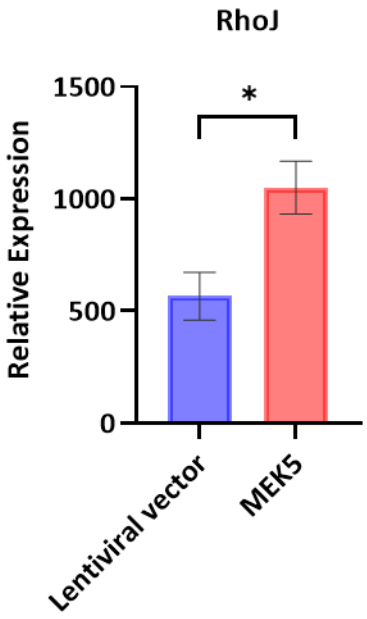

Figure 4.13 Expression of constitutively active MEK5 increases RhoJ expression (GEO Dataset GDS3790). HUVECs were infected with either empty vector or constitutively active MEK5D to activate Erk5 under static conditions to mimic laminar shear to identify the role of MEK5/Erk5 pathway in endothelial function. Expression of each gene was depicted relative to GAPDH and depicted as fold changes compared to empty vector (log ratio changes); three biological replicates were used to determine the mean and error bars show SEM. Statistical analyses were performed using an unpaired t-test to compare RhoJ expression between empty vector and active MEK5 vector samples (*= $P<0.05$)

The next bioinformatic microarray analysis investigated the effect of depleting the transcriptional regulator yes-associated protein (YAP) on endothelial cell gene expression. YAP is a downstream effector of the Hippo pathway which plays an important role in cell mechano-transduction (131). YAP expression, like CLEC14A and RhoJ, is regulated by shear stress with uniform laminar flow inactivating its production and atherogenic disturbed flow activating YAP, with this being shown to promote atherogenesis and plaque progression (132, 133). Changes to CLEC14A and RhoJ gene expression in response to knocking down YAP expression in HUVECs was interrogated in this study. Two different YAP-specific siRNA duplexes and a RISC-free control were used, and RNA was extracted after 30 hours for microarray analysis. YAP knocked down was confirmed through western blot using GAPDH as loading control. Data from four independent experiments for each condition showed that CLEC14A expression relative to HPRT housekeeping gene was no different in YAP-deleted HUVECs compared with the control-treated HUVEC. By contrast, RhoJ expression showed a significant reduction in the HUVEC sample treated with siYAP duplex 2 but not the siYAP duplex 1 compared to RISC-free control (Figure 4.14). The inconsistent results between the two siRNA duplexes indicate that likely one or both siRNA targeting sequences is causing off-target effect and hence no conclusions as to the effects of YAP down-regulation on RhoJ expression can be drawn.

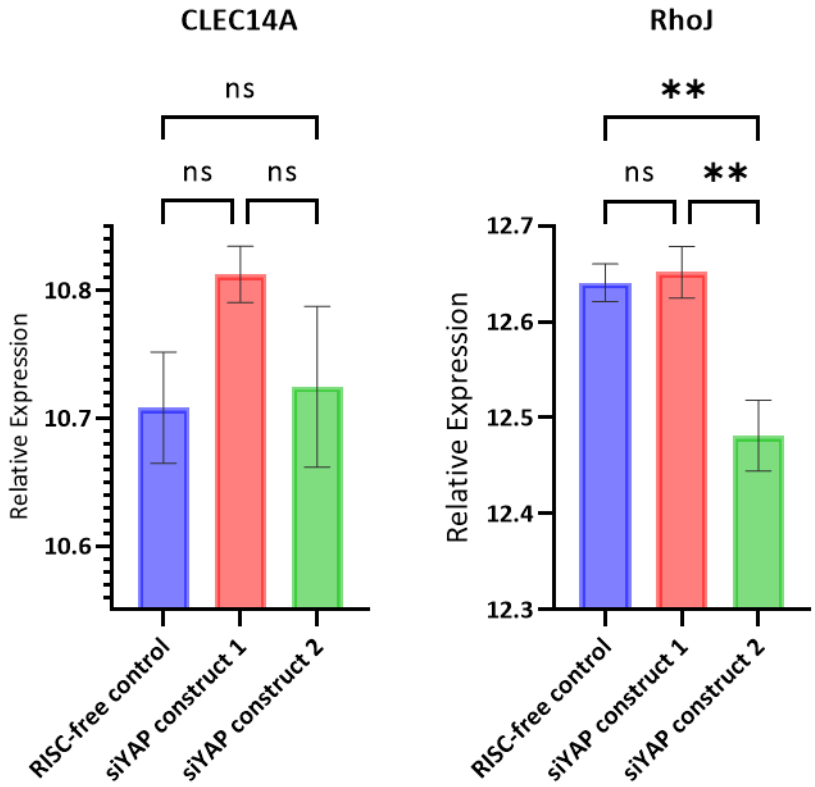

Figure 4.14: HUVECs treated with YAP siRNA Construct 2 resulted in reduction of RhoJ expression in comparison to RISC-free control (GEO Dataset GDS5914). In this study two siRNA constructs were used to knockdown the transcriptional regulator YAP in HUVECs, and RNA was extracted 30 hours post siRNA transfection to undergo expression profiling by microarray to better understand YAP role in endothelial cell proliferation. Each bar represents mean of 4 biological replicates for each condition and the error bars represent the SEM. Gene expression was normalised to HPRT housekeeping gene and data presented as fold change using RISC-free control line as the control group. Statistical analyses were performed using one way ANOVA to determine any significant differences between the subsets (**=P<0.01). Tukey's multiple comparison test was then used to compare control with SiYAP construct 2 (**= P<0.01).

4.3.6 CLEC14A and Rhoj Expression Data from Microarray Study Investigating the Molecular Mechanism of Endothelial Barrier Formation

Endothelial cells become activated by disturbed flow and chronic inflammation which contribute to endothelial dysfunction and loss of healthy endothelial barrier protection (134). A microarray bioinformatic study was analysed to compare gene expression in confluent HUVECs and sub-confluent samples, with the aim to gain insight into the effects of growth and contact inhibition on endothelial barrier formation and function (135). Isolated HUVECs were cultured on a fibronectin-coated surface to confluence and another plate to sub-confluence, with a total of 3 biological replicates for each condition. RNA was extracted and subjected to microarray analysis. The data was interrogated for CLEC14A and RhoJ expression with CLEC14A expression significantly upregulated in confluent HUVECs compared to sub-confluent HUVECs (Figure 4.15). RhoJ expression showed no significant difference between sparse and confluent HUVEC.

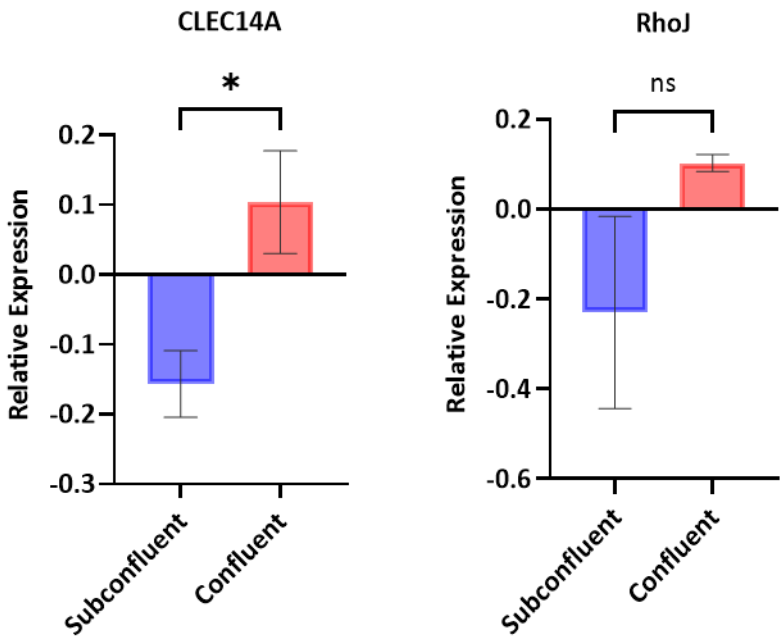

Figure 4.15: CLEC14A expression is significantly different between subconfluent and confluent HUVEC cultures (GEO Dataset GDS3177). Lysates were obtained from HUVECs cultured to confluence and sub-confluence to better understand the molecular mechanism involved in endothelial barrier formation. Data expression is presented as log10 ratio, and gene expression was normalised to β-actin. Mean was calculated using 3 biological repeats for each condition, and error bars depict SEM. Statistical analyses were performed using paired t-tests (*=P<0.05).

4.4 Discussion

4.4.1 Summary

Publicly available microarray databases were interrogated to better understand the expression patterns of CLEC14A and RhoJ. CLEC14A's expression was clearly shown to be shear regulated as had been previously reported (67), but its expression at very high levels of shear stress differed between studies. Analyses of atherosclerotic plaques gave a complex and mixed picture of CLEC14A expression, with some studies showing an overall increase in expression but these data were complicated both by the varying endothelial content within plaque samples and considerable sample variation. *In vitro*, CLEC14A expression was downregulated by TNF-α, reduced after transduction of the EGR1 transcription factor and regulated by cell confluence. *In vitro*, RhoJ expression was down-regulated with siRNA- mediated knockdown of the transcription regulators ERG and the lentiviral transduction of the transcription factor EGR1. Its expression was not affected by cell confluence and there was conflicting data with respect to shear stress. Where data were available, the overall expression levels of RhoJ were unchanged in atherosclerotic plaques, when normalised to the expression of the endothelial specific vWF gene, there was a decrease in RhoJ message levels. By contrast, RhoJ expression was up-regulated in a model of ischaemia-reperfusion injury.

4.4.2 *In vitro* Regulation of CLEC14A Expression

Previously, Mura *et al.* demonstrated that laminar shear stress of 2 Pa for 24 h resulted in the down regulation of CLEC14A expression relative to cells in static culture (67). The two studies examined in this chapter explore CLEC14A expression at higher shear stress levels of

7.5 and 10 Pa, levels that are observed as blood flows around atherosclerotic plaques with at least 40% stenosis (115). The two studies showed opposite patterns of expression, however it should be noted that the sources of cells were different, as were the precise levels of shear stress applied. Endothelial cells sourced from veins (HUVECs) showed a reduction in CLEC14A expression when increasing shear stress from 1.5 Pa to 7.5 Pa, whereas arterial endothelial cells (bovine aorta) showed decreased CLEC14A expression with shear stress increased from 2 Pa to 10 Pa. The different levels of very high shear stress between the two studies make their comparison difficult. In combination they suggest that CLEC14A expression would drop until about 7.5Pa and then sharply increase thereafter. Further experiments would be required to determine whether there is differential CLEC14A expression in vein or arterial endothelial cells, between endothelial cells sourced from different species or whether there might be a difference between 7.5 or 10 Pa. It should be noted that the endothelial cells in these studies are adhered to rigid substrates and are subjected to relatively short periods of shear stress. This is very different from the *in vivo* environment where alterations in shear stress result in adaptive remodelling of the vascular endothelium and the expansion of arteries (108), which will likely impact shear stress response gene expression. Other factors were also shown to influence CLEC14A expression, both long- and short-term exposure to TNF-α down-regulated expression of CLEC14a in neonatal murine endothelial cells, CLEC14A expression was found to increase on cell confluence. These were novel findings of this study, and it would be interesting to further explore their mechanism of regulation of CLEC14A, and how this may impact endothelial biology. CLEC14A expression was found to be down-regulated following transduction of the transcription factor EGR-1. This transcription factor is itself induced by disturbed flow and

has a role in regulating atherosclerosis (127) and so may play a role in regulating CLEC14A transcription during this pathology.

4.4.3 *In vivo* Atherosclerotic Plaque Study Interrogation for CLEC14A Expression

There were several different sets of data from human atherosclerotic plaques which enabled an analysis of CLEC14A expression in this pathology; these compared either stable with unstable plaques, or atherosclerotic tissue with control vessels. Unstable plaques had a small but statistically insignificant increase in CLEC14A expression compared with stable plaques; by contrast another study showed a significant increase in CLEC14A in carotid plaques compared with control arterial tissue. However, the data was complicated by fact that atherosclerotic plaques vary in their composition and in particular their endothelial content. This was addressed by also analysing the expression of an endothelial specific gene vWF (68, 136) and a shear regulated endothelial expressed gene TIE1 (68, 137). In a large number of the samples, levels of CLEC14A mirrored that of vWF and TIE1; and when CLEC14A expression was normalised to vWF expression, its expression was significantly decreased in carotid plaques relative to normal arterial tissue. In unstable plaques there was a trend towards an increased CLEC14A expression in the unstable plaques compared with stable plaques, this was not statistically significant, and analyses were confounded by a small number of data points and considerable variability between the paired samples. The source of the variability in endothelial content was unclear and the endothelial cells could have been derived from the arterial lumen or from angiogenic vessels within the plaque. Angiogenic vessels derived from vasa vasorum increases endothelial content of atherosclerotic plaques (138, 139) and this in turn could increase CLEC14A expression levels.

In particular, intraplaque microvasculature is found at the proximal end of unstable plaques (140, 141). Since CLEC14A expression is known to be shear-regulated, another confounding factor is the complex flow pattern in plaques which may account for some of the variation seen in CLEC14A expression (142). Not only were there variations between data from different patients, but there was also considerable variation in data in different samples from the same patient, indicating that regional differences in plaque composition are likely to significantly influence the data generated and limit the utility of transcriptomic analyses such as these. Combining this with methodologies such as immunofluorescence or immunohistochemistry to better the define the localisation of CLEC14A expression within plaques would be highly informative.

4.4.4 *In vitro* Regulation of RhoJ Expression

One of the aims of my project was to determine whether RhoJ is regulated by shear stress and one of the ways to do this was through interrogation of bioinformatic analyses. In one bioinformatic study using cultured bovine aortic ECs, RhoJ expression was shown to be negatively regulated by laminar shear stress with a significant stepwise decrease after 24 hours at 2 Pa and 10 Pa laminar shear stress (Figure 4.2). However, in another study, endothelial cells sourced from veins (HUVECs) subjected to 24 hours of 1.5 Pa and 7.5 Pa laminar shear stress showed no significant change in RhoJ expression (Figure 4.1). The differences in the two results may be explained by the different cell lines used. Aortic endothelial cells are known to respond to shear stress more acutely than HUVECs (143) highlighting the importance of determining adequate flow time for selected endothelial cell type.

Interrogating potential pathways such as the MEK5/Erk5 pathway, which is activated by laminar shear stress, revealed that RhoJ may be modulated through this pathway. The transcription factor ERG was confirmed to promote RhoJ expression which supports findings Yuan L *et al* (89). RhoJ may be a potential target for the transcriptional regulator YAP, however an inconsistency in results obtained by two different siRNA duplexes make interpretation impossible, ideally a pool of siRNA should be used to minimise off-target effects (144).

4.4.5 *In vivo* Atherosclerotic Plaque Study Interrogation for RhoJ Expression

RhoJ signalling pathways are important in regulating endothelial motility and tube formation in angiogenesis (87, 90), but its expression levels in vascular diseases such as atherosclerosis are not known. Changes in other Rho GTPase signalling pathways are associated with atherogenesis (145) but no role for RhoJ has been reported. In at least two of these bioinformatic studies of atherosclerotic plaques, there is a small reduction in the expression of RhoJ relative to expression levels of vWF, in at least one study of plaques from carotid arteries this was a statistically significant change. Both our own experimental data from the previous chapter and data from at least one of the high shear stress microarrays indicate that RhoJ expression is negatively regulated by laminar shear stress. High pulsatile arterial laminar flow in healthy plaque-free carotid arteries is replaced by complex disturbed flow patterns in carotid artery plaque lesions (146), and it would be interesting to determine how disturbed flow pattern affect RhoJ expression. As noted in the discussion above, the plaque tissue will contain endothelial cells from both the lumen of the large arteries and from the small vessels of the vasa vasorum (147), so these cells will have experienced a range of flow

pattern making it difficult to predict how changes in blood flow might affect RhoJ expression in whole plaque tissue.

While the inflammatory cytokine TNF-α did not influence RhoJ expression (Figure 4.10), significant changes in RhoJ were observed in cerebral ischemia-reperfusion injury rat models (Figure 4.9), with a significant upregulation of expression, both when considered alone and when relative to vWF expression. This is a model oxidative stress, a stressor also seen in atherosclerosis pathology (148). However manifold cellular changes occur during ischaemia and reperfusion. The ischaemia causes hypoxia, cell swelling and rupture, necrosis, apoptosis and autophagy; the ensuing reperfusion restores oxygen levels but the large increase in reactive oxygen species is accompanied by neutrophil infiltration (149). Which of these different cellular changes contributes of changes in RhoJ expression would be interesting to determine.

4.5 Conclusions

Interrogating bioinformatic databases can give interesting and novel insight into gene expression yielding a wealth of information about how different genes may regulated by different cellular conditions, exposure to soluble factors, altered levels of transcription factors and in different pathologies. There are limitations and particularly the loss of spatial resolution of expression in tissue samples hampers a clear understanding of how gene expression changes in pathology. However, the data they yield also prompts further questions. For example, what causes RhoJ upregulation in ischaemia reperfusion injury and does RhoJ contribute to the pathology, or alternatively, how does cell confluence affect

CLEC14A expression and which signalling pathways are involved? All this is beyond the scope of this project but could inform and inspire future studies.

List of References

1. Givens C, Tzima E. Endothelial Mechanosignaling: Does One Sensor Fit All? Antioxid Redox Signal. 2016;25(7):373-88.

2. Urschel K, Tauchi M, Achenbach S, Dietel B. Investigation of Wall Shear Stress in Cardiovascular Research and in Clinical Practice-From Bench to Bedside. Int J Mol Sci. 2021;22(11).

3. Conway D, Schwartz MA. Lessons from the endothelial junctional mechanosensory complex. F1000 Biol Rep. 2012;4:1.

4. Sprague B, Chesler NC, Magness RR. Shear stress regulation of nitric oxide production in uterine and placental artery endothelial cells: experimental studies and hemodynamic models of shear stresses on endothelial cells. Int J Dev Biol. 2010;54(2-3):331-9.

5. Berk BC. Atheroprotective signaling mechanisms activated by steady laminar flow in endothelial cells. Circulation. 2008;117(8):1082-9.

6. Cunningham KS, Gotlieb AI. The role of shear stress in the pathogenesis of atherosclerosis. Lab Invest. 2005;85(1):9-23.

7. Chiu JJ, Chien S. Effects of disturbed flow on vascular endothelium: pathophysiological basis and clinical perspectives. Physiol Rev. 2011;91(1):327-87.

8. Wragg JW, Durant S, McGettrick HM, Sample KM, Egginton S, Bicknell R. Shear stress regulated gene expression and angiogenesis in vascular endothelium. Microcirculation. 2014;21(4):290-300.

9. Davies PF. Hemodynamic shear stress and the endothelium in cardiovascular pathophysiology. Nat Clin Pract Cardiovasc Med. 2009;6(1):16-26.

10. Heo KS, Fujiwara K, Abe J. Shear stress and atherosclerosis. Mol Cells. 2014;37(6):435-40.

11. Liu Y, Sweet DT, Irani-Tehrani M, Maeda N, Tzima E. Shc coordinates signals from intercellular junctions and integrins to regulate flow-induced inflammation. J Cell Biol. 2008;182(1):185-96.

12. Weinbaum S, Tarbell JM, Damiano ER. The structure and function of the endothelial glycocalyx layer. Annu Rev Biomed Eng. 2007;9:121-67.

13. Reitsma S, Slaaf DW, Vink H, van Zandvoort MA, oude Egbrink MG. The endothelial glycocalyx: composition, functions, and visualization. Pflugers Arch. 2007;454(3):345-59.

14. Mensah SA, Cheng MJ, Homayoni H, Plouffe BD, Coury AJ, Ebong EE. Regeneration of glycocalyx by heparan sulfate and sphingosine 1-phosphate restores inter-endothelial communication. PLoS One. 2017;12(10):e0186116.

15. Shi ZD, Wang H, Tarbell JM. Heparan sulfate proteoglycans mediate interstitial flow mechanotransduction regulating MMP-13 expression and cell motility via FAK-ERK in 3D collagen. PLoS One. 2011;6(1):e15956.

16. Curry FE, Adamson RH. Endothelial glycocalyx: permeability barrier and mechanosensor. Ann Biomed Eng. 2012;40(4):828-39.

17. Frati-Munari AC. [Medical significance of endothelial glycocalyx]. Arch Cardiol Mex. 2013;83(4):303-12.

18. Wang G, Kostidis S, Tiemeier GL, Sol W, de Vries MR, Giera M, et al. Shear Stress Regulation of Endothelial Glycocalyx Structure Is Determined by Glucobiosynthesis. Arterioscler Thromb Vasc Biol. 2020;40(2):350-64.

19. Warboys CM, Ghim M, Weinberg PD. Understanding mechanobiology in cultured endothelium: A review of the orbital shaker method. Atherosclerosis. 2019;285:170-7.

20. Zhou J, Li YS, Chien S. Shear stress-initiated signaling and its regulation of endothelial function. Arterioscler Thromb Vasc Biol. 2014;34(10):2191-8.

21. Yao Y, Rabodzey A, Dewey CF, Jr. Glycocalyx modulates the motility and proliferative response of vascular endothelium to fluid shear stress. Am J Physiol Heart Circ Physiol. 2007;293(2):H1023-30.

22. dela Paz NG, Melchior B, Shayo FY, Frangos JA. Heparan sulfates mediate the interaction between platelet endothelial cell adhesion molecule-1 (PECAM-1) and the Galphaq/11 subunits of heterotrimeric G proteins. J Biol Chem. 2014;289(11):7413-24.

23. Conway DE, Coon BG, Budatha M, Arsenovic PT, Orsenigo F, Wessel F, et al. VE-Cadherin Phosphorylation Regulates Endothelial Fluid Shear Stress Responses through the Polarity Protein LGN. Curr Biol. 2017;27(17):2727.

24. Conway DE, Schwartz MA. Mechanotransduction of shear stress occurs through changes in VE-cadherin and PECAM-1 tension: implications for cell migration. Cell Adh Migr. 2015;9(5):335-9.

25. Coon BG, Baeyens N, Han J, Budatha M, Ross TD, Fang JS, et al. Intramembrane binding of VE-cadherin to VEGFR2 and VEGFR3 assembles the endothelial mechanosensory complex. J Cell Biol. 2015;208(7):975-86.

26. Baeyens N, Nicoli S, Coon BG, Ross TD, Van den Dries K, Han J, et al. Vascular remodeling is governed by a VEGFR3-dependent fluid shear stress set point. Elife. 2015;4.

27. Schimmel L, Gordon E. The precise molecular signals that control endothelial cell-cell adhesion within the vessel wall. Biochem Soc Trans. 2018;46(6):1673-80.

28. Sun Z, Li X, Massena S, Kutschera S, Padhan N, Gualandi L, et al. VEGFR2 induces c-Src signaling and vascular permeability in vivo via the adaptor protein TSAd. J Exp Med. 2012;209(7):1363-77.

29. Dejana E, Orsenigo F, Lampugnani MG. The role of adherens junctions and VE-cadherin in the control of vascular permeability. J Cell Sci. 2008;121(Pt 13):2115-22.

30. Yamada S, Nelson WJ. Localized zones of Rho and Rac activities drive initiation and expansion of epithelial cell-cell adhesion. J Cell Biol. 2007;178(3):517-27.

31. Privratsky JR, Newman PJ. PECAM-1: regulator of endothelial junctional integrity. Cell Tissue Res. 2014;355(3):607-19.

32. Taveau JC, Dubois M, Le Bihan O, Trepout S, Almagro S, Hewat E, et al. Structure of artificial and natural VE-cadherin-based adherens junctions. Biochem Soc Trans. 2008;36(Pt 2):189-93.

33. Naumann DN. Early Microcirculatory Dysfunction Following Traumatic Haemorrhage: University of Birmingham; 2018.

34. Dorland YL, Huveneers S. Cell-cell junctional mechanotransduction in endothelial remodeling. Cell Mol Life Sci. 2017;74(2):279-92.

35. Lupu F, Kinasewitz G, Dormer K. The role of endothelial shear stress on haemodynamics, inflammation, coagulation and glycocalyx during sepsis. J Cell Mol Med. 2020;24(21):12258-71.

36. Chappell D, Dorfler N, Jacob M, Rehm M, Welsch U, Conzen P, et al. Glycocalyx protection reduces leukocyte adhesion after ischemia/reperfusion. Shock. 2010;34(2):133-9.

37. Dekker RJ, Boon RA, Rondaij MG, Kragt A, Volger OL, Elderkamp YW, et al. KLF2 provokes a gene expression pattern that establishes functional quiescent differentiation of the endothelium. Blood. 2006;107(11):4354-63.

38. Boon RA, Leyen TA, Fontijn RD, Fledderus JO, Baggen JM, Volger OL, et al. KLF2-induced actin shear fibers control both alignment to flow and JNK signaling in vascular endothelium. Blood. 2010;115(12):2533-42.

39. Bai K, Wang W. Shear stress-induced redistribution of the glycocalyx on endothelial cells in vitro. Biomech Model Mechanobiol. 2014;13(2):303-11.

40. Chu HR, Sun YC, Gao Y, Guan XM, Yan H, Cui XD, et al. Function of Kruppel-like factor 2 in the shear stress-induced cell differentiation of endothelial progenitor cells to endothelial cells. Mol Med Rep. 2019;19(3):1739-46.

41. Dekker RJ, van Soest S, Fontijn RD, Salamanca S, de Groot PG, VanBavel E, et al. Prolonged fluid shear stress induces a distinct set of endothelial cell genes, most specifically lung Kruppel-like factor (KLF2). Blood. 2002;100(5):1689-98.

42. Lin Z, Kumar A, SenBanerjee S, Staniszewski K, Parmar K, Vaughan DE, et al. Kruppel-like factor 2 (KLF2) regulates endothelial thrombotic function. Circ Res. 2005;96(5):e48-57.

43. Moncada S, Higgs EA. The discovery of nitric oxide and its role in vascular biology. Br J Pharmacol. 2006;147 Suppl 1(Suppl 1):S193-201.

44. Parmar KM, Larman HB, Dai G, Zhang Y, Wang ET, Moorthy SN, et al. Integration of flow-dependent endothelial phenotypes by Kruppel-like factor 2. J Clin Invest. 2006;116(1):49-58.

45. SenBanerjee S, Lin Z, Atkins GB, Greif DM, Rao RM, Kumar A, et al. KLF2 Is a novel transcriptional regulator of endothelial proinflammatory activation. J Exp Med. 2004;199(10):1305-15.

46. Fledderus JO, Boon RA, Volger OL, Hurttila H, Yla-Herttuala S, Pannekoek H, et al. KLF2 primes the antioxidant transcription factor Nrf2 for activation in endothelial cells. Arterioscler Thromb Vasc Biol. 2008;28(7):1339-46.

47. Psefteli PM, Kitscha P, Vizcay G, Fleck R, Chapple SJ, Mann GE, et al. Glycocalyx sialic acids regulate Nrf2-mediated signaling by fluid shear stress in human endothelial cells. Redox Biol. 2021;38:101816.

48. Takabe W, Warabi E, Noguchi N. Anti-atherogenic effect of laminar shear stress via Nrf2 activation. Antioxid Redox Signal. 2011;15(5):1415-26.

49. Mochizuki S, Vink H, Hiramatsu O, Kajita T, Shigeto F, Spaan JA, et al. Role of hyaluronic acid glycosaminoglycans in shear-induced endothelium-derived nitric oxide release. Am J Physiol Heart Circ Physiol. 2003;285(2):H722-6.

50. Jin ZG, Ueba H, Tanimoto T, Lungu AO, Frame MD, Berk BC. Ligand-independent activation of vascular endothelial growth factor receptor 2 by fluid shear stress regulates activation of endothelial nitric oxide synthase. Circ Res. 2003;93(4):354-63.

51. Mui KL, Chen CS, Assoian RK. The mechanical regulation of integrin-cadherin crosstalk organizes cells, signaling and forces. J Cell Sci. 2016;129(6):1093-100.

52. Dekker RJ, van Thienen JV, Rohlena J, de Jager SC, Elderkamp YW, Seppen J, et al. Endothelial KLF2 links local arterial shear stress levels to the expression of vascular tone-regulating genes. Am J Pathol. 2005;167(2):609-18.

53. Fleming I, Busse R. Molecular mechanisms involved in the regulation of the endothelial nitric oxide synthase. Am J Physiol Regul Integr Comp Physiol. 2003;284(1):R1-12.

54. Hsieh HJ, Liu CA, Huang B, Tseng AH, Wang DL. Shear-induced endothelial mechanotransduction: the interplay between reactive oxygen species (ROS) and nitric oxide (NO) and the pathophysiological implications. J Biomed Sci. 2014;21(1):3.

55. Urbich C, Walter DH, Zeiher AM, Dimmeler S. Laminar shear stress upregulates integrin expression: role in endothelial cell adhesion and apoptosis. Circ Res. 2000;87(8):683-9.

56. Tzima E, Irani-Tehrani M, Kiosses WB, Dejana E, Schultz DA, Engelhardt B, et al. A mechanosensory complex that mediates the endothelial cell response to fluid shear stress. Nature. 2005;437(7057):426-31.

57. Khan KA, McMurray JL, Mohammed F, Bicknell R. C-type lectin domain group 14 proteins in vascular biology, cancer and inflammation. FEBS J. 2019;286(17):3299-332.

58. Jang J, Kim MR, Kim TK, Lee WR, Kim JH, Heo K, et al. CLEC14a-HSP70-1A interaction regulates HSP70-1A-induced angiogenesis. Sci Rep. 2017;7(1):10666.

59. Ho M, Yang E, Matcuk G, Deng D, Sampas N, Tsalenko A, et al. Identification of endothelial cell genes by combined database mining and microarray analysis. Physiol Genomics. 2003;13(3):249-62.

60. Herbert JM, Stekel D, Sanderson S, Heath VL, Bicknell R. A novel method of differential gene expression analysis using multiple cDNA libraries applied to the identification of tumour endothelial genes. BMC Genomics. 2008;9:153.

61. Khan KA, Naylor AJ, Khan A, Noy PJ, Mambretti M, Lodhia P, et al. Multimerin-2 is a ligand for group 14 family C-type lectins CLEC14A, CD93 and CD248 spanning the endothelial pericyte interface. Oncogene. 2017;36(44):6097-108.

62. Zelensky AN, Gready JE. The C-type lectin-like domain superfamily. FEBS J. 2005;272(24):6179-217.

63. Borah S, Vasudevan D, Swain RK. C-type lectin family XIV members and angiogenesis. Oncol Lett. 2019;18(4):3954-62.

64. Rho SS, Choi HJ, Min JK, Lee HW, Park H, Park H, et al. Clec14a is specifically expressed in endothelial cells and mediates cell to cell adhesion. Biochem Biophys Res Commun. 2011;404(1):103-8.

65. Liang Z, Yang L, Zheng J, Zuo H, Weng S, He J, et al. A low-density lipoprotein receptor (LDLR) class A domain-containing C-type lectin from Litopenaeus vannamei plays opposite roles in antibacterial and antiviral responses. Dev Comp Immunol. 2019;92:29-34.

66. Noy PJ, Swain RK, Khan K, Lodhia P, Bicknell R. Sprouting angiogenesis is regulated by shedding of the C-type lectin family 14, member A (CLEC14A) ectodomain, catalyzed by rhomboid-like 2 protein (RHBDL2). FASEB J. 2016;30(6):2311-23.

67. Mura M, Swain RK, Zhuang X, Vorschmitt H, Reynolds G, Durant S, et al. Identification and angiogenic role of the novel tumor endothelial marker CLEC14A. Oncogene. 2012;31(3):293-305.

68. Robinson J, Whitworth K, Jinks E, Nagy Z, Bicknell R, Lee SP. An evaluation of the tumour endothelial marker CLEC14A as a therapeutic target in solid tumours. J Pathol Clin Res. 2020;6(4):308-19.

69. Noy PJ, Lodhia P, Khan K, Zhuang X, Ward DG, Verissimo AR, et al. Blocking CLEC14A-MMRN2 binding inhibits sprouting angiogenesis and tumour growth. Oncogene. 2015;34(47):5821-31.

70. Masiero M, Simoes FC, Han HD, Snell C, Peterkin T, Bridges E, et al. A core human primary tumor angiogenesis signature identifies the endothelial orphan receptor ELTD1 as a key regulator of angiogenesis. Cancer Cell. 2013;24(2):229-41.

71. Sandoval DR, Gomez Toledo A, Painter CD, Tota EM, Sheikh MO, West AMV, et al. Proteomics-based screening of the endothelial heparan sulfate interactome reveals that C-type lectin 14a (CLEC14A) is a heparin-binding protein. J Biol Chem. 2020;295(9):2804-21.

72. Lee S, Rho SS, Park H, Park JA, Kim J, Lee IK, et al. Carbohydrate-binding protein CLEC14A regulates VEGFR-2- and VEGFR-3-dependent signals during angiogenesis and lymphangiogenesis. J Clin Invest. 2017;127(2):457-71.

73. Zanivan S, Maione F, Hein MY, Hernandez-Fernaud JR, Ostasiewicz P, Giraudo E, et al. SILAC-based proteomics of human primary endothelial cell morphogenesis unveils tumor angiogenic markers. Mol Cell Proteomics. 2013;12(12):3599-611.

74. Lorenzon E, Colladel R, Andreuzzi E, Marastoni S, Todaro F, Schiappacassi M, et al. MULTIMERIN2 impairs tumor angiogenesis and growth by interfering with VEGF-A/VEGFR2 pathway. Oncogene. 2012;31(26):3136-47.

75. Ohura N, Yamamoto K, Ichioka S, Sokabe T, Nakatsuka H, Baba A, et al. Global analysis of shear stress-responsive genes in vascular endothelial cells. J Atheroscler Thromb. 2003;10(5):304-13.

76. Chu TJ, Peters DG. Serial analysis of the vascular endothelial transcriptome under static and shear stress conditions. Physiol Genomics. 2008;34(2):185-92.

77. Zhuang X, Cross D, Heath VL, Bicknell R. Shear stress, tip cells and regulators of endothelial migration. Biochem Soc Trans. 2011;39(6):1571-5.

78. Hagg S, Skogsberg J, Lundstrom J, Noori P, Nilsson R, Zhong H, et al. Multi-organ expression profiling uncovers a gene module in coronary artery disease involving transendothelial migration of leukocytes and LIM domain binding 2: the Stockholm Atherosclerosis Gene Expression (STAGE) study. PLoS Genet. 2009;5(12):e1000754.

79. Grainger AT, Jones MB, Chen MH, Shi W. Polygenic Control of Carotid Atherosclerosis in a BALB/cJ x SM/J Intercross and a Combined Cross Involving Multiple Mouse Strains. G3 (Bethesda). 2017;7(2):731-9.

80. Shi TT, Li G, Xiao HT. The Role of RhoJ in Endothelial Cell Biology and Tumor Pathology. Biomed Res Int. 2016;2016:6386412.

81. Lawson CD, Ridley AJ. Rho GTPase signaling complexes in cell migration and invasion. J Cell Biol. 2018;217(2):447-57.

82. Zubor P, Dankova Z, Kolkova Z, Holubekova V, Brany D, Mersakova S, et al. Rho GTPases in Gynecologic Cancers: In-Depth Analysis toward the Paradigm Change from Reactive to Predictive, Preventive, and Personalized Medical Approach Benefiting the Patient and Healthcare. Cancers (Basel). 2020;12(5).

83. Mosaddeghzadeh N, Ahmadian MR. The RHO Family GTPases: Mechanisms of Regulation and Signaling. Cells. 2021;10(7).

84. Ridley AJ. Rho GTPase signalling in cell migration. Curr Opin Cell Biol. 2015;36:103-12.

85. Vadodaria KC, Jessberger S. Maturation and integration of adult born hippocampal neurons: signal convergence onto small Rho GTPases. Front Synaptic Neurosci. 2013;5:4.

86. Jaffe AB, Hall A. Rho GTPases: biochemistry and biology. Annu Rev Cell Dev Biol. 2005;21:247-69.

87. Kaur S, Leszczynska K, Abraham S, Scarcia M, Hiltbrunner S, Marshall CJ, et al. RhoJ/TCL regulates endothelial motility and tube formation and modulates actomyosin contractility and focal adhesion numbers. Arterioscler Thromb Vasc Biol. 2011;31(3):657-64.

88. Takase H, Matsumoto K, Yamadera R, Kubota Y, Otsu A, Suzuki R, et al. Genome-wide identification of endothelial cell-enriched genes in the mouse embryo. Blood. 2012;120(4):914-23.

89. Yuan L, Sacharidou A, Stratman AN, Le Bras A, Zwiers PJ, Spokes K, et al. RhoJ is an endothelial cell-restricted Rho GTPase that mediates vascular morphogenesis and is regulated by the transcription factor ERG. Blood. 2011;118(4):1145-53.

90. Wilson E, Leszczynska K, Poulter NS, Edelmann F, Salisbury VA, Noy PJ, et al. RhoJ interacts with the GIT-PIX complex and regulates focal adhesion disassembly. J Cell Sci. 2014;127(Pt 14):3039-51.

91. Kim C, Yang H, Fukushima Y, Saw PE, Lee J, Park JS, et al. Vascular RhoJ is an effective and selective target for tumor angiogenesis and vascular disruption. Cancer Cell. 2014;25(1):102-17.

92. Fukushima Y, Nishiyama K, Kataoka H, Fruttiger M, Fukuhara S, Nishida K, et al. RhoJ integrates attractive and repulsive cues in directional migration of endothelial cells. EMBO J. 2020;39(12):e102930.

93. Feng Q, Baird D, Yoo S, Antonyak M, Cerione RA. Phosphorylation of the cool-1/beta-Pix protein serves as a regulatory signal for the migration and invasive activity of Src-transformed cells. J Biol Chem. 2010;285(24):18806-16.

94. Richards M, Hetheridge C, Mellor H. The Formin FMNL3 Controls Early Apical Specification in Endothelial Cells by Regulating the Polarized Trafficking of Podocalyxin. Curr Biol. 2015;25(17):2325-31.

95. Sundararaman A, Mellor H. A functional antagonism between RhoJ and Cdc42 regulates fibronectin remodelling during angiogenesis. Small GTPases. 2021;12(4):241-5.

96. Al-Yafeai Z, Yurdagul A, Jr., Peretik JM, Alfaidi M, Murphy PA, Orr AW. Endothelial FN (Fibronectin) Deposition by alpha5beta1 Integrins Drives Atherogenic Inflammation. Arterioscler Thromb Vasc Biol. 2018;38(11):2601-14.

97. Fukushima Y, Okada M, Kataoka H, Hirashima M, Yoshida Y, Mann F, et al. Sema3E-PlexinD1 signaling selectively suppresses disoriented angiogenesis in ischemic retinopathy in mice. J Clin Invest. 2011;121(5):1974-85.

98. Arts JJG, Mahlandt EK, Schimmel L, Gronloh MLB, van der Niet S, Klein B, et al. Endothelial Focal Adhesions Are Functional Obstacles for Leukocytes During Basolateral Crawling. Front Immunol. 2021;12:667213.

99. Jaipersad AS, Lip GY, Silverman S, Shantsila E. The role of monocytes in angiogenesis and atherosclerosis. J Am Coll Cardiol. 2014;63(1):1-11.

100. Ye J, Coulouris G, Zaretskaya I, Cutcutache I, Rozen S, Madden TL. Primer-BLAST: a tool to design target-specific primers for polymerase chain reaction. BMC Bioinformatics. 2012;13:134.

101. Livak KJ, Schmittgen TD. Analysis of relative gene expression data using real-time quantitative PCR and the 2(-Delta Delta C(T)) Method. Methods. 2001;25(4):402-8.

102. Clough E, Barrett T. The Gene Expression Omnibus Database. Methods Mol Biol. 2016;1418:93-110.

103. Edgar R, Domrachev M, Lash AE. Gene Expression Omnibus: NCBI gene expression and hybridization array data repository. Nucleic Acids Res. 2002;30(1):207-10.

104. Kolberg L, Raudvere U, Kuzmin I, Vilo J, Peterson H. gprofiler2 -- an R package for gene list functional enrichment analysis and namespace conversion toolset g:Profiler. F1000Res. 2020;9.

105. Leszczynska K, Kaur S, Wilson E, Bicknell R, Heath VL. The role of RhoJ in endothelial cell biology and angiogenesis. Biochem Soc Trans. 2011;39(6):1606-11.

106. Melchionna R, Porcelli D, Mangoni A, Carlini D, Liuzzo G, Spinetti G, et al. Laminar shear stress inhibits CXCR4 expression on endothelial cells: functional consequences for atherogenesis. FASEB J. 2005;19(6):629-31.

107. Nayak L, Lin Z, Jain MK. "Go with the flow": how Kruppel-like factor 2 regulates the vasoprotective effects of shear stress. Antioxid Redox Signal. 2011;15(5):1449-61.

108. Dolan JM, Sim FJ, Meng H, Kolega J. Endothelial cells express a unique transcriptional profile under very high wall shear stress known to induce expansive arterial remodeling. Am J Physiol Cell Physiol. 2012;302(8):C1109-18.

109. Nakajima H, Mochizuki N. Flow pattern-dependent endothelial cell responses through transcriptional regulation. Cell Cycle. 2017;16(20):1893-901.

110. Duchemin AL, Vignes H, Vermot J. Mechanically activated piezo channels modulate outflow tract valve development through the Yap1 and Klf2-Notch signaling axis. Elife. 2019;8.

111. Galvagni F, Nardi F, Spiga O, Trezza A, Tarticchio G, Pellicani R, et al. Dissecting the CD93-Multimerin 2 interaction involved in cell adhesion and migration of the activated endothelium. Matrix Biol. 2017;64:112-27.

112. Coumans JV, Gau D, Poljak A, Wasinger V, Roy P, Moens P. Green fluorescent protein expression triggers proteome changes in breast cancer cells. Exp Cell Res. 2014;320(1):33-45.

113. Das AT, Zhou X, Metz SW, Vink MA, Berkhout B. Selecting the optimal Tet-On system for doxycycline-inducible gene expression in transiently transfected and stably transduced mammalian cells. Biotechnol J. 2016;11(1):71-9.

114. Dardik A, Chen L, Frattini J, Asada H, Aziz F, Kudo FA, et al. Differential effects of orbital and laminar shear stress on endothelial cells. J Vasc Surg. 2005;41(5):869-80.

115. White SJ, Hayes EM, Lehoux S, Jeremy JY, Horrevoets AJ, Newby AC. Characterization of the differential response of endothelial cells exposed to normal and elevated laminar shear stress. J Cell Physiol. 2011;226(11):2841-8.

116. Souilhol C, Serbanovic-Canic J, Fragiadaki M, Chico TJ, Ridger V, Roddie H, et al. Endothelial responses to shear stress in atherosclerosis: a novel role for developmental genes. Nat Rev Cardiol. 2020;17(1):52-63.

117. Stary HC, Chandler AB, Dinsmore RE, Fuster V, Glagov S, Insull W, Jr., et al. A definition of advanced types of atherosclerotic lesions and a histological classification of atherosclerosis. A report from the Committee on Vascular Lesions of the Council on Arteriosclerosis, American Heart Association. Circulation. 1995;92(5):1355-74.

118. Woo KV, Baldwin HS. Role of Tie1 in shear stress and atherosclerosis. Trends Cardiovasc Med. 2011;21(4):118-23.

119. Ayari H, Bricca G. Identification of two genes potentially associated in iron-heme homeostasis in human carotid plaque using microarray analysis. J Biosci. 2013;38(2):311-5.

120. Cagnin S, Biscuola M, Patuzzo C, Trabetti E, Pasquali A, Laveder P, et al. Reconstruction and functional analysis of altered molecular pathways in human atherosclerotic arteries. BMC Genomics. 2009;10:13.

121. Victor VM, Rocha M, Sola E, Banuls C, Garcia-Malpartida K, Hernandez-Mijares A. Oxidative stress, endothelial dysfunction and atherosclerosis. Curr Pharm Des. 2009;15(26):2988-3002.

122. Yi D, Wang Q, Zhao Y, Song Y, You H, Wang J, et al. Alteration of N (6) - Methyladenosine mRNA Methylation in a Rat Model of Cerebral Ischemia-Reperfusion Injury. Front Neurosci. 2021;15:605654.

123. Griffin GK, Newton G, Tarrio ML, Bu DX, Maganto-Garcia E, Azcutia V, et al. IL-17 and TNF-alpha sustain neutrophil recruitment during inflammation through synergistic effects on endothelial activation. J Immunol. 2012;188(12):6287-99.

124. Rajashekhar G, Grow M, Willuweit A, Patterson CE, Clauss M. Divergent and convergent effects on gene expression and function in acute versus chronic endothelial activation. Physiol Genomics. 2007;31(1):104-13.

125. De Val S, Black BL. Transcriptional control of endothelial cell development. Dev Cell. 2009;16(2):180-95.

126. Yamamoto S, Yamane M, Yoshida O, Waki N, Okazaki M, Matsukawa A, et al. Early Growth Response-1 Plays an Important Role in Ischemia-Reperfusion Injury in Lung Transplants by Regulating Polymorphonuclear Neutrophil Infiltration. Transplantation. 2015;99(11):2285-93.

127. Khachigian LM. Early Growth Response-1, an Integrative Sensor in Cardiovascular and Inflammatory Disease. J Am Heart Assoc. 2021;10(22):e023539.

128. Blee AM, Huang H. ERG-Mediated Cell Invasion: A Link between Development and Tumorigenesis. Medical Epigenetics. 2015;3(2-3):19-29.

129. Komaravolu RK, Adam C, Moonen JR, Harmsen MC, Goebeler M, Schmidt M. Erk5 inhibits endothelial migration via KLF2-dependent down-regulation of PAK1. Cardiovasc Res. 2015;105(1):86-95.

130. Ohnesorge N, Viemann D, Schmidt N, Czymai T, Spiering D, Schmolke M, et al. Erk5 activation elicits a vasoprotective endothelial phenotype via induction of Kruppel-like factor 4 (KLF4). J Biol Chem. 2010;285(34):26199-210.

131. Moroishi T, Hansen CG, Guan KL. The emerging roles of YAP and TAZ in cancer. Nat Rev Cancer. 2015;15(2):73-9.

132. Yuan P, Hu Q, He X, Long Y, Song X, Wu F, et al. Laminar flow inhibits the Hippo/YAP pathway via autophagy and SIRT1-mediated deacetylation against atherosclerosis. Cell Death Dis. 2020;11(2):141.

133. Sun C, He B, Sun M, Lv X, Wang F, Chen J, et al. Yes-Associated Protein in Atherosclerosis and Related Complications: A Potential Therapeutic Target That Requires Further Exploration. Front Cardiovasc Med. 2021;8:704208.

134. Ricard N, Bailly S, Guignabert C, Simons M. The quiescent endothelium: signalling pathways regulating organ-specific endothelial normalcy. Nat Rev Cardiol. 2021;18(8):565-80.

135. Fontijn RD, Volger OL, Fledderus JO, Reijerkerk A, de Vries HE, Horrevoets AJ. SOX-18 controls endothelial-specific claudin-5 gene expression and barrier function. Am J Physiol Heart Circ Physiol. 2008;294(2):H891-900.

136. Zanetta L, Marcus SG, Vasile J, Dobryansky M, Cohen H, Eng K, et al. Expression of Von Willebrand factor, an endothelial cell marker, is up-regulated by angiogenesis factors: a potential method for objective assessment of tumor angiogenesis. Int J Cancer. 2000;85(2):281-8.

137. Porat RM, Grunewald M, Globerman A, Itin A, Barshtein G, Alhonen L, et al. Specific induction of tie1 promoter by disturbed flow in atherosclerosis-prone vascular niches and flow-obstructing pathologies. Circ Res. 2004;94(3):394-401.

138. Dong S, Hou J, Zhang C, Lu G, Qin W, Huang L, et al. Diagnostic Performance of Atherosclerotic Carotid Plaque Neovascularization with Contrast-Enhanced Ultrasound: A Meta-Analysis. Comput Math Methods Med. 2022;2022:7531624.

139. Doyle B, Caplice N. Plaque neovascularization and antiangiogenic therapy for atherosclerosis. J Am Coll Cardiol. 2007;49(21):2073-80.

140. Cai Y, Pan J, Li Z. Mathematical modeling of intraplaque neovascularization and hemorrhage in a carotid atherosclerotic plaque. Biomed Eng Online. 2021;20(1):42.

141. Wang Y, Qiu J, Luo S, Xie X, Zheng Y, Zhang K, et al. High shear stress induces atherosclerotic vulnerable plaque formation through angiogenesis. Regen Biomater. 2016;3(4):257-67.

142. Samady H, Eshtehardi P, McDaniel MC, Suo J, Dhawan SS, Maynard C, et al. Coronary artery wall shear stress is associated with progression and transformation of atherosclerotic plaque and arterial remodeling in patients with coronary artery disease. Circulation. 2011;124(7):779-88.

143. Maurya MR, Gupta S, Li JY, Ajami NE, Chen ZB, Shyy JY, et al. Longitudinal shear stress response in human endothelial cells to atheroprone and atheroprotective conditions. Proc Natl Acad Sci U S A. 2021;118(4).

144. Neumeier J, Meister G. siRNA Specificity: RNAi Mechanisms and Strategies to Reduce Off-Target Effects. Front Plant Sci. 2020;11:526455.

145. Rolfe BE, Worth NF, World CJ, Campbell JH, Campbell GR. Rho and vascular disease. Atherosclerosis. 2005;183(1):1-16.

146. Gnasso A, Irace C, Carallo C, De Franceschi MS, Motti C, Mattioli PL, et al. In vivo association between low wall shear stress and plaque in subjects with asymmetrical carotid atherosclerosis. Stroke. 1997;28(5):993-8.

147. Mulligan-Kehoe MJ. The vasa vasorum in diseased and nondiseased arteries. Am J Physiol Heart Circ Physiol. 2010;298(2):H295-305.

148. Kattoor AJ, Pothineni NVK, Palagiri D, Mehta JL. Oxidative Stress in Atherosclerosis. Curr Atheroscler Rep. 2017;19(11):42.

149. Kalogeris T, Baines CP, Krenz M, Korthuis RJ. Cell biology of ischemia/reperfusion injury. Int Rev Cell Mol Biol. 2012;298:229-317.

Appendix

Search DataSet Record using
https://www.ncbi.nlm.nih.gov/geo/ or https://www.ncbi.nlm.nih.gov/geo/query/acc.cgi

DataSet Record	Title	Organism
GSE120521	RNA-seq of stable and unstable section of human atherosclerotic plaques	*Homo sapiens*
GDS3698	Atherosclerotic left anterior descendent coronary artery: high scan	*Homo sapiens*
GDS5083	Carotid artery atheroma	*Homo sapiens*
GDS4525	Aortic endothelial cell a response to very high wall shear stress	Bos taurus
GDS2773	Endothelial cell response to acute vs chronic activation by tumour necrosis factor	Mus musculus
GDS3868	Elevated laminar shear stress effect on umbilical endothelial cells	*Homo sapiens*
GDS2009	Sustained EGR1 expression in endothelial cells: time course	*Homo sapiens*
GDS2040	Endothelial cell morphogenesis	*Homo sapiens*
GDS2322	Vascular endothelial cell differentiation in vitro	*Mus musculus*
GDS3557	ERG transcription factor depletion effect on endothelial cell	*Homo sapiens*
GDS1597	Human coronary artery study	Homo sapiens

GDS3818	Atherosclerotic lesion regression: aorta	Mus musculus
GDS1968	Endothelial cell response to hypoxia and subsequent reoxygenation	*Homo sapiens*
GDS1701	Endothelial progenitor cells in fetal liver	*Mus musculus*
GDS2889	Air pollutant and oxidized lipid effect on microvascular endothelial cells: dose response	*Homo sapiens*
GDS1553	Fullerene effect on vascular endothelial cells.	*Homo sapiens*
GDS1354	Cirrhosis and liver endothelial cells.	*Rattus norvegicus*
GDS2484	Dermal lymphatic endothelial cell response to tumor necrosis factor alpha	*Homo sapiens*
GDS2571	Bone morphogenic protein 6 effect on an endothelial cell line: time course	*Mus musculus*
GDS5651	DNA methyltransferase inhibitor 5-Aza-2'deoxycytidine effect on partially-ligated left carotid artery	Mus musculus
GDS5083	Carotid artery atheroma	*Homo sapiens*
GDS2902	Hypoxia and lymphathic endothelial cells	*Homo sapiens*
GDS3060	Endometriosis: endometrial endothelial cells	*Homo sapiens*
GDS5007	Fetal and neonatal ductus arteriosus and aorta: endothelial cells	*Rattus norvegicus*

GDS3683	ACE inhibitor captopril effect on atherosclerosis model: aorta	*Mus musculus*
GDS3177	Confluent and sub-confluent umbilical vein endothelial cell cultures	*Homo sapiens*
GDS3355	Angiopoietin-1 stimulation of vascular endothelial cells	*Homo sapiens*
GDS3310	Human herpesvirus-8 infection of primary pulmonary microvascular cells	*Homo sapiens*
GDS3440	Aortic endothelial cell response to dominant negative PPAR gamma expression in vitro	*Mus musculus*
GDS3600	Endothelial cell response to estradiol in vitro	*Homo sapiens*
GDS3810	TNF receptor and lymphotoxin beta -receptor activation effect on aortic endothelial cells in vitro	*Mus musculus*
GDS3848	HMEC-1 endothelial cell line response to infection by Rickettsia prowazekii	*Homo sapiens*
GDS4463	Endothelial cells from P8 neonatal retina	*Mus musculus*
GDS4777	Freshly-isolated and cultured arterial and venous endothelial cells	*Homo Sapiens*
GDS4773	Peripheral venous congestion model: endothelial cells	*Homo Sapiens*
GDS4778	Freshly-isolated umbilical cord arterial and venous endothelial cells	*Homo Sapiens*
GDS5633	Peroxisome proliferator-activated receptor β,δ agonist	*Homo Sapiens*

	and hypoxia effects on umbilical vein endothelial cells	
GDS5417	Embryonic lung and brain cortex-endothelial cells	*Homo Sapiens*
GDS5914	YAP transcriptional regulator depletion effect on endothelial cells	*Homo Sapiens*
GDS5432	Age effect on corneal endothelium	*Homo Sapiens*
GDS3790	Erk5 activation effect on endothelial cells	*Homo Sapiens*
GDS4262	Oxidized low-density lipoprotein effect on LOX-1 overexpressing aortic endothelial cell line HAECT: time course	*Homo Sapiens*
GSE162072	Transcriptome profiling following focal ischemic stroke in female rats	*Rattus norvegicus*
GSE163614	Gene expression profile in cerebral ischemia-reperfusion injury of rat model	*Rattus norvegicus*
GDS1300	Hyperlipidemic model of adaptive immunity in aorta during atherogenesis	*Mus musculus*
GDS4527	Atherosclerosis susceptibility model: macrophages	*Mus musculus*
GSE166162	Expression data from the cortex after middle cerebral artery occlusion (MCAO) between young and aged rats	*Rattus norvegicus*
GDS3811	β-Catenin stabilized cardiac progenitor cells *in vivo*	*Mus musculus*

GSE148219	Expression profiling of human foetal and calcified adult aortic valves links inflammation to aging and identifying early disease gene markers	*Homo sapiens*